A GEOLOGIC MAP AND STRATIGRAPHY OF UPPER GUADALUPIAN – LOWER OCHOAN (PERMIAN) STRATA ALONG AND EAST OF FM 2185 IN THE NORTHWESTERN APACHE MOUNTAINS NEAR VAN HORN, WEST TEXAS

by

MICHAEL JAMES SWEATT

Presented to the Faculty of the Graduate School of

The University of Texas at Arlington in Partial Fulfillment

of the Requirements

for the Degree of

MASTER OF SCIENCE IN GEOLOGY

THE UNIVERSITY OF TEXAS AT ARLINGTON

December 2009

ACKNOWLEDGEMENTS

I am grateful for the guidance, advice, and patience from my adviser Merlynd Nestell and his wife Galina. Merlynd and Galina's expertise in and help with fusulinacean and small foraminifers identification contributed to the completion of this thesis. I also wish to thank Bruce Wardlaw for the identification of conodont elements, Gorden Bell Jr. and Lance Lambert for thoughtful insights and constructive criticism, and especially for the ranch owners, George Snyder, Kit Bramblett, and Gabe Price, for allowing me access to their properties and use of their facilities. I extend my most sincere thanks and appreciation to my field partner, peer, and friend, Walter Kennedy. And lastly, I would like to thank all my friends (especially T.I.) and family members for their support, encouragement, and understanding during this endeavor.

October 31, 2009

ABSTRACT

A GEOLOGIC MAP AND STRATIGRAPHY OF UPPER GUADALUPIAN – LOWER OCHOAN (PERMIAN) STRATA ALONG AND EAST OF FM 2185 IN THE NORTHWESTERN APACHE MOUNTAINS NEAR VAN HORN, WEST TEXAS

Michael James Sweatt, M.S.

The University of Texas at Arlington, 2009

Supervising Professor: Merlynd K. Nestell

A surface geologic map is constructed for an area of approximately four square miles east of Texas FM 2185, 35 miles northeast of Van Horn, West Texas in the northwestern part of the Apache Mountains. Middle Permian Guadalupian-Late Permian Ochoan age strata containing Capitan Reef debris and shelf to basinal beds are exposed and can be correlated to similar age strata of the Guadalupe Mountains to the north and northwest of the map area. In the area of study, three formations of the uppermost Middle and Upper Permian, Bell Canyon, Castile, and Rustler, expose strata that can be seen in a series of road cuts along Texas FM 2185. The Bell Canyon

Formation, a sequence of approximately two hundred meters of strata consisting of limestone, siltstone and debris flows, is the oldest unit exposed in the map area. The strata of the Castile and Rustler Formations successively overlie the strata of the Bell Canyon Formation. The Castile Formation is an evaporite with alternating dark and light gray laminations at the base and is brecciated towards the top. The Rustler Formation is also an evaporite, primarily brecciated, with rare exposures of red sandstone at the base. The strata exposed in this area are structurally complex due to the intersection of the Stocks fault, the Border fault zone, and the Seven Heart graben complex. The main goals of this study are: 1) to construct a geologic map of the area, 2) to use microfossil data from conodonts, fusulinaceans, and small foraminifers to correlate the Bell Canyon succession in the map area to similar age strata in the Guadalupe Mountains located about 50 miles to the north, 3) present a discussion of the carbonate facies and depositional processes that resulted in the extensive debris flow exposed in the latest Middle Permian, uppermost part of the Bell Canyon Formation (Reef Trail equivalent age) strata.

TABLE OF CONTENTS

LIST OF ILLUSTRATIONS

CHAPTER 1

INTRODUCTION

1.1 Geographic Setting

The Apache Mountains of West Texas are part of the Capitan Reef complex formed during the Middle Permian. This reef outlines the well-known Delaware basin and is exposed on the surface in the Guadalupe, Apache and Glass mountains (figure 1.1) where parts of the reef complex were uplifted and exposed during the Cenozoic (King, 1948).

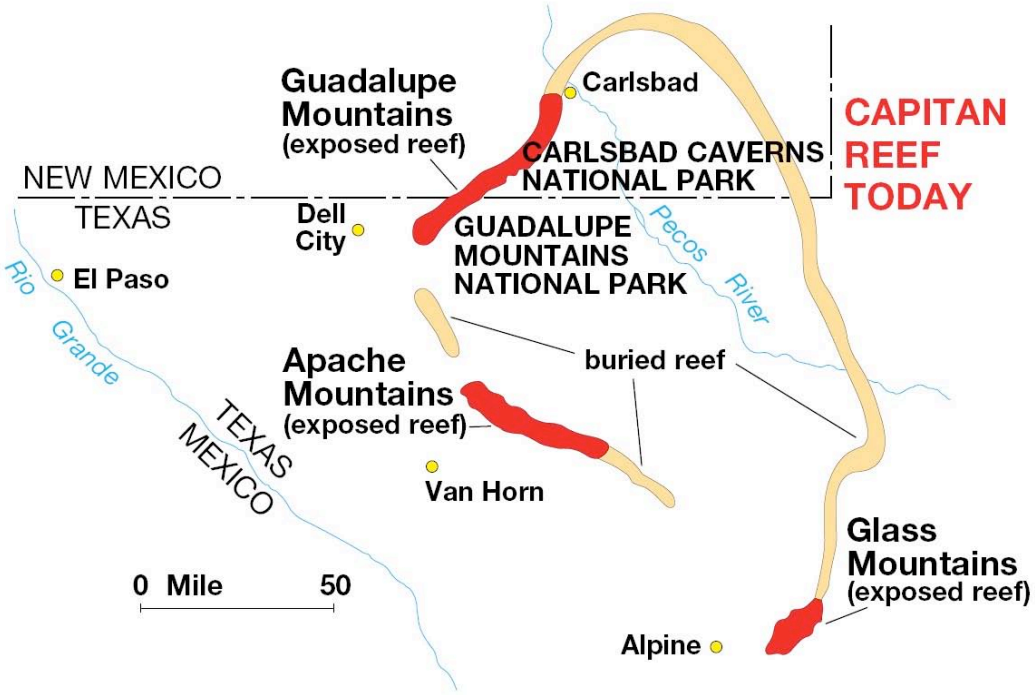

Figure 1.1: Location of the exposed (red) and buried (yellow) Capitan Reef in the Delaware Basin, West Texas (From Gorden Bell Jr., personal communication, 2007; Image is also available via the National Park Service website: www.nps.gov/gumo/naturescience/geologicformations.htm.)

The Delaware basin started to form during the end of the Pennsylvanian as subsidence took place and three monoclinal flexures began to down warp the region: the Bone Spring, Babb, and Victorio flexures (figure 1.2). The subsiding basin received marine water from the Hovey channel (figure 1.3), which separated the area of the present-day Apache and Glass mountains (King, 1942, 1948). This channel is thought to have been deep enough to circulate water into and from the basin (Hills, 1942). At the end of the deposition of the Guadalupian Series, the Hovey channel was uplifted and possibly partially blocked with reef growth, reducing flow from the open ocean and resulting in the formation of the evaporitic Castile lagoon containing evaporate deposits of Ochoan age (Hill, 1999).

During the Permian, a reef thrived along the edges of the Delaware basin keeping virtually the same rate of growth as with the rate of basin subsidence. This reef was mostly composed of calcareous algae (most commonly: *Archaeolithoporella* and *Mizzia*), sponges, *Tubiphytes*, bryozoans, brachiopods and foraminifers (King, 1942, 1948; Newell, 1953). The basin is estimated to have reached a maximum water depth of up to 2000 feet during the Guadalupian, and with subsidence, 3000-5000 feet of silt and sand of the Delaware Mountain Group was deposited in the basin (King, 1942, 1948; Newell et al., 1953; Harms, 1974).

Little or no structural deformation occurred during the Mesozoic, but during the Tertiary, Basin and Range tectonism formed the Delaware uplift and exposed strata in the Guadalupe, Apache, Delaware and Glass mountains (King, 1942, 1948; Wood, 1965). The map area exhibits at least two trends of Tertiary faulting, the Stocks fault and the

Seven Heart graben complex, and possible influence from the Border fault zone (King, 1948). These stages of faulting produced a number of large fault blocks that have made correlation of the strata of the area challenging.

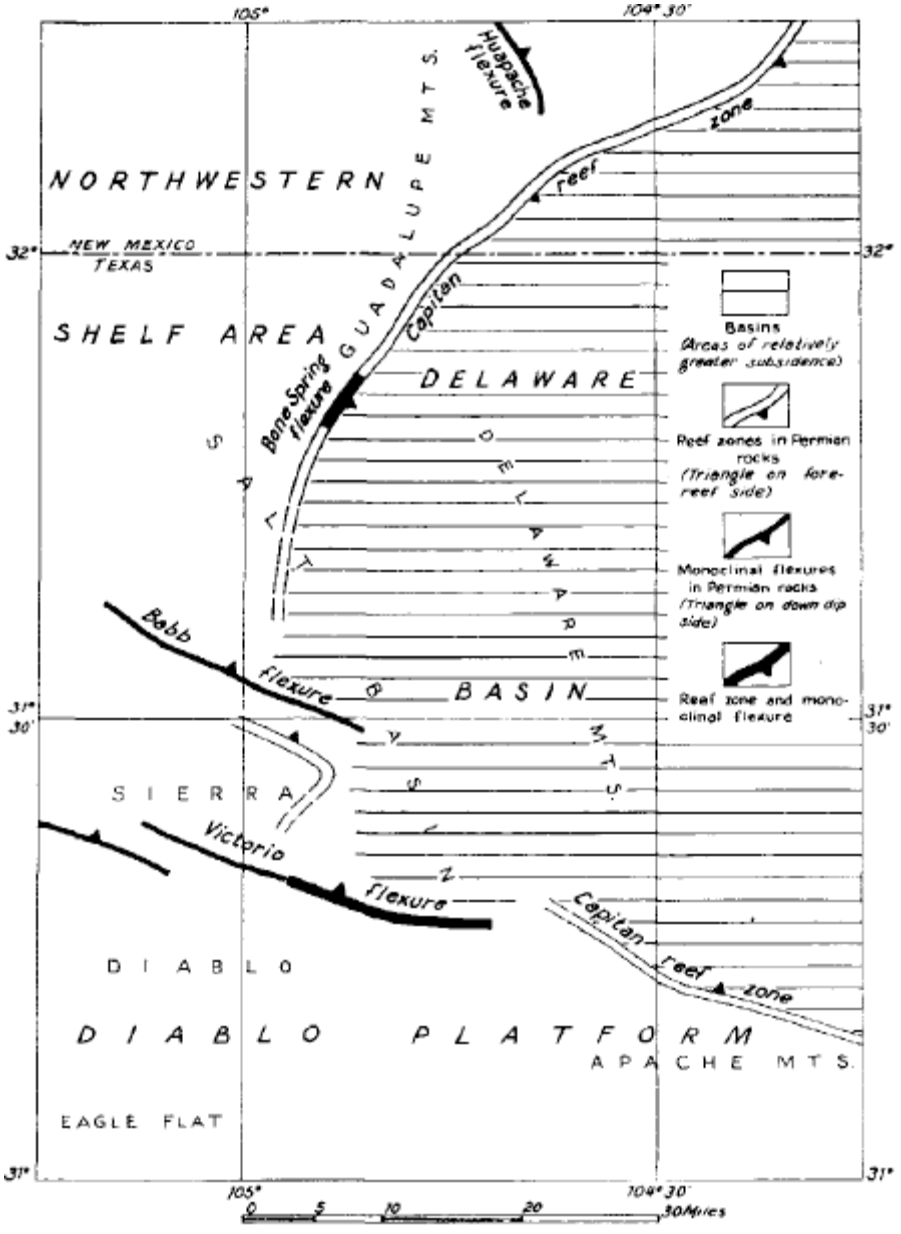

Figure 1.2: Location of the Bone Spring, Babb, and Victorio flexures bordering the Delaware basin, West Texas (from King, 1942).

1.2 Location

The map area is located approximately 35 miles north of Van Horn, Culberson county, West Texas along FM 2185 (figure 1.3) where three formations, Bell Canyon, Castile, and Rustler, are exposed in a series of road cuts. The map area is bounded by FM 2185 to the north and extends south to the 31° 16'30" North latitudinal line. It is bounded on the west by the Seven Heart Ranch access road and on the east by the 104° 31' West longitudinal line.

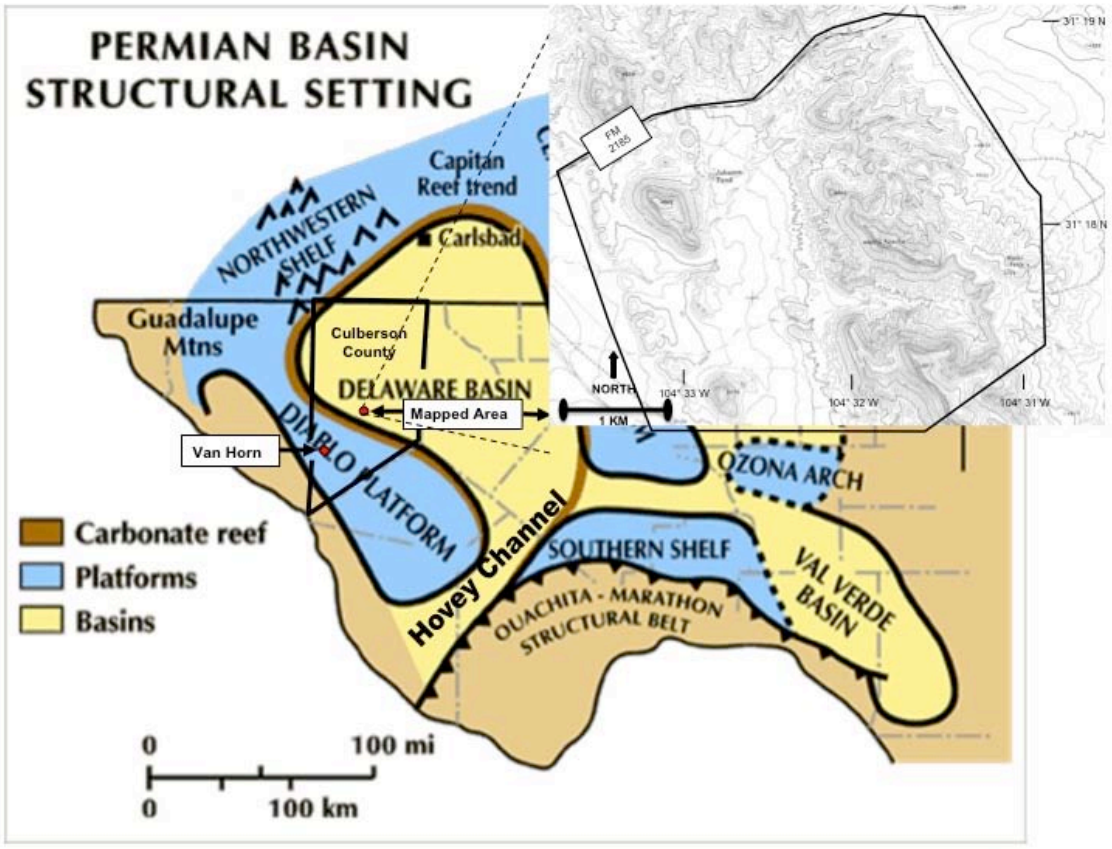

Figure 1.3: Location of the map area northeast of Van Horn in Culberson County, Texas, with the Middle Permian paleogeography superimposed over present day West Texas (After Dutton et al., 2000 and Lambert et al., 2002). Bold line in the inset map outlines the map area.

1.3 Previous Work

A brief description of the Apache Mountains was included in Richardson's (1904) report of a Reconnaissance in Trans-Pecos Texas. The reconnaissance of this area was primarily conducted to determine the conditions and occurrences of underground water. Richardson (1904) established that the strata exposed in the Apache Mountains were Permian in age by observing that the Apache Mountains were an extension of the Delaware Mountains located to the northwest. Richardson's fossil collections from the Apache Mountains, described by Girty (1908), verified that the Apache Mountains strata were Permian in age. Girty (1908) included his work on Richardson's fossils in his well-known monograph "The Guadalupian Fauna." Later, Richardson (1914) summarized his work on the lithology and fossil content of the strata of the western part of the Apache Mountains.

Workers like King and King (1928), and Schuchert (1928) recognized the reefal characteristics of the Capitan Limestone in the Guadalupe Mountains. These observations prompted Lloyd (1929) to further study the Capitan Limestone and consider the fossiliferous limestones as being reefal in origin, which improved the interpretation of the stratigraphy in the Delaware basin. Lloyd also inferred that the massive limestones of the Apache and Glass mountains were also reefal in origin. Crandall (1929), and Blanchard and Davis (1929), provided further evidence to support Lloyd's reefal origin of the Capitan Limestone by studying and comparing the Capitan Reef to other known fossil reef complexes such as the reefal dolomites of the Tyrolean Alps and modern reefs such as in the Bahamas. These works also helped to establish the interpretation of the

different lithofacies surrounding the Capitan reef, such as the back reef, lagoonal, fore reef and basinal facies.

With the recognition of the importance of fusulinaceans for the use of stratigraphic correlation, Dunbar and Skinner published in 1937 "The Permian Fusulinidae of Texas". Their work details the identification, morphologies, classification, correlation and zonation of the Permian fusulinaceans from several areas in the state with emphasis on Middle Permian taxa. This publication provided a useful biostratigraphic framework for the fusulinacean succession in the Middle Permian strata of West Texas.

P. B. King greatly contributed to the understanding of the Permian in West Texas with his monumental works on the geology of the Glass, Guadalupe and Apache mountains, in which he described in detail the geologic framework of the Permian System in West Texas and southeastern New Mexico (King 1926, 1935, 1942, 1948). However, he concentrated most of his work in the Guadalupe Mountains. As a consequence, his geological work in the Apache and Glass mountains does not have the same amount of detail as his work in the Guadalupe Mountains. Like King, Bybee (1931) also worked with general structural problems in West Texas, and also concentrated most of his work to the Guadalupe Mountains area.

A number of Middle Permian stratigraphic units were first described in the Guadalupe Mountains and some of these units can be recognized in the Apache Mountains. For example, the Bell Canyon Formation in the Guadalupe Mountains is a sandstone/siltstone sequence interbedded with five limestone members in ascending order: Hegler, Pinery, Rader, McCombs ("flaggy limestone"), Lamar Limestone, and

Reef Trail ("Post Lamar Beds") Members. King (1948) gave brief descriptions of these limestone members and their fossil content. The Bell Canyon Formation has also been considered by many workers as valid unit in the Apache Mountains.

Wilde et al. (1999) recently designated the "Post Lamar Beds" of the Bell Canyon Formation (as described by King, 1948) as the Reef Trail Member and summarized fusulinacean zones of the Guadalupian and Lopingian series. A modified fusulinacean biostratigraphic zonation used as a basis for correlation in this study is illustrated in figure 1.4 (corrected from Wilde et al. 1999). A number of problems presented in Wilde's fusulinacean zonation and the stratigraphic concept and age of the Reef Trail Member will be discussed later.

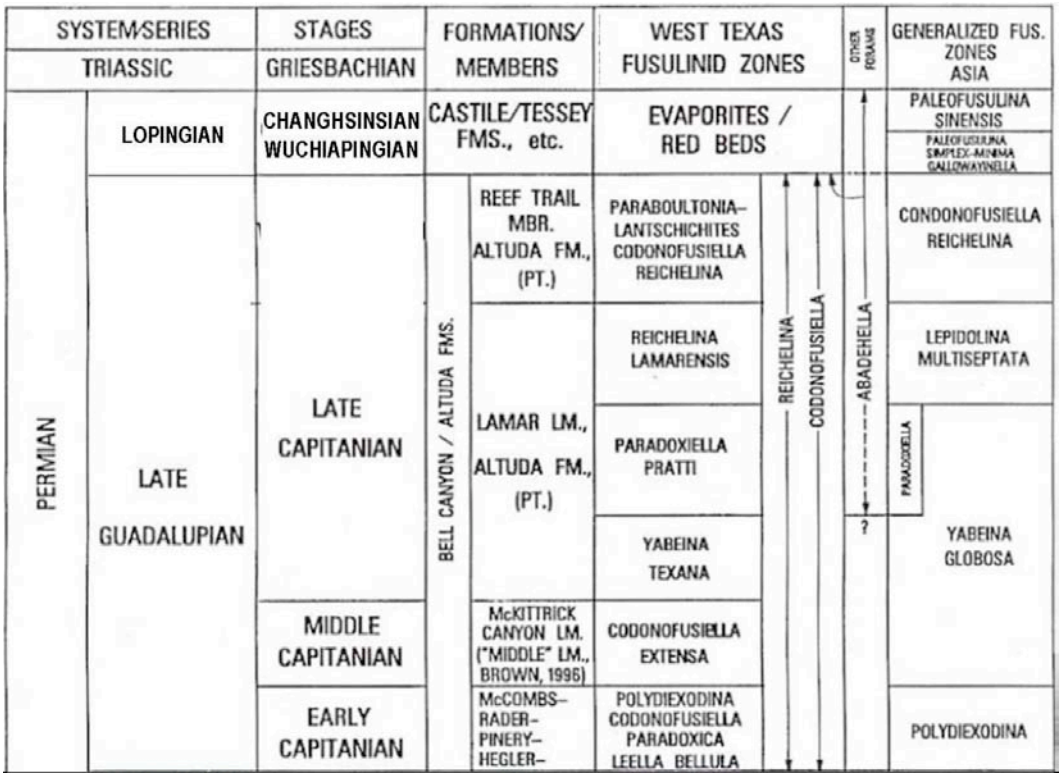

Figure 1.4: Fusulinacean biostratigraphic zones (corrected from Wilde et al., 1999). Wilde designated, incorrectly, the Reef Trail Member of the Bell Canyon Formation as Lopingian in age. The chart has been corrected to include the Reef Trail in the late Guadalupian based on conodont data.

In the Guadalupe Mountains area, the large diagnostic fusulinacean *Polydiexodina* is only present in the Hegler, Pinery, Rader, and McCombs Members and is absent in the Lamar Limestone and Reef Trail Members. These limestone members are separated by significant siltstone/sandstone intervals of the Delaware Mountain Group. In the Guadalupe Mountains, the oldest member in the Bell Canyon Formation is the Hegler Member, which is about 30 to 40 feet thick and consists of dark gray fine grained limestone interbedded with siltstone and sandstone. It was named after the Hegler Ranch by King (1948). The next overlying member is the Pinery. It was named after the old stage station at the mouth of Pine Spring Canyon. It lies about 75 feet above the Hegler, and it is about 30 feet thick consisting of dark gray fine grained limestone interbedded with siltstone and sandstone (King, 1948). The Rader Member lies about 30 to 40 feet above the Pinery Member and is about 15-20 feet thick consisting of limestone interbedded with siltstone and sandstone (King, 1948), and several debris flows known as the Rader slides in many guide books (Nestell et al. 2006b). The next member in the Bell Canyon Formation is the McCombs. It is about 100 feet above the Rader Member and is about 10 feet thick consisting of thin bedded, fine grained, gray limestone (King, 1948). A series of limestone beds was first described by King (1948) as a "flaggy limestone" between the Rader and Lamar Limestone Members. Later in 1956, King and Newell formally named the "flaggy limestone" the McCombs Member. The McCombs Member is significant because it contains the highest occurrence of *Polydiexodina* and the first appearance of the fusulinacean *Codonofusiella extensa* in the Guadalupe Mountains (Newell et al., 1953). The Lamar Limestone Member lies above the McCombs Member

and is described as being variable in its thickness and texture. It ranges from 10's to 100's of feet thick and is fossiliferous and fine grained in texture. Wilde et al. (1999) also introduced the name McKittrick Canyon Member (figure 1.4), but with no description, for a thin interval of limestone beds several meters above the McCombs Member and exposed in the McKittrick Canyon area. This name has never been substantiated nor described and its status is questionable. The Lamar Limestone is absent of *Polydiexodina*, except for reworked fragments sometimes found in scattered debris flows within the member. The fusulinacean *Yabeina texana* Skinner and Wilde is found at the base of the Lamar Limestone (its lowest known occurrence) and the very distinctive fusulinacean *Paradoxiella* first appears approximately in the middle of the Lamar Limestone (figure 1.4). The upper part of the Lamar Limestone Member contains *Reichelina lamarensis* Skinner and Wilde with the occurrence of the small foraminifer *Abadehella.* The Reef Trail Member, formally designated by Wilde et al. (1999), contains the fusulinaceans *Paraboultonia splendens* Skinner and Wilde, and *Codonofusiella extensa.*

Detailed mapping was conducted in the southern end of the Delaware Mountains and in the northwestern part of the Apache Mountains by McNutt (1948) in his doctoral dissertation at The University of Oklahoma. McNutt's map was the first extensive geologic map made of the northwestern part of the Apache Mountains. After McNutt, several other students conducted mapping projects in and around the Apache Mountains; most of them were from The University of Texas at Austin and supervised by R. K. DeFord. DeFord (1951), in his guidebook "The Apache Mountains of Trans-Pecos

Texas", showcased many of his students' work, but most notably, that of Owen (1951). Owen produced a detailed structural map of the Seven Heart Gap area located just northeast of the main trend of the Apache Mountains and a few kilometers east of the map area of this project. His map helped with the understanding of the complexity of the structural trends in the map area. Two other students from The University of Texas: Snider (1955) and Wood (1965) also did mapping theses in the Apache Mountains. Snider constructed a detailed geologic map of the Seven Heart Quadrangle, and discussed the general geology of the area. Snider also discussed in detail the subsurface geology using data from several test wells drilled by various petroleum companies. Wood (1965) summarized the history of the previous works done in the Apache Mountains and in West Texas, and presented a detailed map of the main body of the Apache Mountains with specific emphasis given to the geologic history and rock correlations across the facies changes throughout the Apache Mountains. Wilde and Todd (1968) duplicated Wood's correlation work using surface and subsurface fusulinacean data. They presented stratigraphic columns of the backreef, reef and basin deposits from both the Apache and Guadalupe mountains. Their work reiterated the importance of fusulinaceans in stratigraphic correlations, especially in structurally and stratigraphically complex areas such as the Apache and Guadalupe mountains.

Recent works in the Apache Mountains have been primarily detailed bio-stratigraphic studies. As noted earlier, Wilde et al. (1999) described the previously known "Post-Lamar-Beds" as the new Reef Trail Member of the uppermost Bell Canyon Formation with type locality at the entrance to McKittrick Canyon in the Guadalupe

Mountains. In Wilde's attempt to establish the boundary between the Middle and Upper Permian strata, he incorrectly assigned the newly described Reef Trail Member to the Upper Permian Lopingian Series. At the time of Wilde et al. (1999) publication, the precise Guadalupian–Lopingian boundary had not been established as at the first occurrence of the conodont *Clarkina postbitteri postbitteri*, a species that has never been found in West Texas. *Clarkina postbitteri hongshuiensis* is the defining conodont species of latest Guadalupian age strata. This species has been found in the uppermost beds of the Bell Canyon Formation in the Patterson Hills (Guadalupe Mountains area) and in the map area (Apache Mountains area). This author's study is part of an ongoing project by M. Nestell, G. Nestell, B. Wardlaw, L. Lambert, and G. Bell Jr. to clarify the correlation of Middle Permian strata in the Guadalupe and Apache mountains.

1.4 Methods

Approximately six weeks were spent conducting field work in the map area which consisted of reconnaissance, measurement of stratigraphic sections, and collection of samples. Samples were chosen on the basis of maximizing conodont yield, high fusulinacean/foraminifer content and interesting textures.

Samples were dissolved by formic acid and the non-soluble residues were examined for conodonts, foraminifers and other fossils. Conodonts were separated from the acid residues by floating the lighter insoluble grains of the residue in a heavy liquid, Tetrabromoethane. The Tetrabromoethane was diluted with acetone until a specific gravity slightly less than that of conodonts (approximately 2.87 g/cm3) allowing the heavier conodonts to sink and then be removed through a petcock at the bottom of the

separation funnel. Tetrabromoethane vapors are highly toxic and the separation process must be conducted under a strong ventilation hood. Additional samples were made into thin-sections and polished slabs to study lithofacies and biofacies.

Stratigraphic columns were constructed to illustrate and describe the lithologies of the measured sections in the map area. The increase of horizontal width of the measured units in the lithology column is in direct proportion to the increase of that measured units resistance to weathering.

Mapping was accomplished by traverse, aerial photographs, vegetation changes, and with the aid of a Garmin Legend eTrek GPS receiver. Drafting of the final map was done with ArcGIS 9.2 and Microsoft Windows Power Point program.

1.5 Purpose of Study

This study consists of: 1) construction of a geologic map of the map area in the northwestern Apache Mountains, with the aim of distinguishing among the various debris flows present in the Bell Canyon Formation and giving only a generalized description of the distribution of the strata of the overlying Castile and Rustler Formations, 2) a general discussion of the correlation problem presented by the various parts of the Bell Canyon Formation bounded by these debris flows in the map area with the well-known Bell Canyon Limestone Members (Hegler, Pinery, Rader, McCombs, Lamar, Reef Trail) as described in the Guadalupe Mountains, 3) discussion and illustration of the carbonates and depositional processes which resulted in the extensive debris flow exposed in the latest Middle Permian (Reef Trail equivalent age) strata.

CHAPTER 2

STRATIGRAPHY

2.1 Introduction

Three rock formations: the Bell Canyon, Castile, and Rustler are exposed in the map area. The Bell Canyon Formation is the uppermost formation in the Delaware Mountain Group of the Guadalupian Series in West Texas. This formation consists of interbedded calcareous siltstone, very fine grained sandstone, silty carbonate mudstone to packstone and several thick debris flows (Lambert et al., 2002). The clastic deposits of the Bell Canyon Formation were possibly deposited by turbidity currents during low stand conditions in the Delaware basin (Dutton et al., 2003). A well-known oil reservoir in the East Ford and Ford Geraldine oil fields in the Delaware basin is the Ramsey Sandstone stratigraphically located between the McCombs and Lamar Limestone Members of the Bell Canyon Formation. One of the unsolved problems in the map area is the presence in two sections (AV and K) of two thick siltstone sequences separated by a package of thin carbonate beds that could be the Ramsey Sand equivalent because of the stratigraphic position of this package below a sequence of carbonate strata that contains the fusulinacean *Yabeina texana* and appears to be the equivalent in age to the Lamar Limestone (M. Nestell, personal communication, 2009).

The Bell Canyon Formation has six limestone members that were originally described from the Guadalupe Mountains area: Hegler, Pinery, Rader, McCombs, Lamar,

and Reef Trail. Some of these limestone members can be differentiated from others by using their particular fossil assemblages, especially the conodonts and fusulinaceans. The rock sequences in the Apache Mountains can be correlated biostratigraphically to strata present in the Guadalupe Mountains by using the fossil assemblages. However, the individual limestone members of the Bell Canyon Formation of the Guadalupe Mountains cannot be identified lithologically in the Apache Mountains, although some Bell Canyon names, e.g., Rader and Lamar have been used for strata in the Apache Mountains (Silver, 1968).

The Castile Formation is an evaporite that was deposited in early Ochoan time. It has varve-like laminations of gypsum and bituminous dark gray calcite; and in the subsurface, anhydrite and bituminous dark gray calcite, and occasional halite (King, 1948; Kirkland et al., 2000). The strata of the Castile Formation in the map area are slightly different lithologically from those of the Castile Formation in the Guadalupe Mountains area. The Castile Formation in the map area has strata that exhibit the 1-2 mm thick alternating dark and light lamina like the Castile Formation in the Guadalupe Mountains area, but it also displays quite different lithologies with sections of conglomerate and breccia similar to those known in the Tessey Limestone in the Glass Mountains (King, 1948). Near the base of the formation in the map area there is an interval of lamina with mud cracks.

In the eastern part of the Delaware basin, the Salado Formation, a thick sequence of halite interbedded with red shale (Hills, 1972), lies between strata of the Castile and

Rustler Formations. The Salado Formation is not present in the map area; either it was not deposited (Hills, 1972), or was removed due to erosion or dissolution (Owen, 1951).

The Rustler Formation lies above the Castile Formation in the map area, and is composed mostly of brecciated dolomite with rare red sandstone at its base. The red sandstone is thought to have been derived from the Salado Formation (Hills, 1972), and this sandstone is so rarely exposed in the map area that it was not useful to map as the contact between strata of the Castile and Rustler Formations. The age of the Rustler Formation was determined to be Ochoan by the discovery of fossils described by Walter (1953) in the uppermost part of the formation, which was not found in the map area.

2.2 Bell Canyon Formation

Deposited in Late Guadalupian time, the Bell Canyon Formation, named by King (1942) after its type section locality in Bell Canyon in the Guadalupe Mountains area consists of siltstone and very fine grained sandstone interbedded with limestone. The Bell Canyon Formation in the map area has an upper conformable contact with the Castile Formation. There are approximately 200 meters of exposed Bell Canyon age strata in the map area where several sequences of the formation can be seen in the road cuts along TX FM 2185. Traveling northeast along FM 2185 through the map area, each of the road cuts containing the Bell Canyon strata has been given a section name beginning a few hundred meters north-northeast from the gate to the Seven Heart Ranch: the M section, EF section, B section, A section, and G section (figures 2.1 and 2.2, and the geologic map in Appendix A) (Nestell et al., 2006a). One additional section, the K section, is exposed on a hill and adjacent valley to the southeast, in the northeast portion

of the map area (figure 2.2). Determination of the stratigraphic ordering of the rock sequences in the numbered sections is complicated due to the Tertiary faulting in the map area and has been determined biostratigraphically using conodonts and fusulinaceans (Nestell and Wardlaw, personal communication, 2009). Also, the fossil content has been used to correlate the strata of the Bell Canyon Formation in the map area with similar age strata of the Bell Canyon Formation exposed in the Guadalupe Mountains area. However, the confident use of the individual member names is not easily transferable from the Guadalupe Mountains to the map area in the Apache Mountains due to lithological differences.

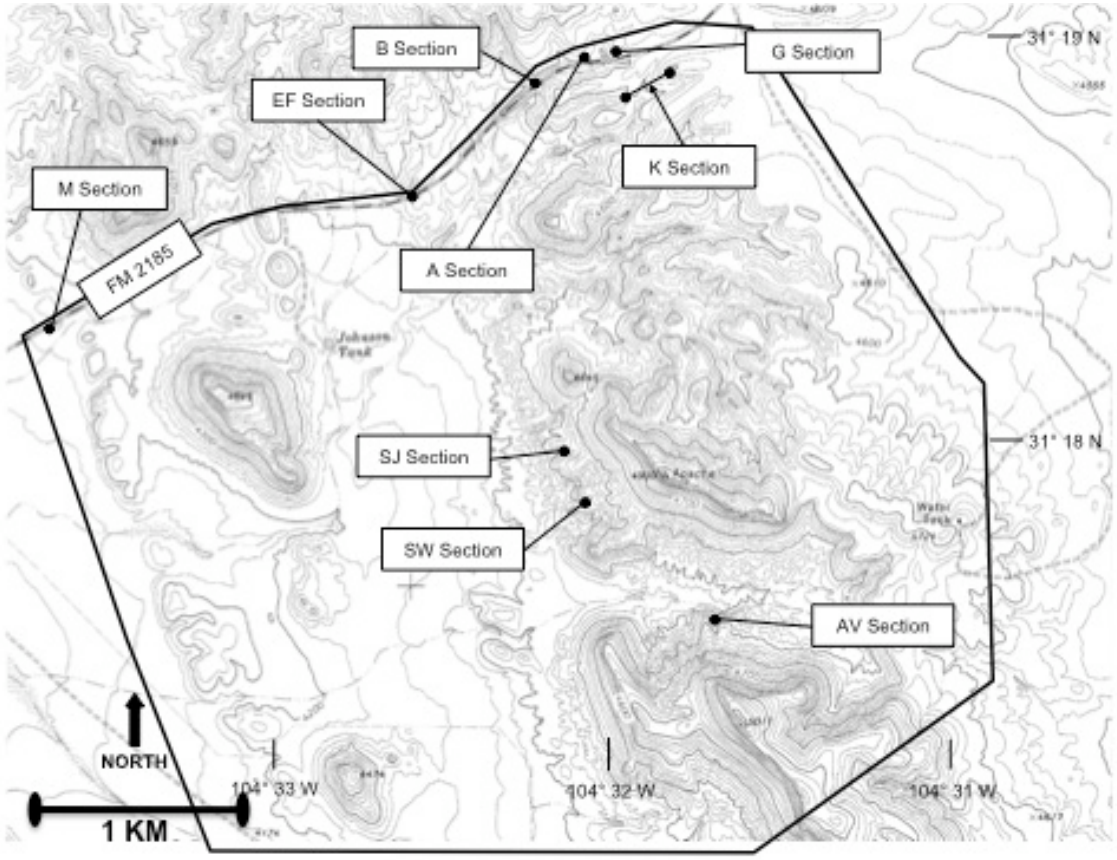

Figure 2.1: Locations of the M, EF, SW, SJ, AV, B, A, G, and K sections. TX FM 2185 runs across the north part of the map along the border of the map area. The map area is outlined with a bold solid line.

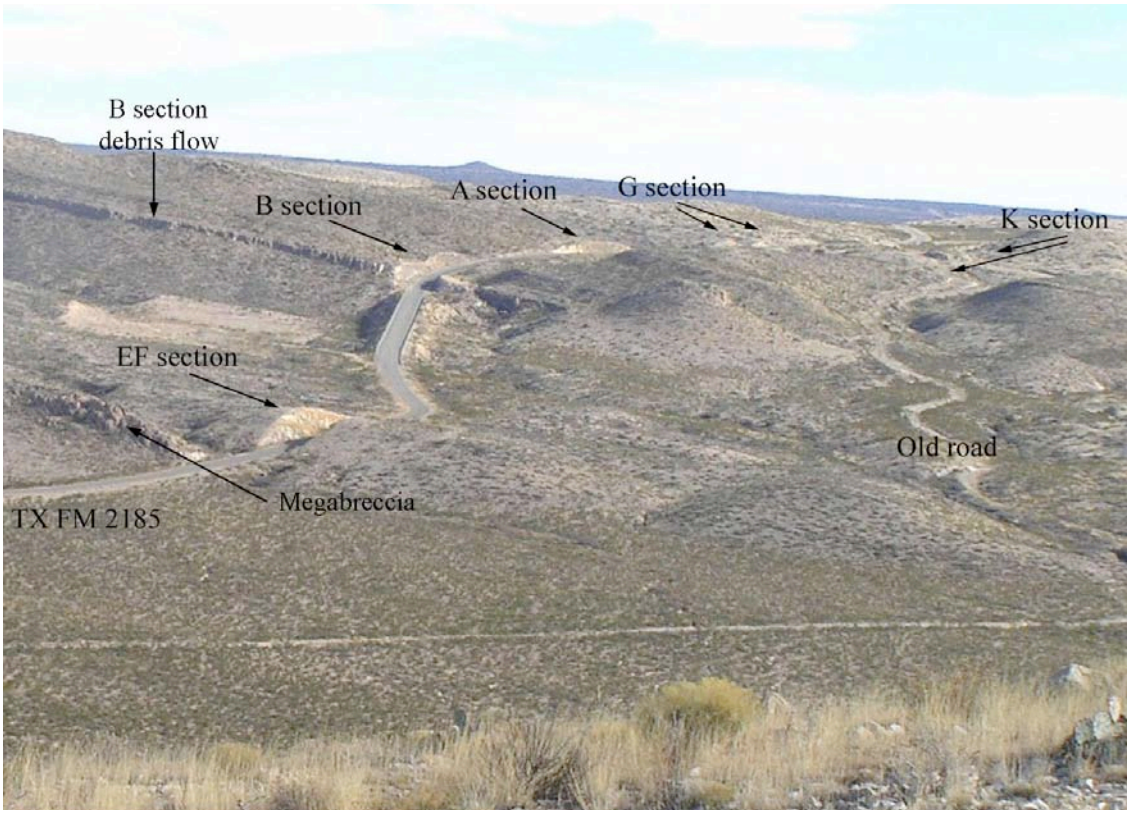

Figure 2.2: Location of the EF section, B section, A section, G section and K section, looking to the northeast along Texas FM 2185 (Nestell et al., 2006a). The B section debris flow and the megabreccia in the base of the EF section can clearly be seen in their respective road cuts.

2.2.1 Biostratigraphic Relations

The major problem in correlating the individual unnamed members of the Bell Canyon Formation in the Apache Mountains with the members of the Bell Canyon Formation in the Guadalupe Mountains is the difference in lithofacies from one location to the other. However, some of the Guadalupe Mountains area Bell Canyon members can be recognized biostratigraphically in the map area in the Apache Mountains. The occurrence of particular species, used in conjunction with other key species (a fossil assemblage), can create zones in which an age range can be assigned whenever that particular species is encountered. Generalized correlations can be made for the B, A, G,

and K sections and confident more precise correlations can be made for the EF SW, SJ, AV and M sections. These correlations can be accomplished by using biostratigraphic data from several key faunas present in both the Apache and Guadalupe mountains such as particular species of the fusulinacean genera *Paraboultonia, Polydiexodina, Paradoxiella, Reichelina, Yabeina*, and *Codonofusiella* and conodont species of the genera *Jinogondolella* and *Clarkina* (figure 2.3) (Nestell et al., 2006a). For example, the uppermost part of the Bell Canyon Formation of the Apache Mountains contains an evolutionary trend from the conodont species *Jinogondolella altudaensis* (Kozur) to *Jinogondolella crofti* (Kozur and Lucas) and then to *Clarkina postbitteri hongshuiensis* Henderson, Mei, and Wardlaw, both of which occur in the EF and M sections of the map area (Nestell et al., 2006a). *Clarkina postbitteri* is divided into two subspecies: *Clarkina postbitteri postbitteri* Mei and Wardlaw, and *Clarkina postbitteri hongshuiensis*. *Clarkina postbitteri postbitteri* has not been found in West Texas and its significance is that its first appearance marks the GSSP for the lower boundary of the Upper Permian Lopingian Series in the Penglaitan section in South China (Gradstein et al., 2004). The recent discovery of the conodont *Clarkina postbitteri hongshuiensis* in West Texas is significant because its presence marks the uppermost conodont zone for the Guadalupian Series in North America (Nestell et al., 2006a). It has been found in the uppermost few meters of equivalent age strata of the Reef Trail Member in the Guadalupe Mountains at one locality in the Patterson Hills (south boundary section SBR1 of Gorden Bell Jr., personal communication, 2009), and its correlative strata in the Apache Mountains.

Clarkina postbitteri hongshuiensis has not been found in the type section of the Reef Trail Member at McKittrick Canyon as designated by Wilde et al. (1999).

Strata of the sections B, A, G, and K all contain the fusulinacean *Polydiexodina* thus placing them as pre-Lamar in age. The EF section is void of *Polydiexodina* except as reworked pre-Lamar debris particles incorporated into debris flows. The presence of the fusulinacean *Paraboultonia splendens* and the conodonts *Jinogondolella crofti* and *Clarkina postbitteri hongshuiensis* in the EF section suggests that the strata of the EF section is essentially equivalent in age to that of the Reef Trail Member as expanded by newly discovered complete sections in the Patterson Hills just to the west of Guadalupe Peak (Nestell et al, 2007b). Much of the conodont, fusulinacean, and radiolarian data presented in this thesis are from unpublished work in progress by Nestell, Nestell and Wardlaw.

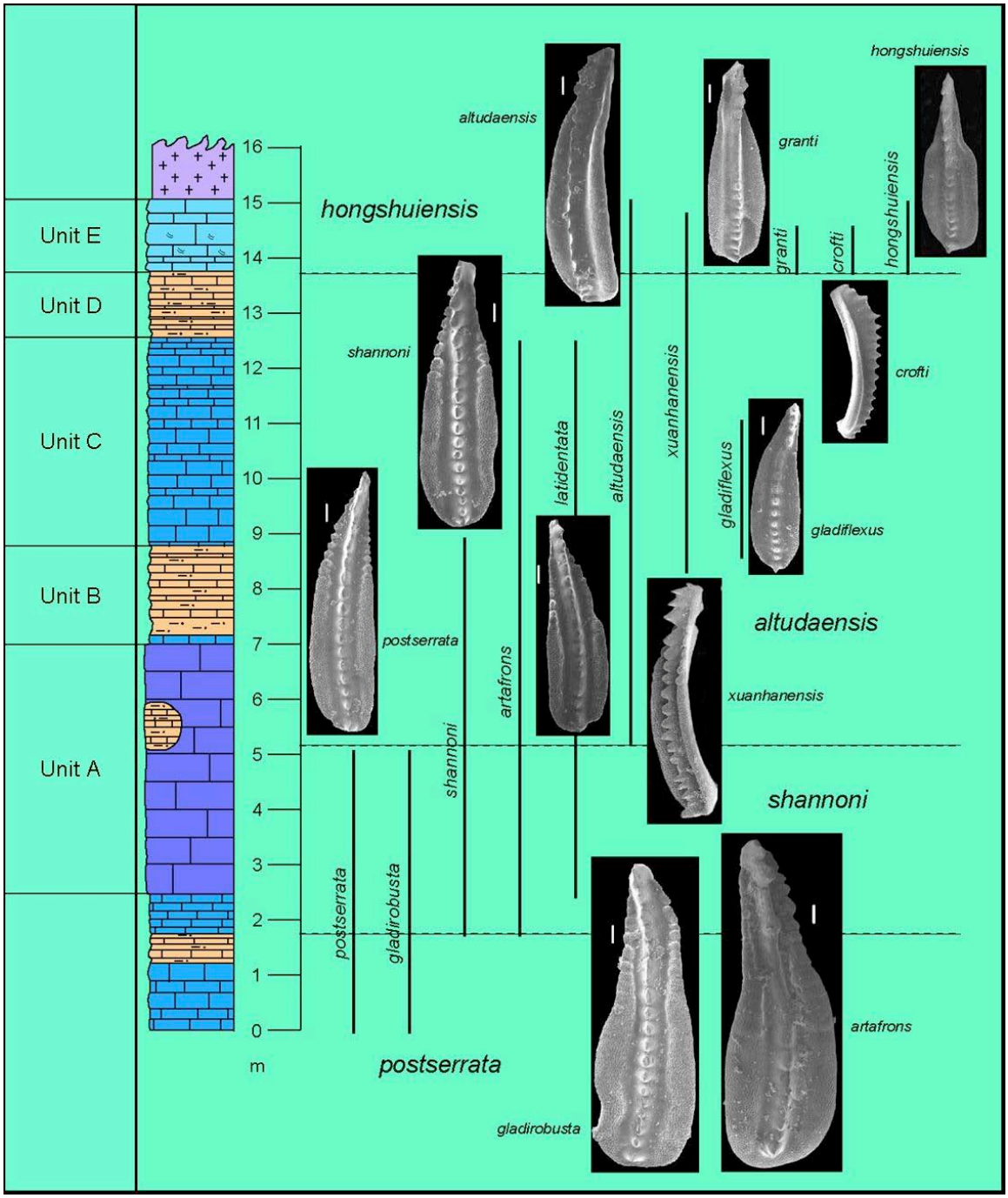

Figure 2.3: Conodont zonal distribution of P-elements from Units A-E in the EF section showing part of the *Jinogondolella* assemblage and also the youngest conodont found in the map area: *Clarkina postbitteri hongshuiensis* (Nestell and Wardlaw, personal communication, 2009). The white bar with each sample equals 100 micrometers.

2.2.2 B Section

The B section is the oldest exposed strata in the map area and is juxtaposed by a fault against strata of the Castile and Rustler Formations. A several meter thick debris flow is present in the lower middle part of the B section and is discussed in great detail by Kennedy (2009) in his master's thesis. The above mentioned debris flow is only present in this author's map area for roughly 80 meters southeast from TX FM 2185, where the B section is truncated by a fault (Appendix A).

The B section is 47 meters thick and was measured starting at the juxtaposing fault with the Castile Formation in a gully (figures 2.4 and 2.5) on the southeast side of TX FM 2185. The first 4.5 meters is thin bedded tan siltstone interbedded with thin to thick bedded gray limestone with scattered ammonoids tentatively identified as the genus *Mexicoceras* in a bed between the first and second meters of the measured section. The next 15 meters comprise several intervals of the massive carbonate debris flow in the B section (figures 2.6, 2.7 and 2.8). This debris flow can be traced for miles to the northwest in Kennedy's map area and in the valley walls north of his map area. However, it was surprising to find it rarely exposed in this author's map area. The B section road cut is capped with a sequence of thin bedded tan siltstone interbedded with beds of thin to thick gray limestone for 28 meters from the top of the debris flow (figures 2.9 and 2.10).

Fossils found in the B section include radiolarians, small foraminifers, the large fusulinacean *Polydiexodina*, and the conodonts *Jinogondolella aserrata* Mei and Wardlaw of Late Wordian age and in the upper part, *J. postserrata* of Capitanian age.

The presence of both *J. aserrata* and *J. postserrata* suggests that the B section contains the transition from Late Wordian to Early Capitanian strata and is possibly the age equivalent of the Hegler Member in the lower part of the B section and the age equivalent of the Pinery Member in the upper part of the B section (Nestell and Wardlaw, personal communication, 2009).

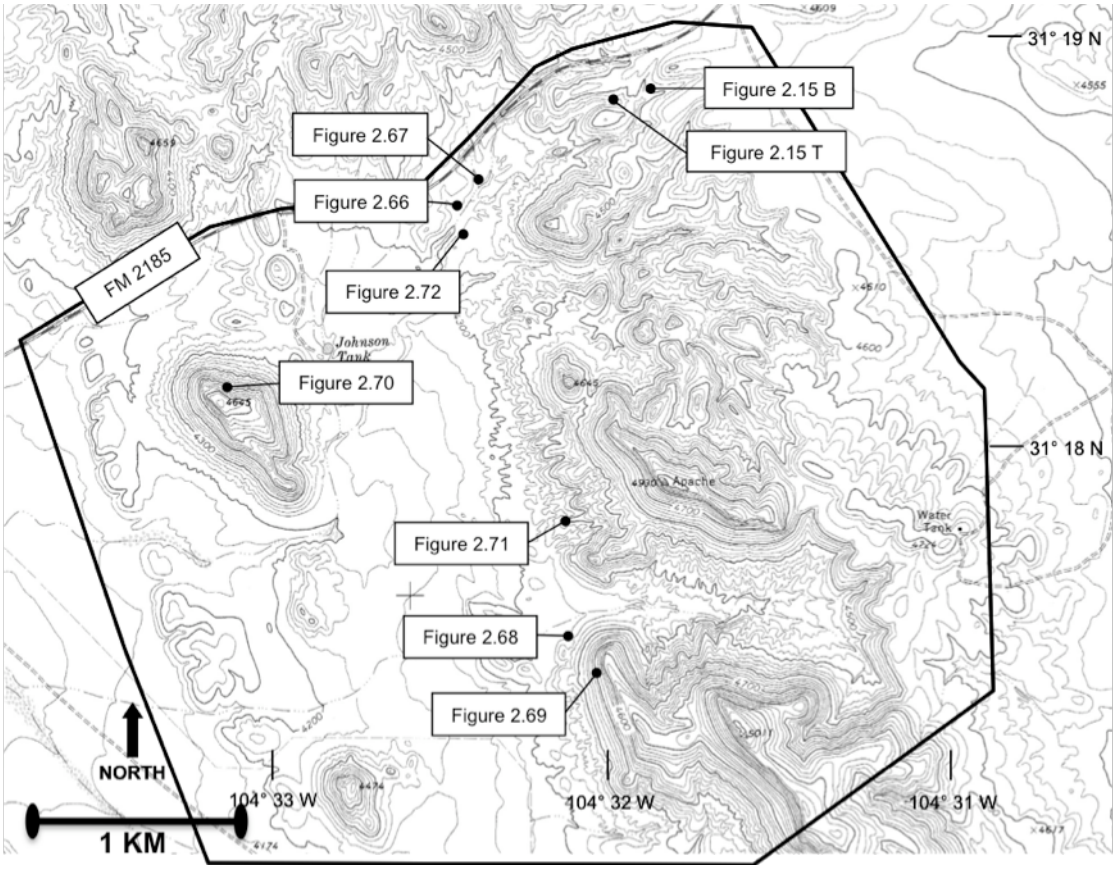

Figure 2.4: Locations of photos displayed in this thesis. The locations are identified by a figure number and the letter, where applicable. T and B represent Top and Bottom with respect to the individual photos in each figure.

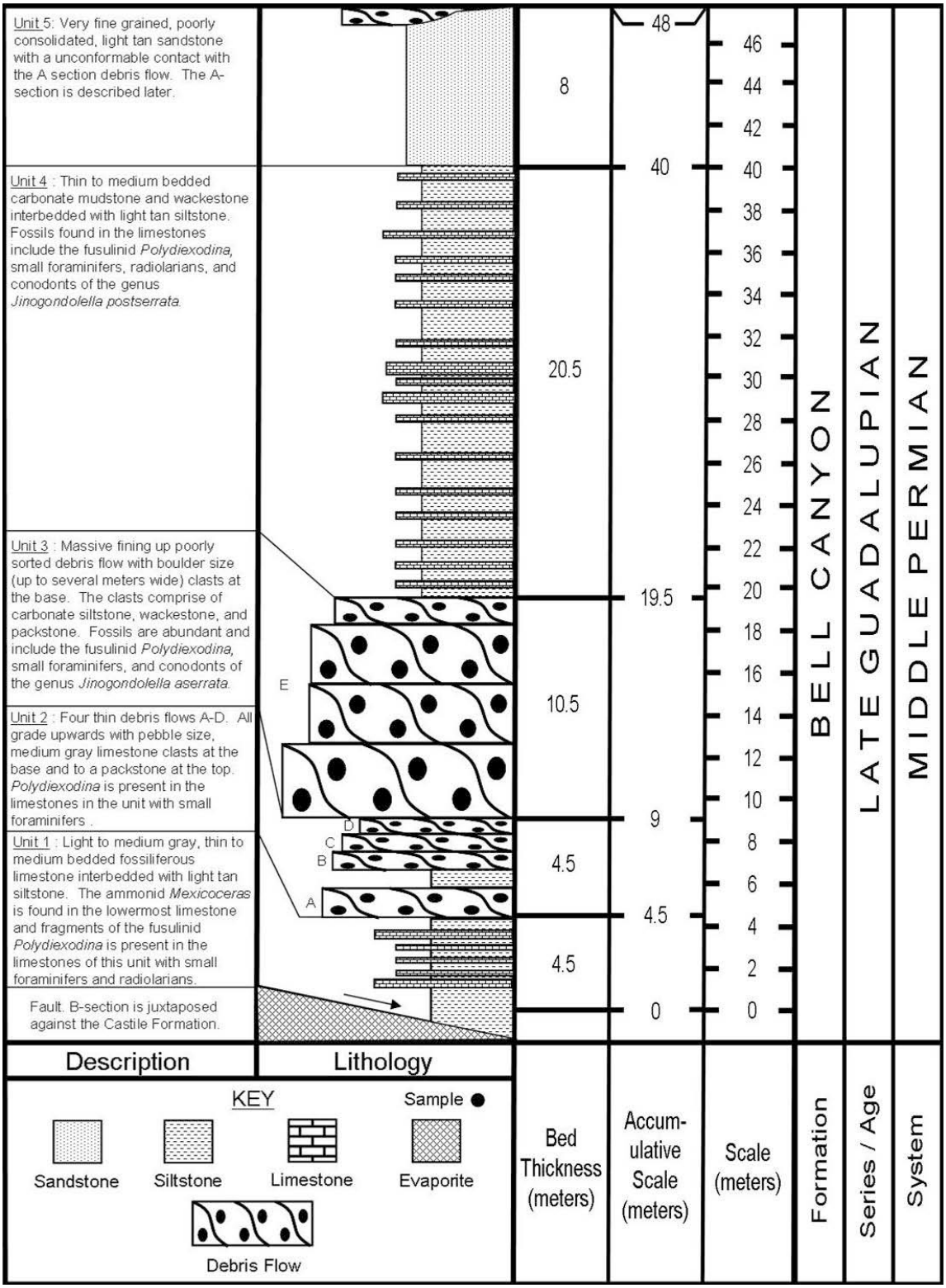

Figure 2.5: Composite stratigraphic column of the B section in a valley and road cut.

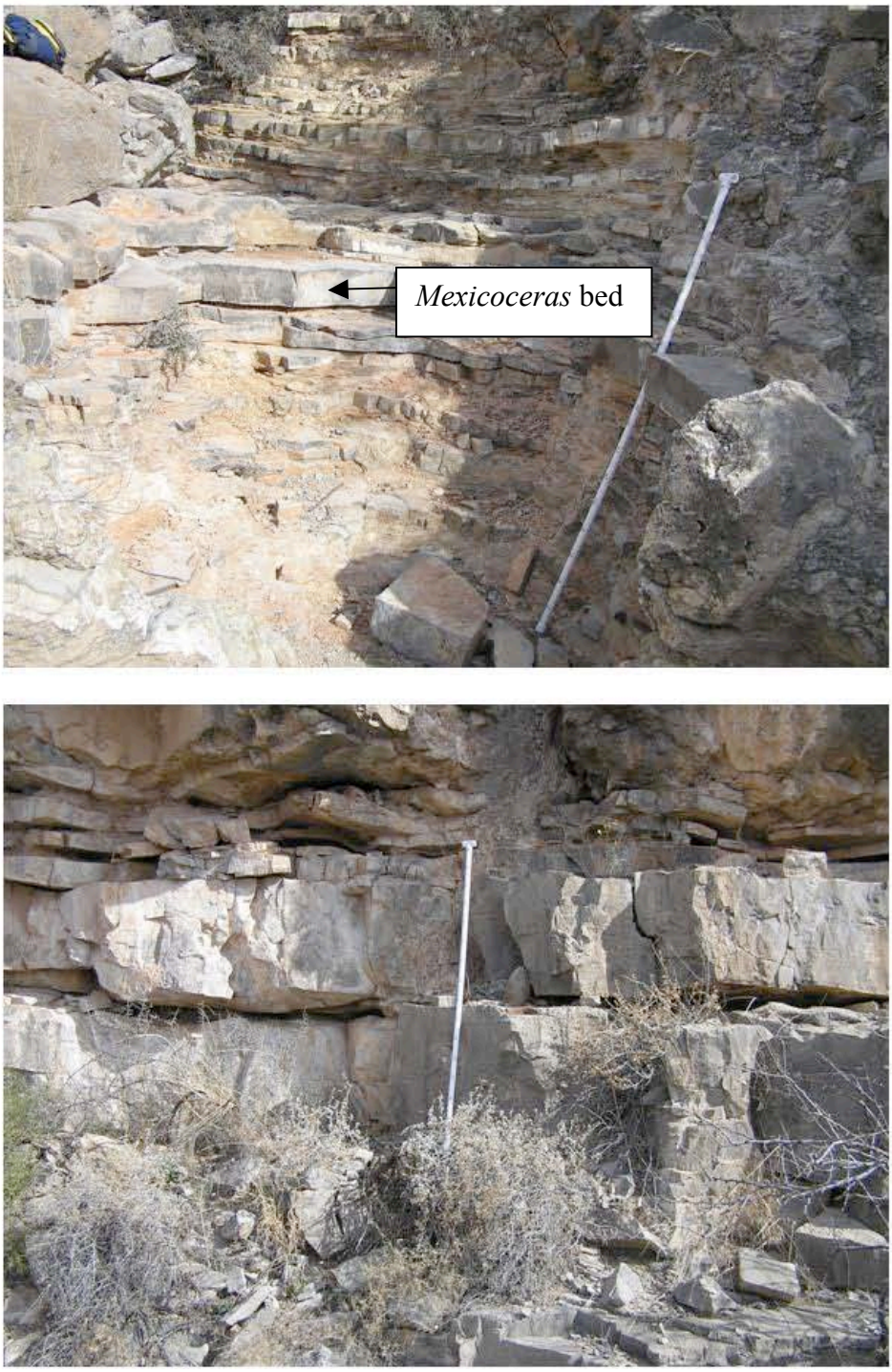

Figure 2.6: B section in the gully just south-southeast of FM 2185. Top: Lowermost beds of the B section containing the ammonoid *Mexicoceras*. Bottom: Lowermost debris flow intervals at the top of the gully and just below the road level.

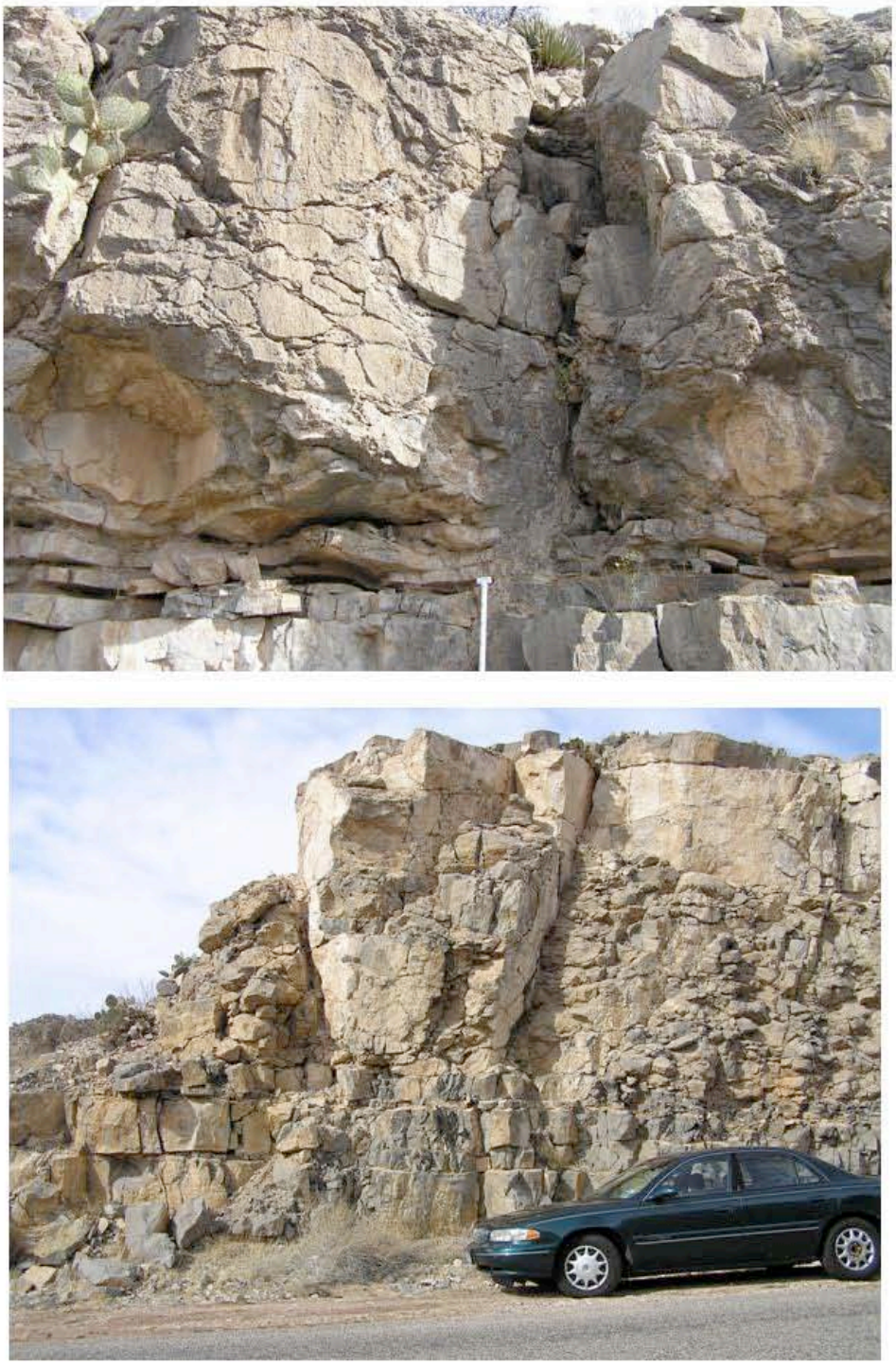

Figure 2.7: Top: B section in the gully south of FM 2185. Massive large (meters in diameter) clast, main interval of the B section debris flow. Bottom: B section in the north-northwest road cut of FM 2185. Massive, large clasts in the main interval of the B section debris flow.

Figure 2.8: B section in the north road cut of FM 2185. Top: Upper part of the B section debris flow with small debris flow that thins to the right of the photo. Bottom: Thin limestone beds with interbedded siltstone of the middle part of the B section, overlying the debris flow.

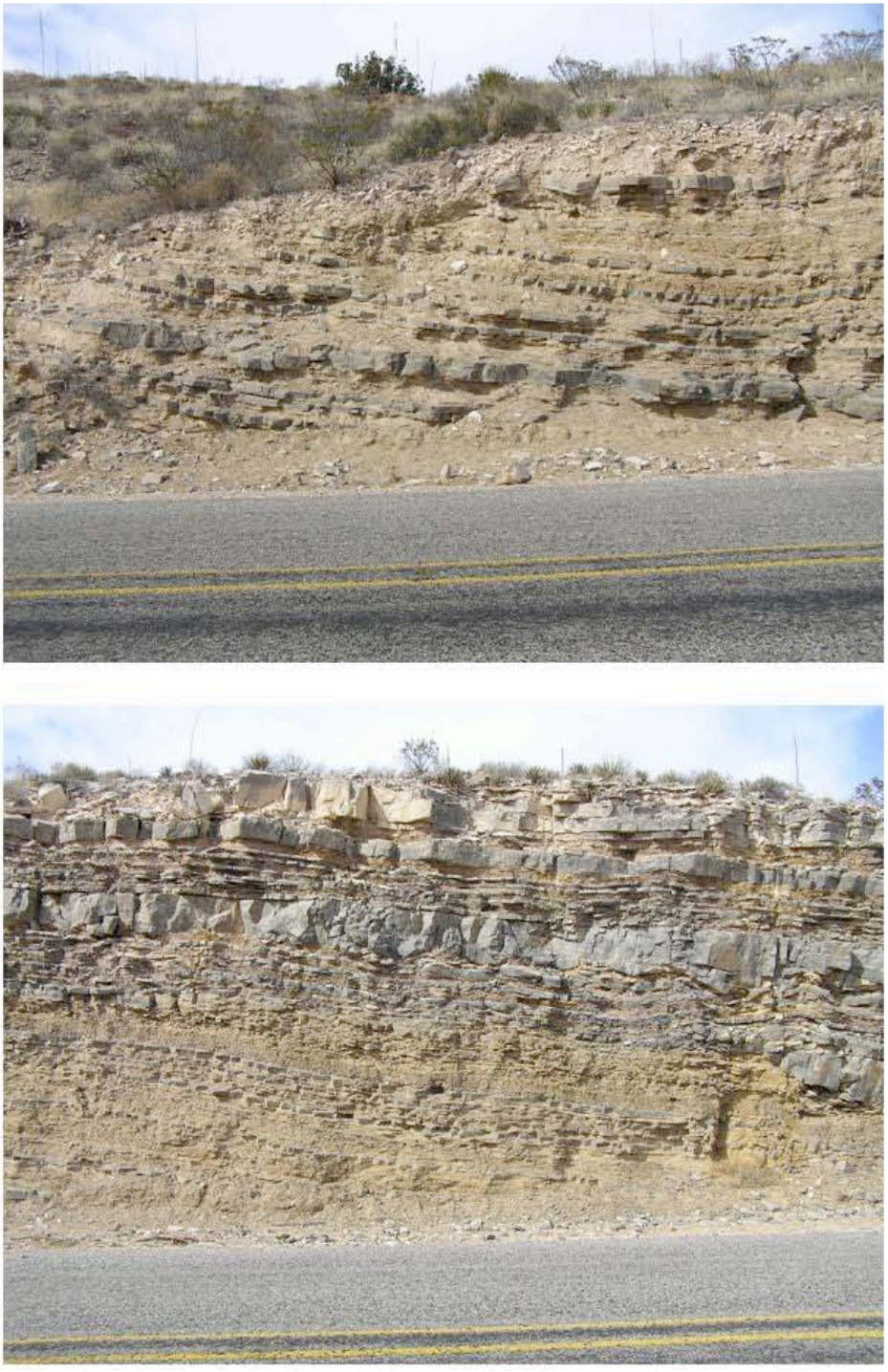

Figure 2.9: Upper B section in the north road cut of FM 2185. Top: Thin to medium limestone with interbedded siltstone of the middle part of the B section. Bottom: Medium to thick limestone beds with interbedded siltstone, overlying the strata in the top photo.

Figure 2.10: Siltstone that marks the top of the B section, with the overlying A debris flow at the base of the A section at the right of the photo.

2.2.3 A Section

Continuing from the top of the B section is the A section, measured at a total thickness of 9 meters starting at the base of a 2.5 meter thick carbonate debris flow (figures 2.11 and 2.12). This debris flow contains conodonts, abundant *Polydiexodina,* small foraminifers, and fragments of bryozoans and brachiopods. The next 6.5 meters of the A section is a tan to brown siltstone interbedded with thin to medium thick, gray limestone beds with radiolarians and small foraminifers. The contact with the overlying G section is within a 9 meter covered section.

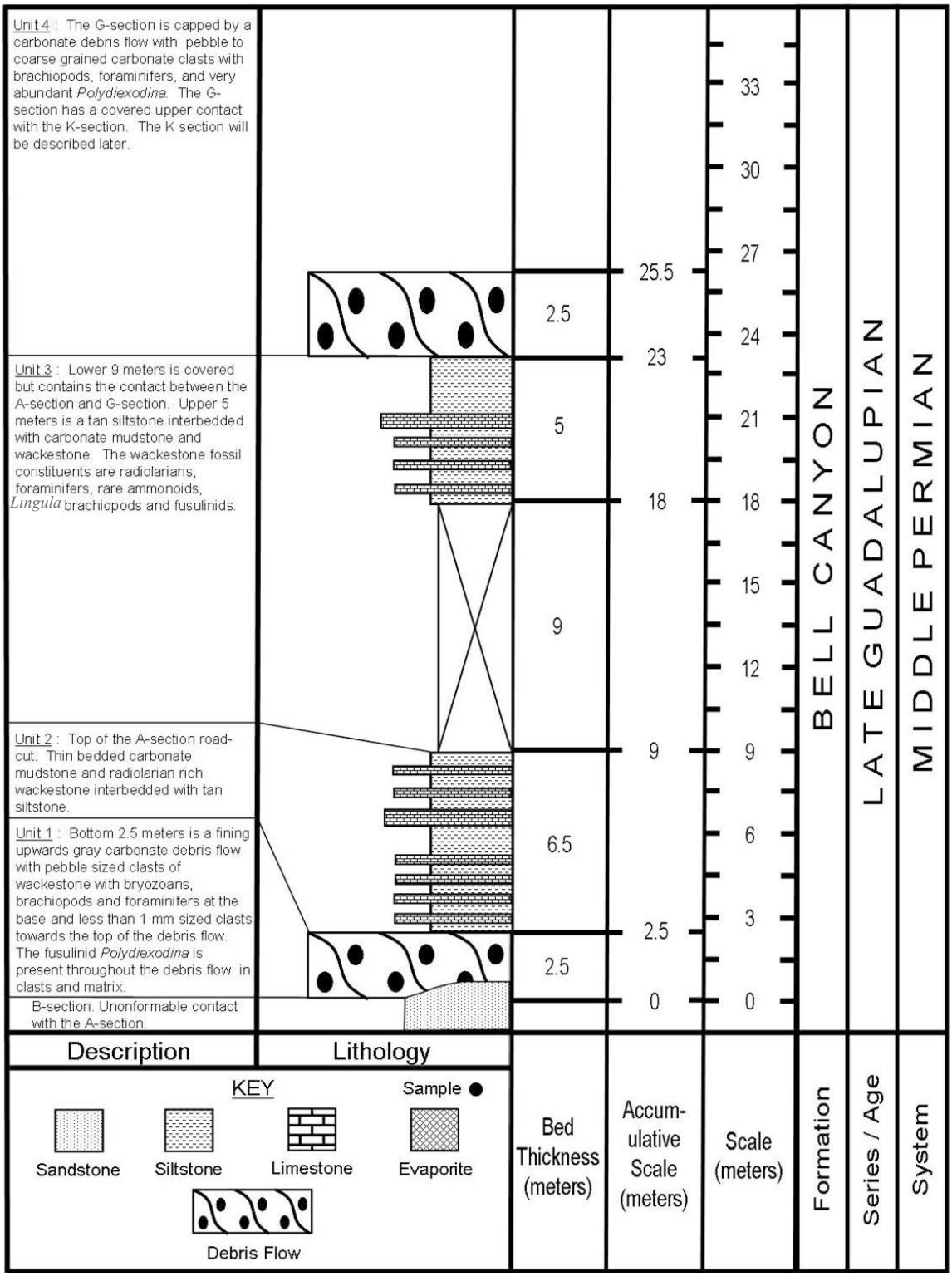

Figure 2.11: Composite stratigraphic column of the A section and G sections.

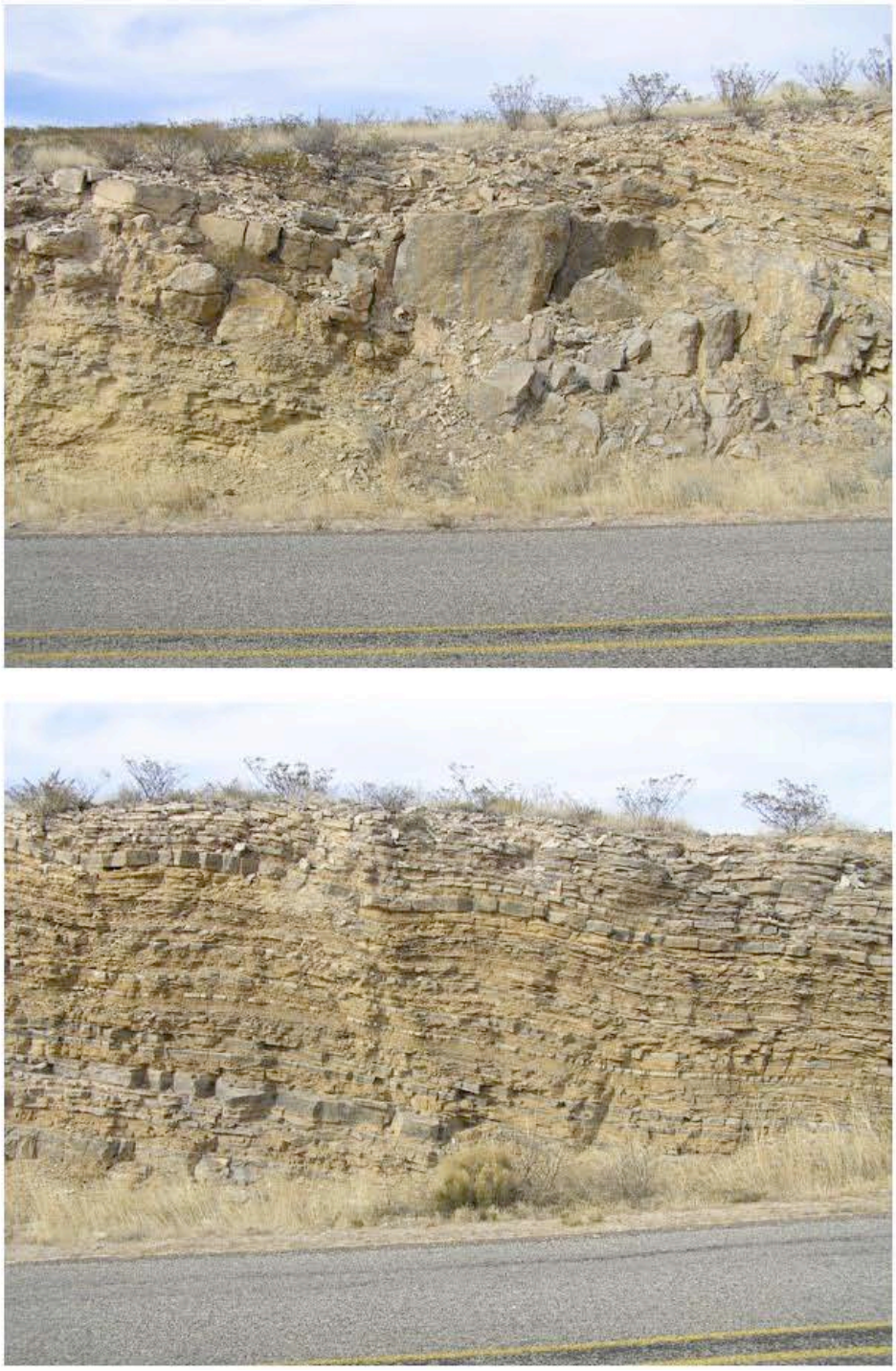

Figure 2.12: Road cut of the A section showing a carbonate debris flow (top photo) at the base overlain by thin interbedded limestone and siltstone (bottom photo).

2.2.4 G Section

Between the A and G sections there is roughly 9 meters of covered section, most likely a thin bedded siltstone package because of its erosive nature (figure 2.11). The measured G section starts at the top of the covered section and is 3 meters of thin to thick bedded gray limestone with radiolarians, brachiopods, ammonoids, small foraminifers, and fragments of the fusulinacean *Polydiexodina* interbedded with thin bedded tan siltstone. Beds of thin tan siltstone are measured for the next 2 meters in the section and then the G section is capped by a 2.5 meter thick carbonate debris flow (figure 2.13). The debris flow grades from cobble sized limestone clasts to a packstone with very abundant fusulinaceans of the genus *Polydiexodina.* A better exposure of strata equivalent to the G section can be seen in a deep valley just south of the FM 2185 G section road cut at the base of the measured K section, and also exposed along a fault in the far southeastern part of the map area (figures 2.4 and 2.14).

Figure 2.13: G section road cut with limestone interbedded with siltstone at the base with the lower part of the G debris flow capping the top of the road cut (top photo). The G debris flow extends to the next road cut to the east from the previous road cut (bottom photo).

Figure 2.14: Top: G section equivalent strata exposed in an adjacent valley to the southeast of the road cut on Fm 2185 (figure 2.4). The G section debris flow is the thick bed at the top of the thin bedded strata. Bottom: Debris flow equivalent to the G section debris flow as exposed to the right of the top photo.

2.2.5 K Section

The K section is approximately 52 meters thick and was measured starting from the top of the G section debris flow in a deep valley approximately 250 meters south of TX FM 2185 and continuing up the valley and then to the top of the hill to the northeast (figures 2.1, 2.15and 2.16). The first 25 meters of the K section comprises mostly thin to thick bedded tan to reddish-tan siltstone interbedded with fossiliferous thin to thick bedded gray limestone. The next 21.5 meters of the section is mostly siltstone with very few thin limestone beds. The upper six meters of the section forms the top of the hill and is comprised of thin to medium thick beds of limestone. The uppermost limestone in the K section is possibly equivalent in age to the McCombs Limestone Member of the Bell Canyon Formation but there is no direct fossil evidence to support this claim. The large body (about 20 meters) of siltstone present below the uppermost limestone beds in the K section may possibly be equivalent in age to the lower part of the well-known petroleum reservoir, the Ramsey Sand, which is stratigraphically below the Lamar Limestone Member and was deposited from a north-westward source into the Delaware basin from the Guadalupe Mountains during cyclic low-stands (Dutton et al., 2003).

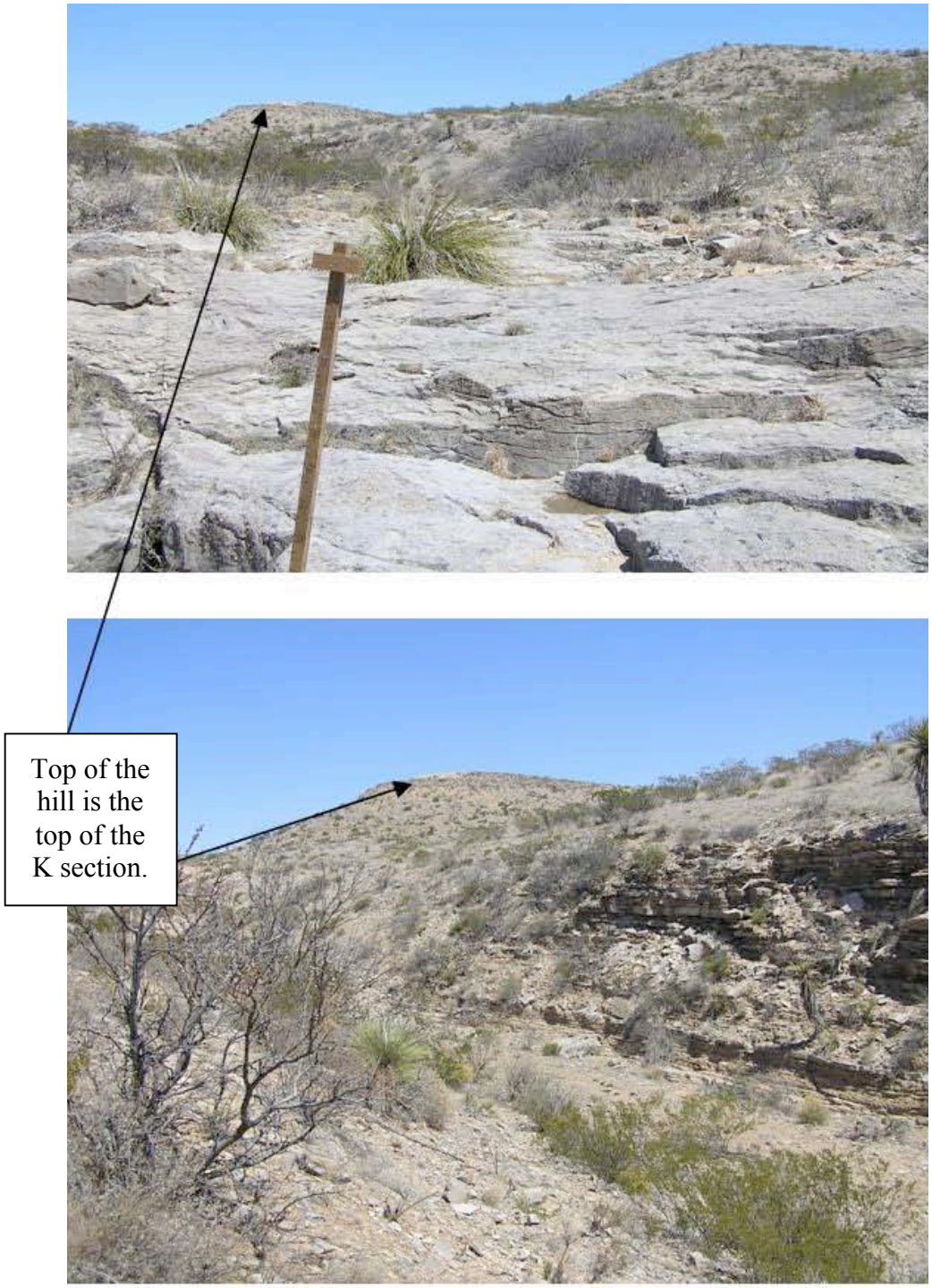

Figure 2.15: Top: The K section begins at the top of the G section debris flow. Bottom: The lower part is mostly limestone with few interbeds of siltstone. The middle part is mostly siltstone with a few limestone and few sandstone beds. The upper part to the top, the cap of the hill, is several meters of siltstone followed by several limestone beds with siltstone interbeds. The limestone unit on top of the hill is possibly the age equivalent of the McCombs Limestone Member. (figure 2.4)

The top of the K section marks the end of a stratigraphic sequence of Bell Canyon age strata that can be considered a continuous composite section. Continuing to the northeast past the top of the K section, the covered strata is sparsely covered with float from a bed of what appears to be a brachiopod rich fine to medium grained wackestone or another debris flow. This brachiopod rich limestone bed can be found in the low lying hills across from the K section over a wide flat covered section that may possibly be the erosional remains of upper Ramsey Sand equivalent strata. The brachiopod rich limestone in the hills to the northeast may be equivalent in age to a thick brachiopod rich limestone that is present in the AV section (this section will be discussed later). The incomplete upper part of the K section causes a problem in the attempt to tie the B, A, G, and K sections to the clearly younger in age strata of the EF section. Several additional sections recently found in the southeastern part of the map area (SJ, SK, and AV, discussed in the next chapter section) may aid in the solution of this correlation problem when conodont and foraminiferal data are finally integrated and interpreted (Nestell and Wardlaw, personal communication, 2009)

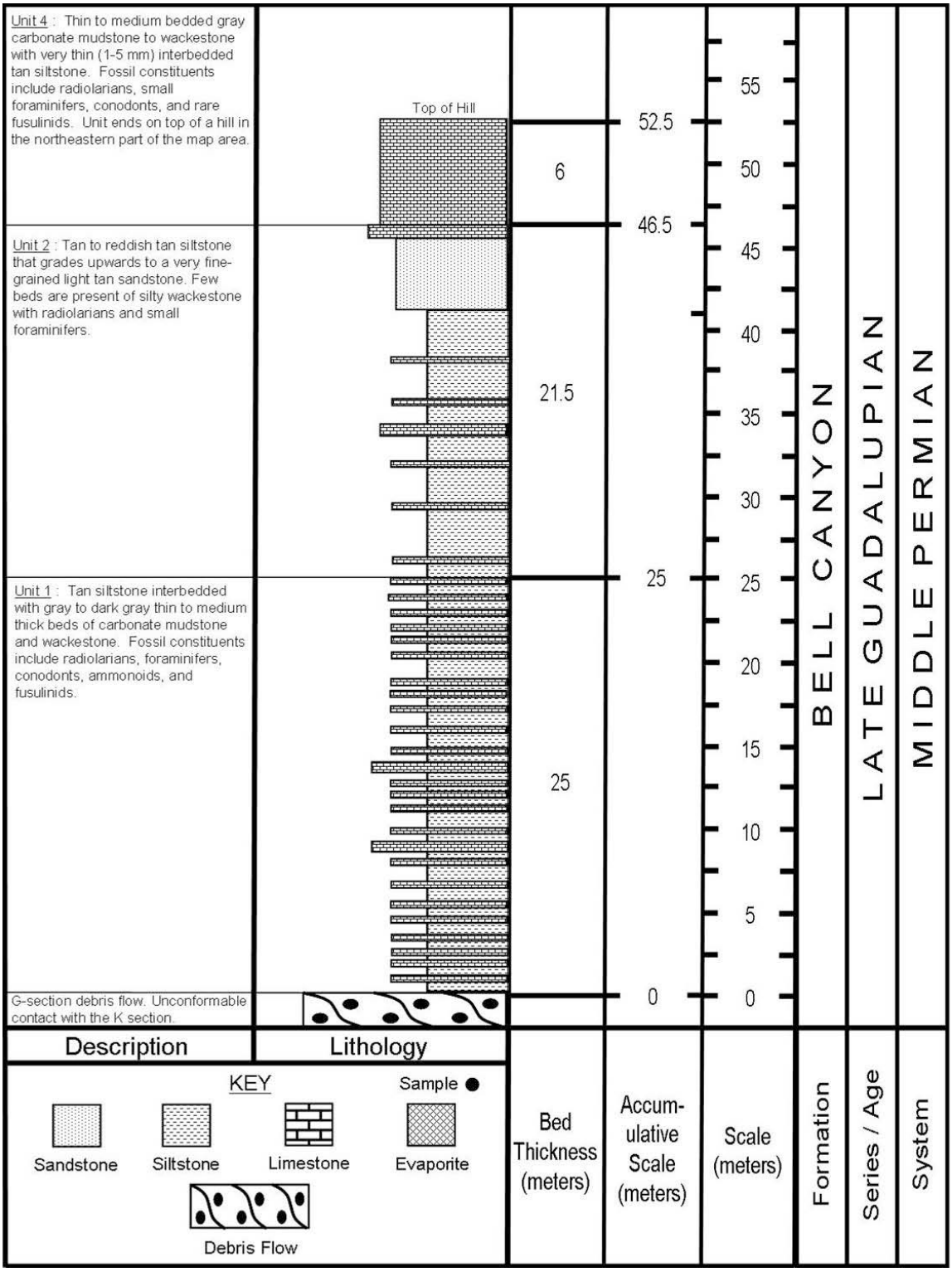

Figure 2.16: K section stratigraphic column.

2.2.6 EF, M, SJ, SW, and AV Sections

The youngest strata in the Bell Canyon Formation deposited in the map area can be map laterally along southeastward trends from the M and EF section road cuts through and beyond the map area. The EF, M, SJ, SW, and AV sections have been measured and correlated. Each of these measured sections except for the M section, have an exposure of a megabreccia present. Exposed strata below the megabreccia in the EF and SJ sections is not present, but the EF and SJ sections do expose strata above and equivalent in age to the EF section megabreccia. Traverses to the southeastern part of the map area reveled exposed strata below the megabreccia in the SW and AV sections. The AV section is the most complete of these sections and with further study, its lowermost beds may be found to correlate to the uppermost beds of the K section.

The most diagnostic feature of these sections is the 0.5-1.0 meter thick dark, petroliferous, laminated limestone with pink calcite and dolomitic nodules at the boundary (contact) of the Bell Canyon and Castile Formations. This mappable limestone marks a transition between the Guadalupian and Lopingian series in this part of the Delaware basin. Beds of strata exposed in this interval have characteristics of both the formations above and below it and it is still unclear as to which formation it belongs. Both King (1948) and McNutt (1948) make reference to a laminated limestone at the base of the Castile Formation conformably in contact with the Bell Canyon Formation. In this thesis, this transitional laminated limestone is included in the Castile Formation to retain consistency with King and McNutt; this laminated bed has been referred to as the Basal Limestone Member of the Castile Formation (Anderson et al., 1972). The beds in this

interval have yielded the conodont subspecies *Clarkina postbitteri hongshuiensis* which defines those beds as being just below the lower Lopingian boundary, thus making the lowermost beds of the Castile Formation not Lopingian, but very uppermost Guadalupian in age. A problem then arises in the assignment of the Castile Formation to the Lopingian Series and an Ochoan age based on the lithological change between the Bell Canyon and Castile Formations. The Castile Formation is herein considered to be primarily of Ochoan age. Some past workers have considered the Ochoan and Lopingian to be the same because of the historic designation of the Guadalupian/Lopingian boundary at a global regression (Gradstein et al., 2004). The discovery of *Clarkina postbitteri hongshuiensis* in the Basal Limestone Member of the Castile Formation allows for the term Ochoan to be applied to the strata above the Bell Canyon and Castile contact based solely on lithological changes. The exact boundary between the Guadalupian and Lopingian is not known in the West Texas area because the presence of *Clarkina postbitteri postbitteri* has not been reported as of yet. Presently, the Guadalupian/Lopingian boundary can only be considered to be somewhere with-in the lower part of the Castile Formation. Future study of the basal strata in the Castile Formation may provide additional data to define a specific Guadalupian/Lopingian boundary.

2.2.6.1 M and EF Sections

The M section is the thinnest measured section (Figure 2.17, from Nestell et al. 2006a) and only has exposures of the uppermost beds of the Bell Canyon Formation in the map area. Traverses to the south have only discovered exposures of the uppermost

part of strata equivalent to the EF debris flow. The M section was measured in the FM 2185 road cut and is an abbreviated and incomplete version of the uppermost part of the measured EF section road cut. The correlation of the M section to part of the EF section is verified by lithofacies packages and the presence of the fusulinacean *Paraboultonia splendens* in several intervals (figures 2.18, 2.19, and 2.20). The EF section is the most studied section because of its more continuous exposure of strata between the debris flow and the Castile Formation and its ease of access. The conodont succession starts with *Jinogondolella postserrata* and ends with the first occurrence of *Clarkina postbitteri hongshuiensis* found in the West Texas area (Lambert et al. 2002).

The EF section is approximately 23 meters thick (figure 2.21) with the first 15 meters being a carbonate debris flow. Figure 2.22 is a detailed stratigraphic column of the upper part of the EF section, and figure 2.23 illustrates the individual lithological units in the road cut. Unit A is the debris flow with a megabreccia at the base (unit A1, figure 2.21) with large clasts of strata. The debris flow then fines upwards with several different lithologies, which will be discussed in a later section (units A2-A6, figure 2.21). Unit B is 1.5 meters thick and is a tan to brown siltstone interbedded with thin to medium bedded carbonate mudstone and a few wackestone beds that pinch and swell, containing radiolarians, foraminifers and the conodont *Jinogondolella altudaensis* (Lambert et al., 2002) (figure 2.24). Unit C is 4 meters thick and is a thinly bedded carbonate mudstone with radiolarians, foraminifers, and conodonts. Unit D is 1.5 meters thick and is a tannish-red siltstone interbedded with beds of thin mudstone and wackestone containing the fusulinacean *Paraboultonia splendens* (Skinner and Wilde) at its base (figure 2.25).

The significance of the presence of *P. splendens* is that its first appearance datum (FAD) marks the beginning of the Reef Trail Member of the Bell Canyon Formation at its type locality (Wilde et al., 1999). It should be noted here that clasts containing *P. splendens* are present in unit A (figure 2.48 Top). Unit E1-E2 comprises the uppermost two beds of the Bell Canyon Formation (figure 2.26). This unit swells and pinches throughout the map area and varies in thickness. Unit E1-E2 contains the fusulinacean *P. splendens,* and the conodonts *Jinogondolella crofti* and *Clarkina postbitteri hongshuiensis* (figures 2.24 and 2.25). Unit E3-E5 is the basal dolomitic laminated limestone of the Castile Formation (figure 2.26). This unit also contains scarce *C. postbitteri hongshuiensis,* which dates this limestone as latest Guadalupian, and which signifies that the original placement of the Guadalupian/Lopingian boundary needs to be revised in the West Texas region.

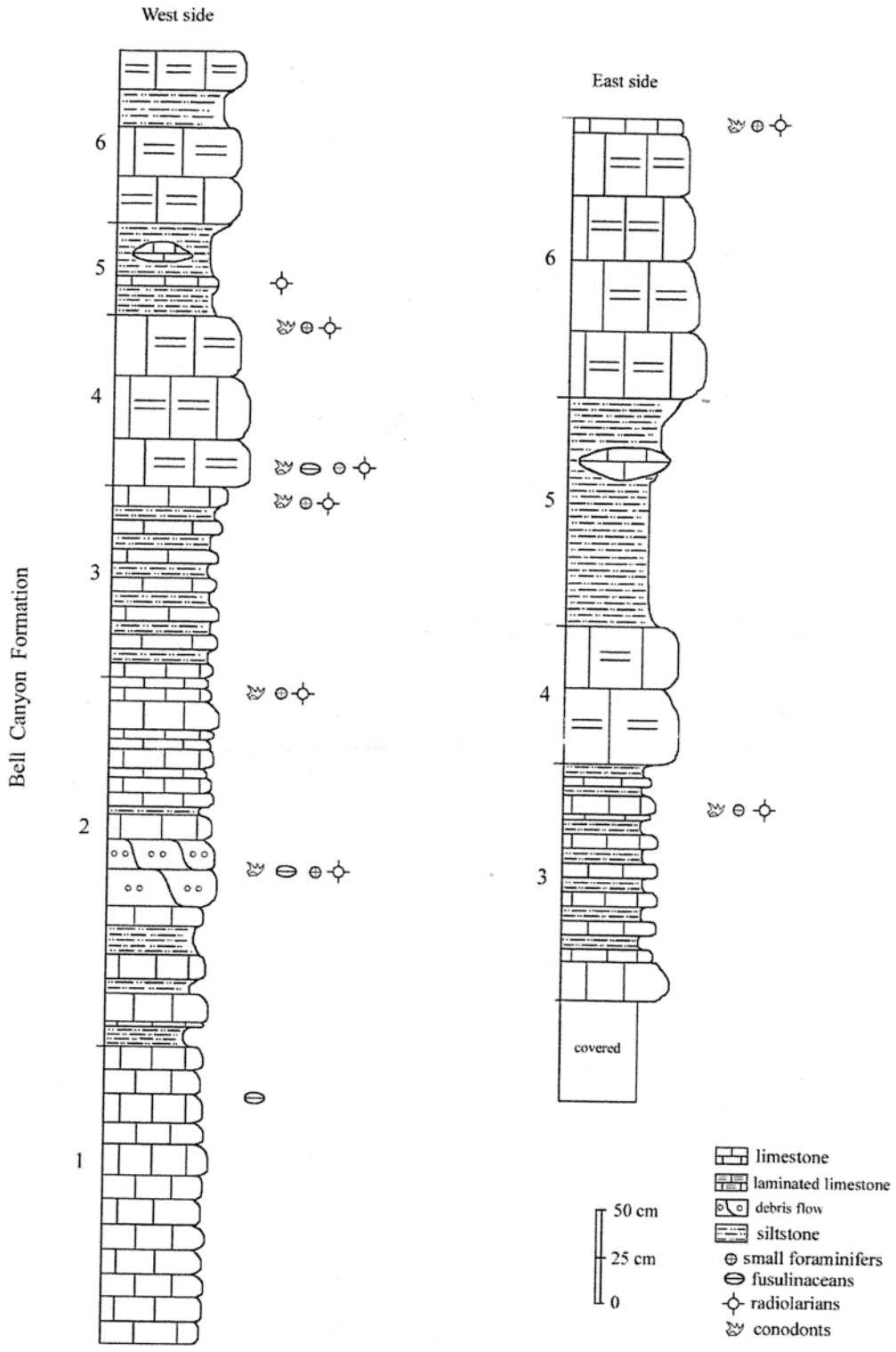

Figure 2.17: M section stratigraphic column (from Nestell et al. 2006a)

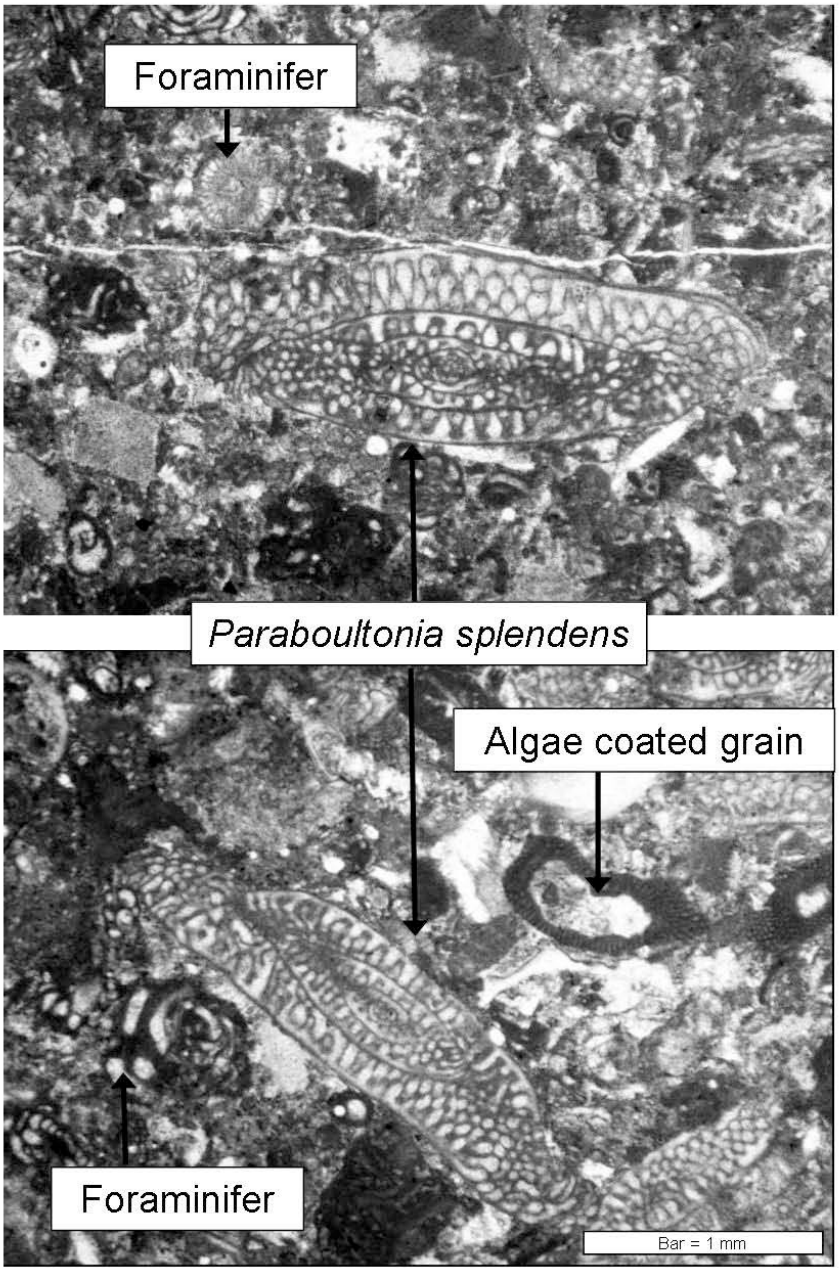

Figure 2.18: Top and bottom micrographs: Lower M section samples (unit 2) of wackestone containing algae. Foraminifers, fusulinacean: *Paraboultonia splendens*, and indistinguishable material.

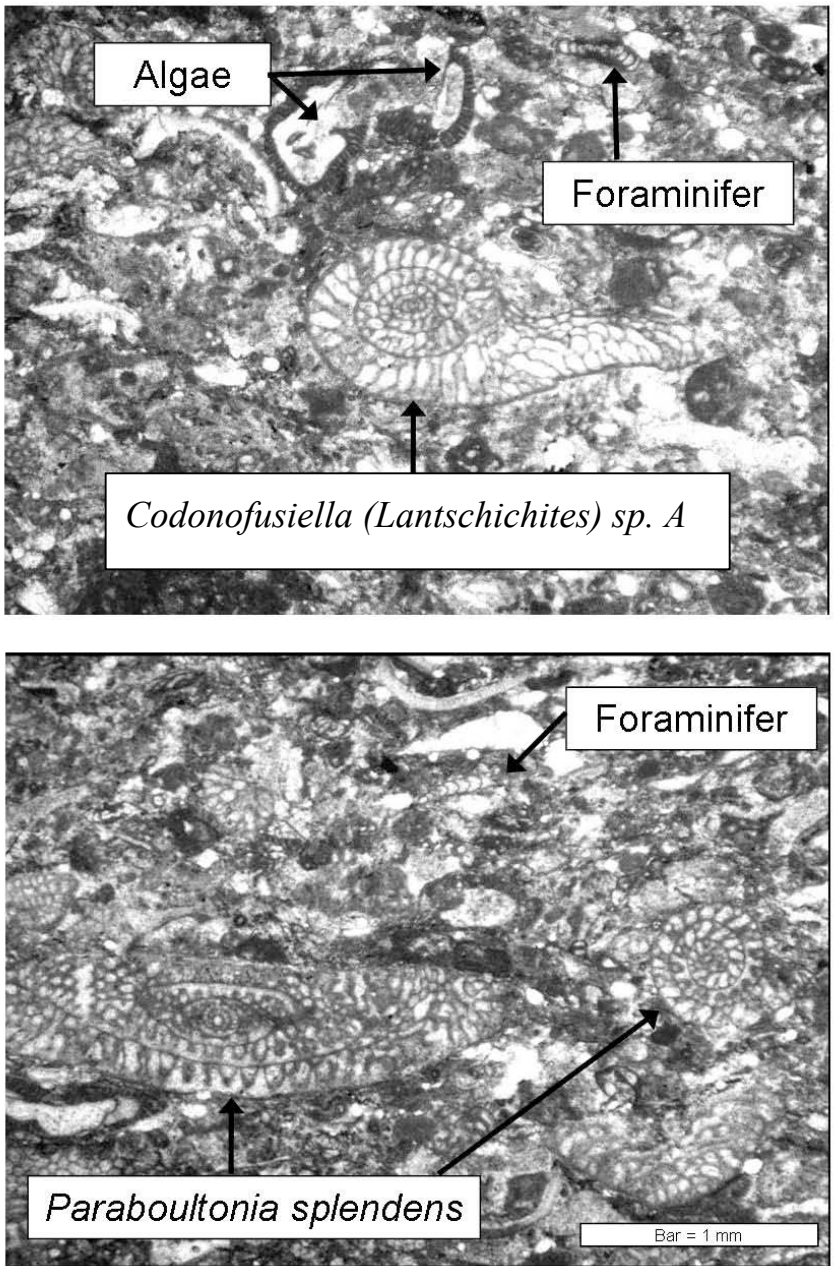

Figure 2.19: Top and bottom micrographs: Upper M section samples (base of unit 4) of wackestone containing algae. Foraminifers, fusulinaceans: *Paraboultonia splendens* and *Codonofusiella (Lantschichites) sp. A,* and indistinguishable material.

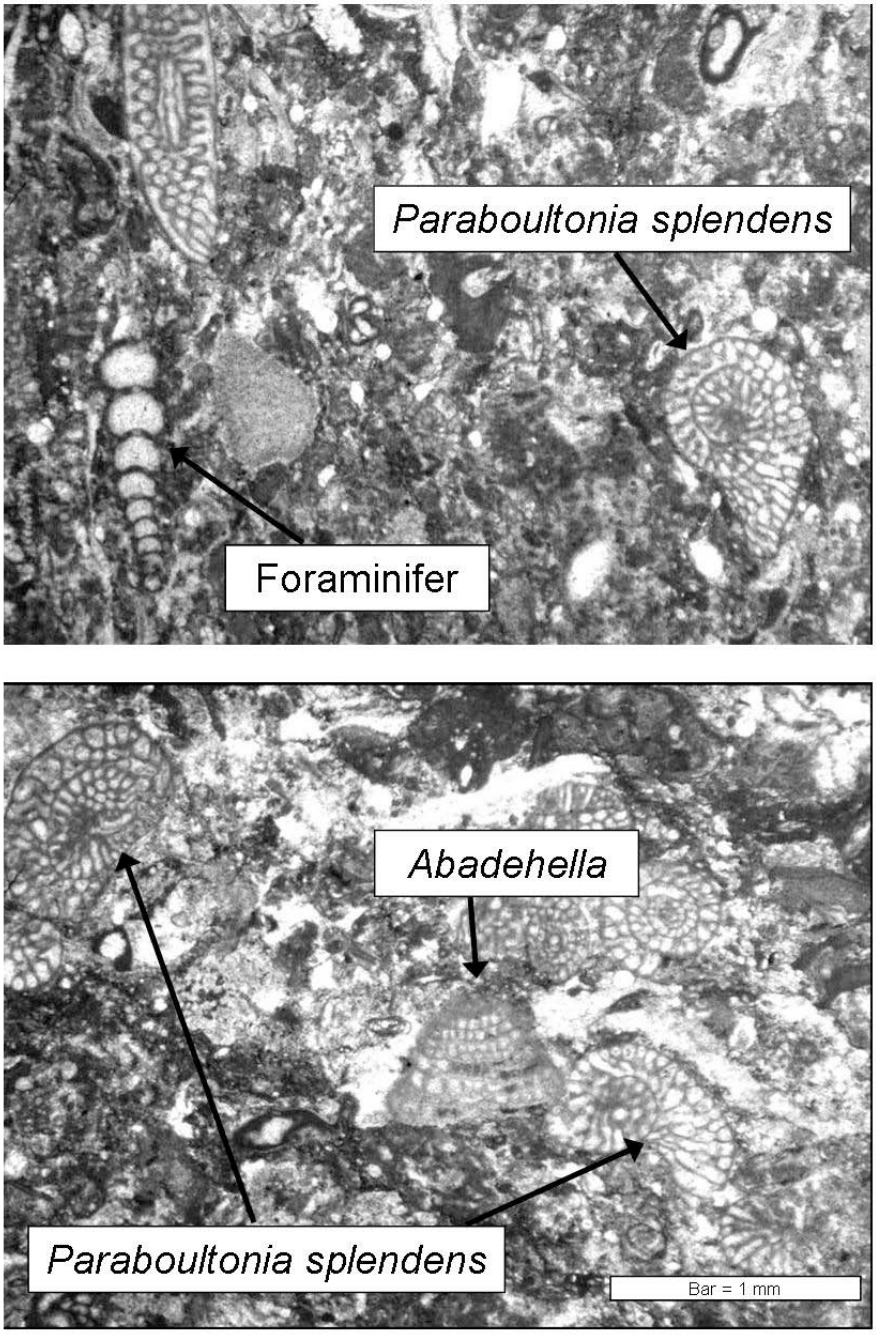

Figure 2.20: Top and bottom micrographs: Upper M section samples (base of unit 4) of wackestone containing algae, foraminifers, the fusulinacean: *Paraboultonia splendens*, and indistinguishable material.

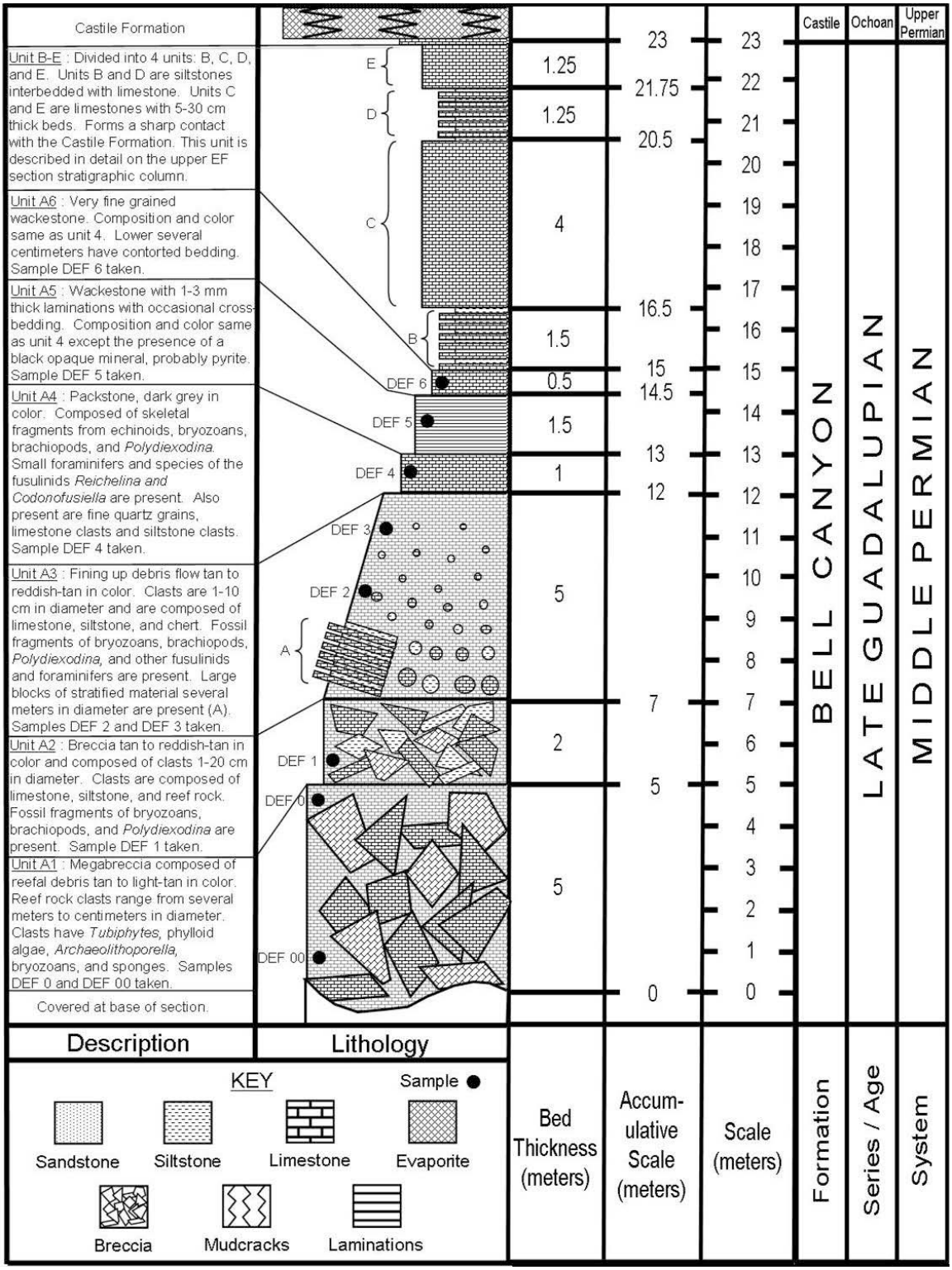

Figure 2.21: Stratigraphic column of the south side EF road cut. DEF samples will be discussed in detail in the debris flow section of this thesis.

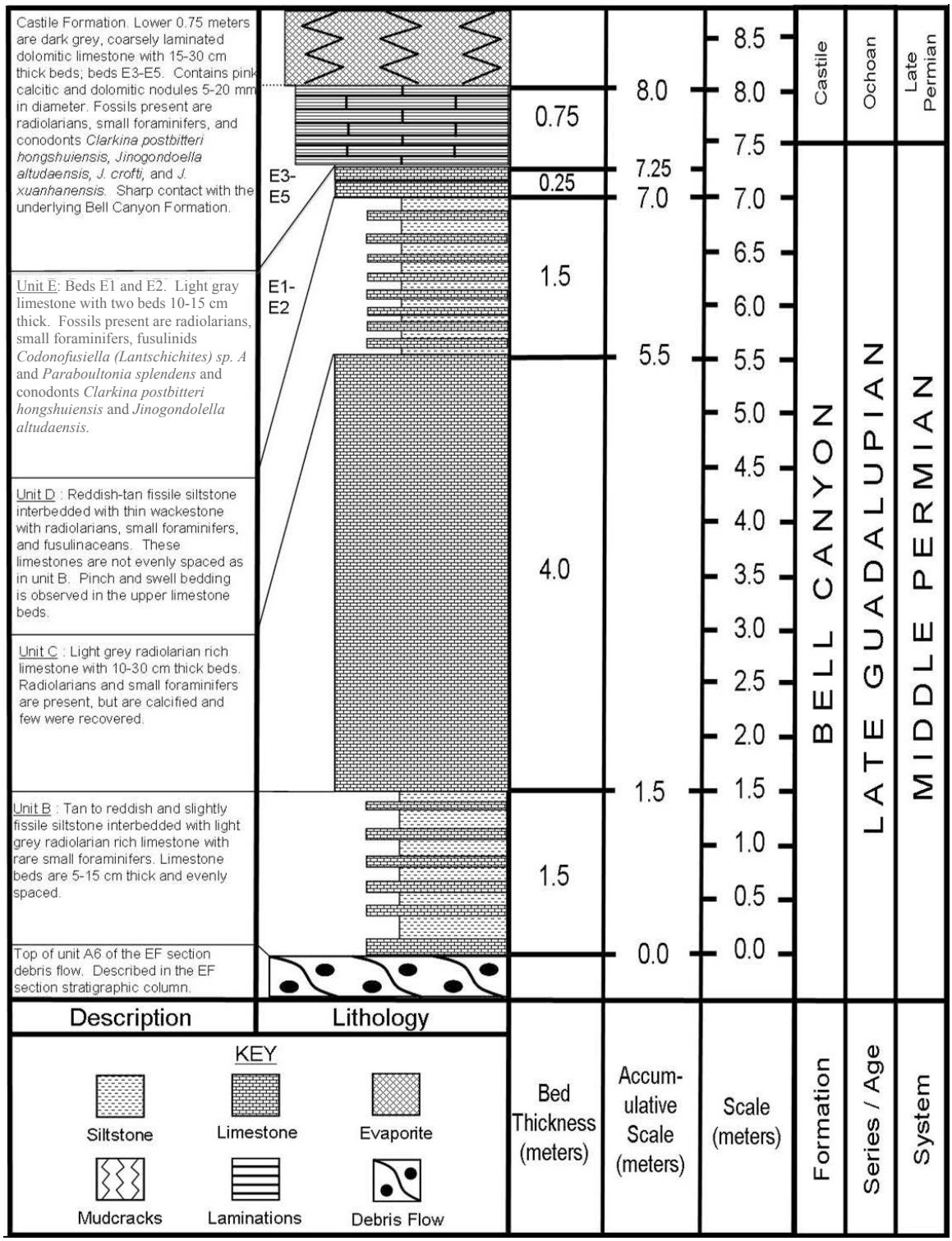

Figure 2.22: Detailed stratigraphic column of the upper part of the EF section (units B-E) north side road cut.

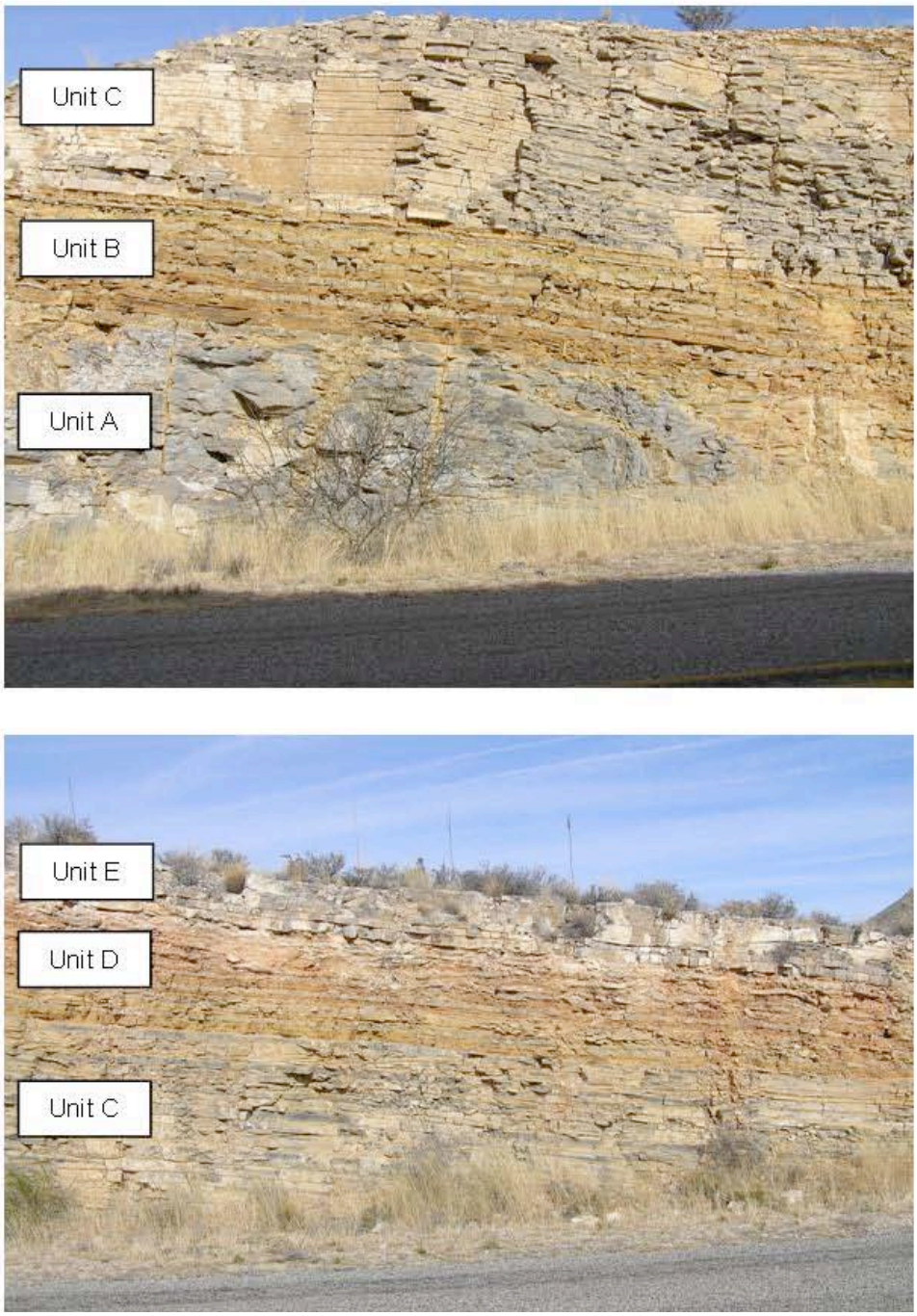

Figure 2.23: The EF section road cut along FM 2185. Unit A is the upper debris flow. Unit B is siltstone interbedded with thin beds of limestone. Unit C is thin to medium bedded limestone. Unit D is similar to unit 2 but contains the fusulinacean *Paraboultonia splendens*. Unit E comprises the uppermost beds of the Bell Canyon Formation in the map area, and it contains the fusulinaceans *Paraboultonia splendens* and *Codonofusiella (Lantschichites) sp. A*, and the conodont *Clarkina postbitteri hongshuiensis*. The uppermost three beds of Unit E contain the laminated dolomitic limestone beds of the Basal Limestone Member of the Castile Formation (Nestell et al., 2006a).

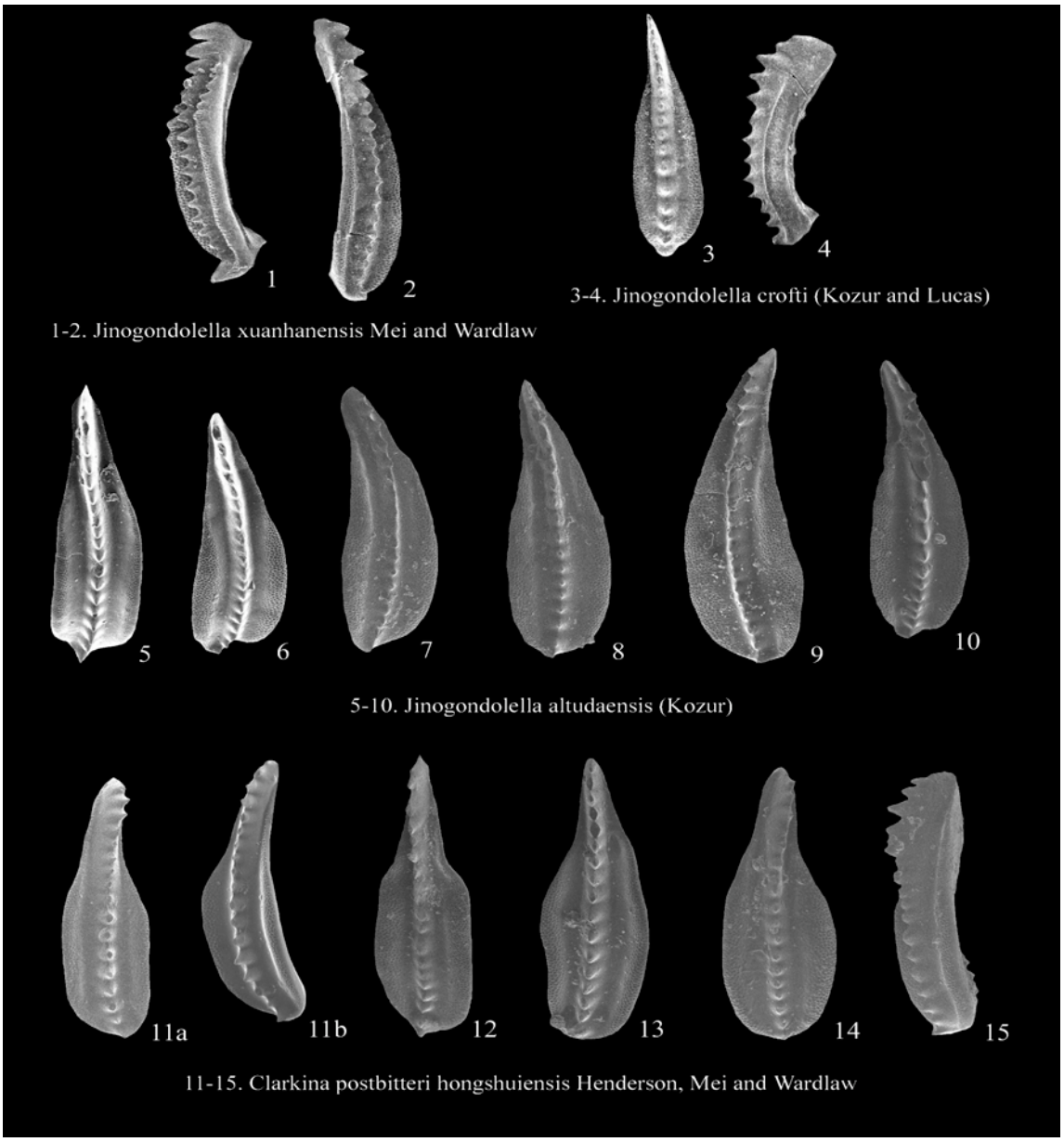

Figure 2.24: Conodont P-elements from the upper EF section showing part of the *Jinogondolella* assemblage and also the youngest conodont found in the map area: *Clarkina postbitteri hongshuiensis* (Nestell et al., 2006a). These conodonts are found in the upper most beds (E1-E2 and E3-E5 of the EF section road cut (figure 2.22).

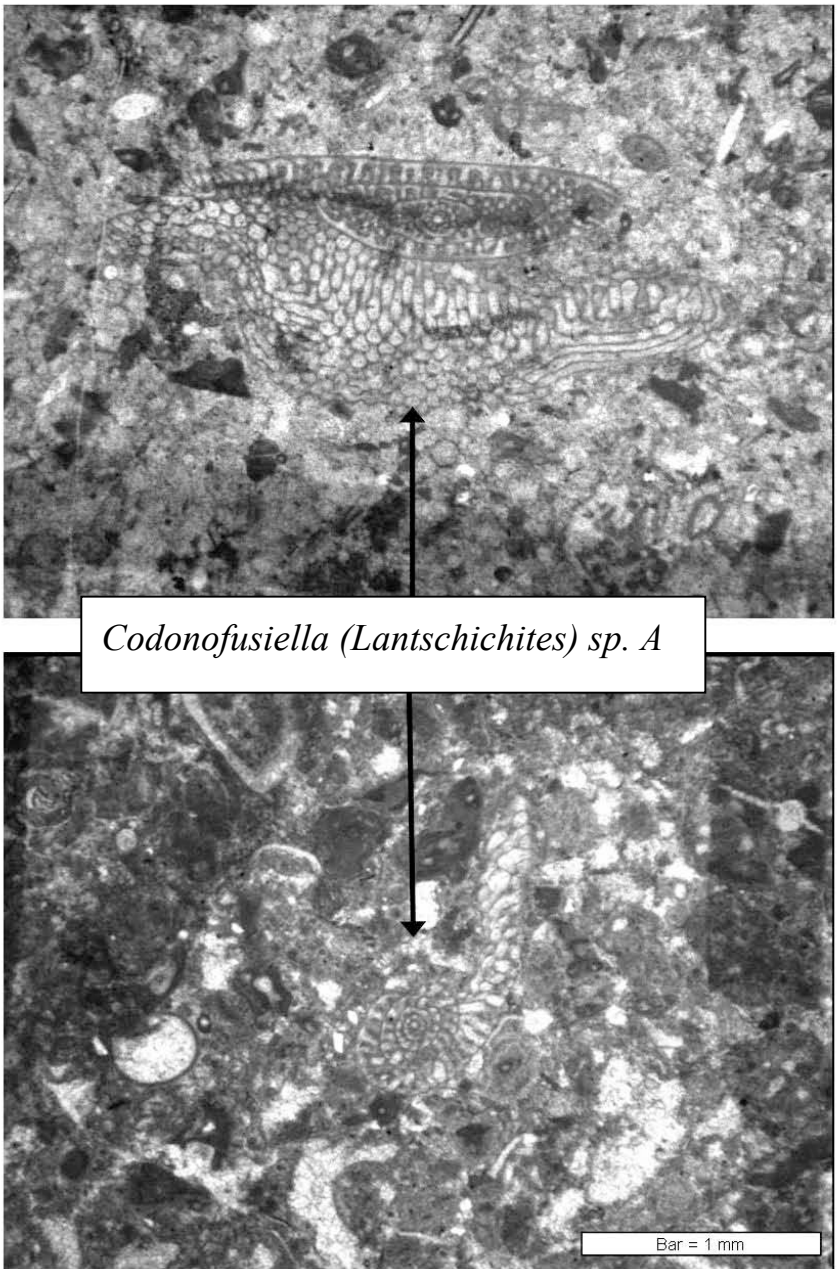

Figure 2.25: Top and bottom micrographs: Upper EF section sample from E1 of wackestone containing algae, foraminifers. Fusulinacean: *Codonofusiella (Lantschichites) sp. A,* and indistinguishable material.

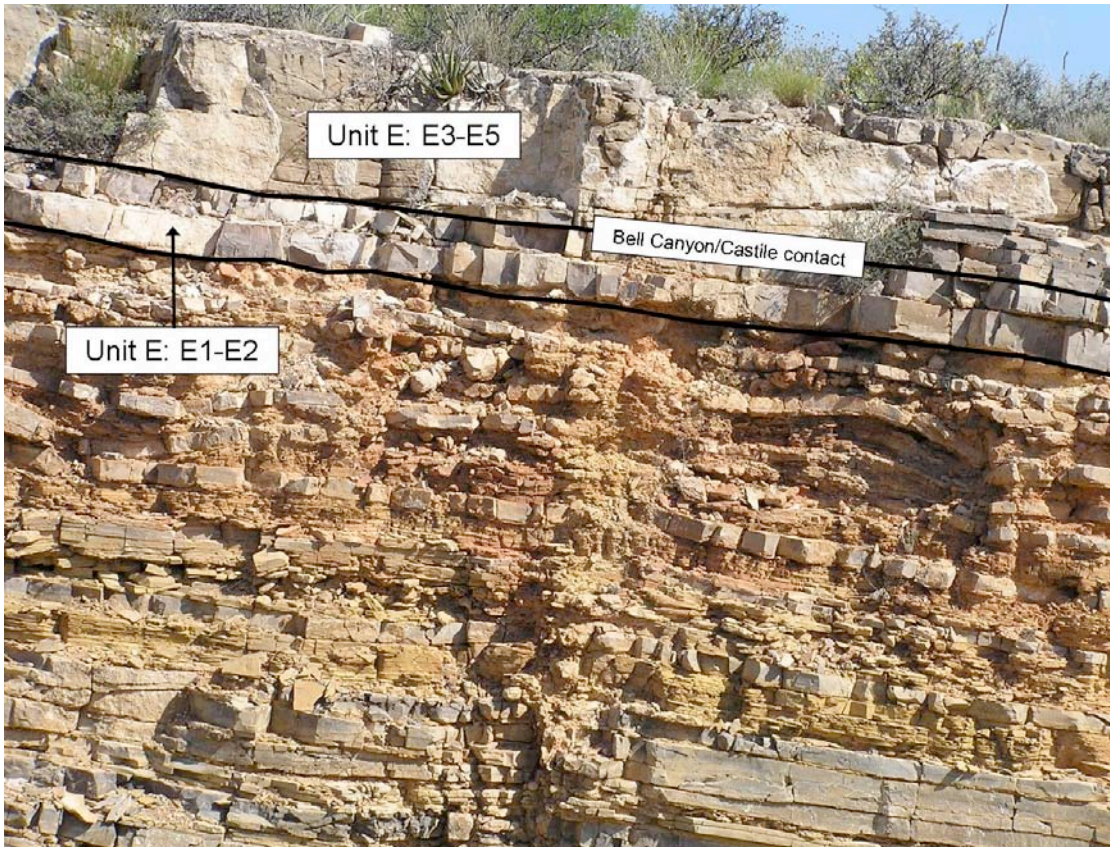

Figure 2.26: Top: The uppermost unit of the EF section: Unit E, shown divided into two groups of bedding: E1-E2 and E3-E5. The dark solid bold lines divide the groups, and the upper line shows the contact between the Bell Canyon Formation (Reef Trail equivalent aged strata) and the Castile Formation (Basal Limestone Member).

2.2.6.2 SJ, SW and AV Sections

Traverses south from the EF section road cut were made to map the EF debris flow and to attempt to discover exposed strata below the debris flow in hopes to form a complete section from the base of the B section up to the Castile Formation (i.e., a nearly complete Bell Canyon Formation). Presently a complete section has not been found. Additional work may discover that the unmapped strata above and west of the K section in the northeastern part of the map area help to clarify this problem.

The SJ section is the first section measured to the southeast from the EF section traverse (figures 2.1 and 2.27). The dark gray cherty limestone sequence present in the SJ section was first measured as an in place section of strata (figure 2.28). After studying the fossil content, the dark gray limestone was discovered to contain the fusulinaceans *Polydiexodina* and *Codonofusiella,* which would date the strata as possibly the equivalent in age to the McCombs Limestone Member. The overlying strata is lithologically correlative to the EF section and thus the dark gray cherty limestone interval was tentatively concluded to be a large block of strata with-in the debris flow similar to the blocks of strata exposed in the base of the EF section road cut in FM 2185. The weathered remnants of another large block of strata in the debris flow can be viewed just a few decameters above the large block of dark gray cherty limestone mentioned above (figure 2.29). The measured section is 25 meters thick and is cut by a fault at the base juxtaposing the section against strata of the Rustler Formation and the section is measured up to the Bell Canyon and Castile Formations contact.

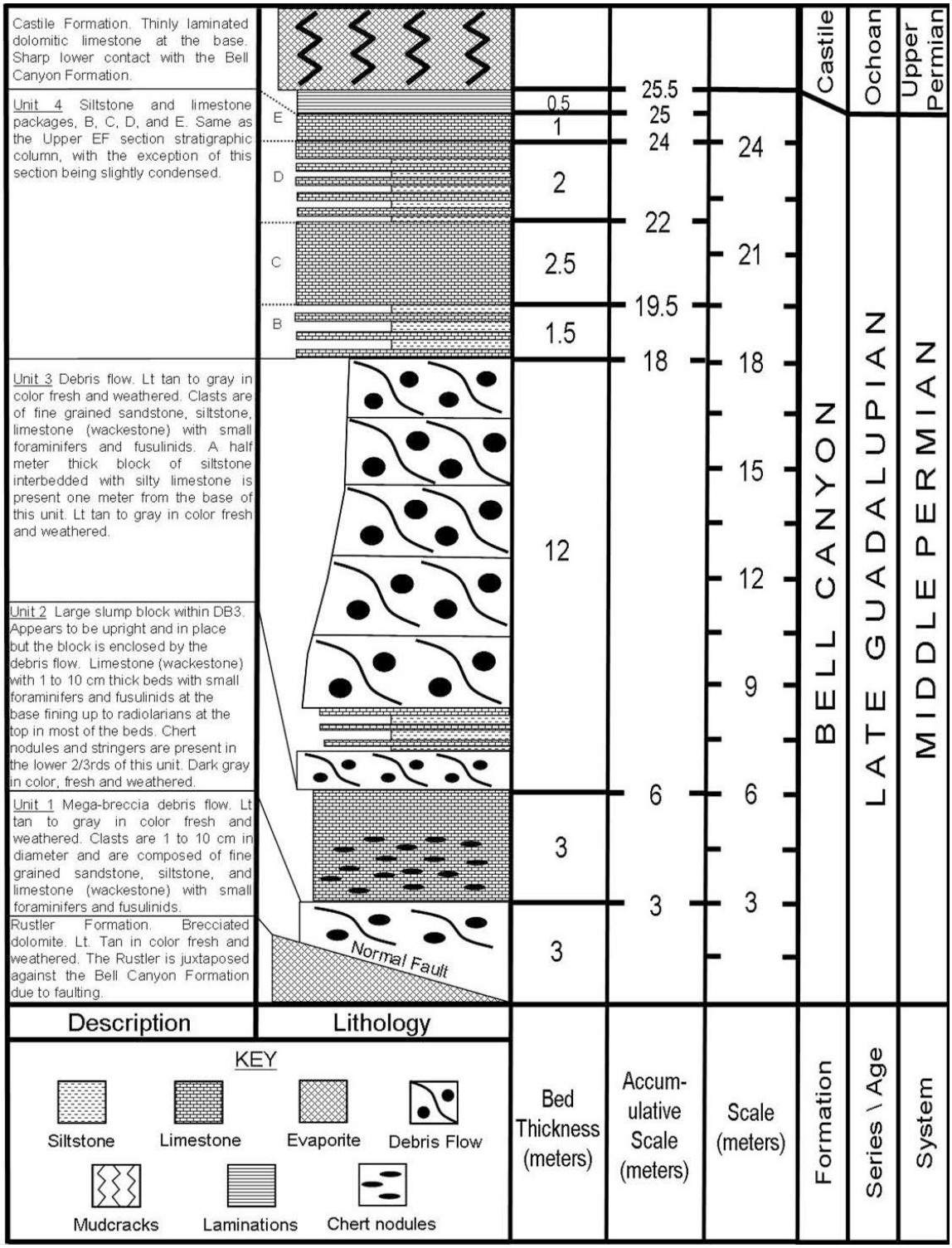

Figure 2.27: SJ section stratigraphic column.

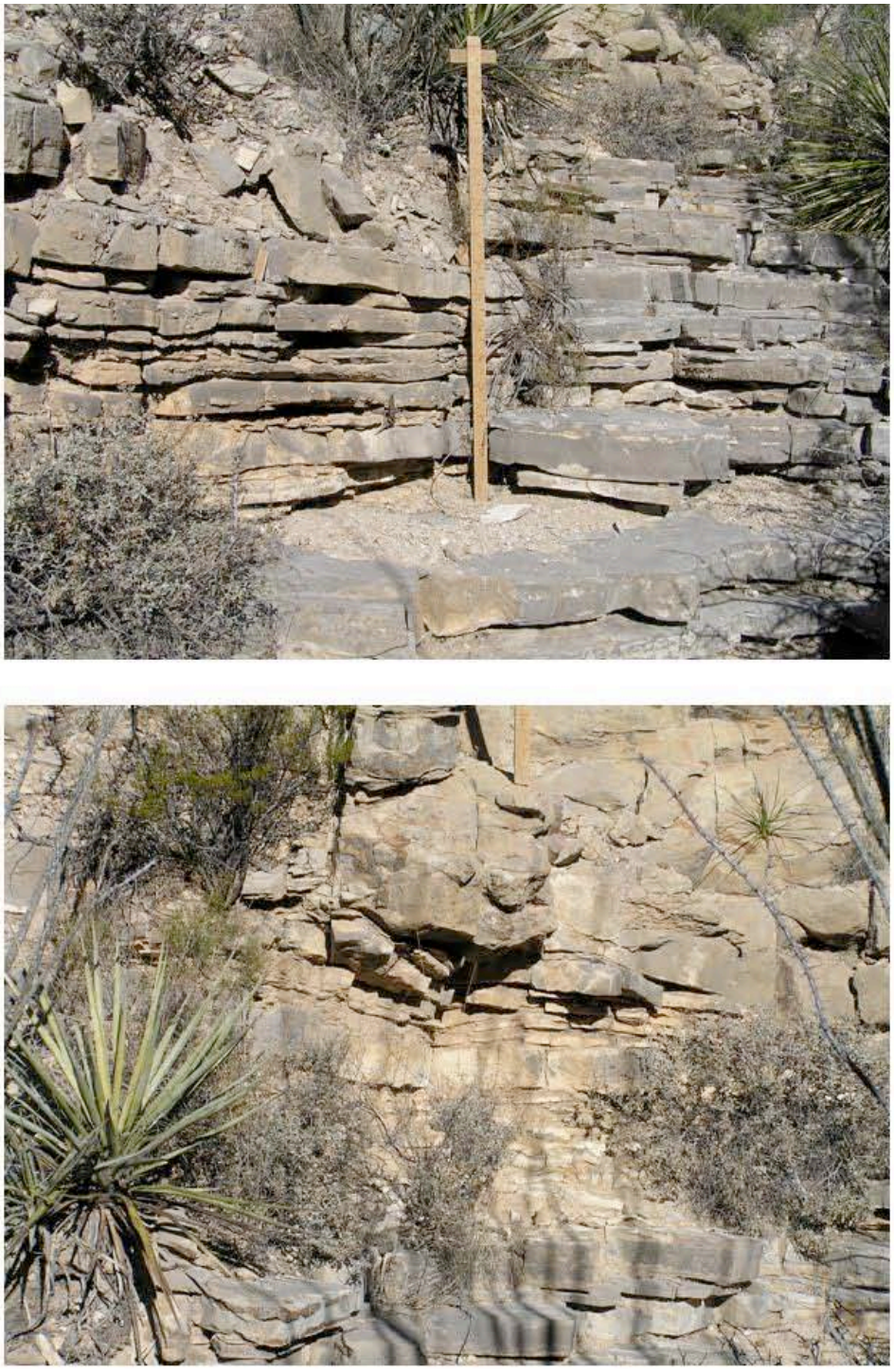

Figure 2.28: Top: The lower part of the SJ section. The Jacob staff is 1.5 meters. The dark, cherty limestone shown appears to be is a very large block of stratified material in the debris flow. Bottom: Top of the block mentioned above, in contact with a debris flow.

Figure 2.29: The lower part of the SJ section. The Jacob staff is 1.5 meters. The debris flow above the previously mentioned block of dark cherty limestone, with remnants of a smaller block in the flow.

The SW section is the second section measured along the traverse to the southeast approximately 1.5 miles southeast from the EF section road cut (figure 2.1). This section has 22 meters of exposed strata below a major debris flow (figure 2.30). The total thickness of the measured section (figure 2.31) is 49 meters and it is cut by the same fault as in the SJ section at the base juxtaposing the section against strata of the Rustler Formation. The lower 22 meters is very fine grained sandstone fining up to a siltstone with a few thin limestone beds containing radiolarians, conodonts, and foraminifers. The lower part of the section is topped by a massive debris flow that is capped by a stratigraphic sequence very similar to that of the upper part of the SJ and the EF sections. A thick section of Castile and Rustler strata tops the SK section.

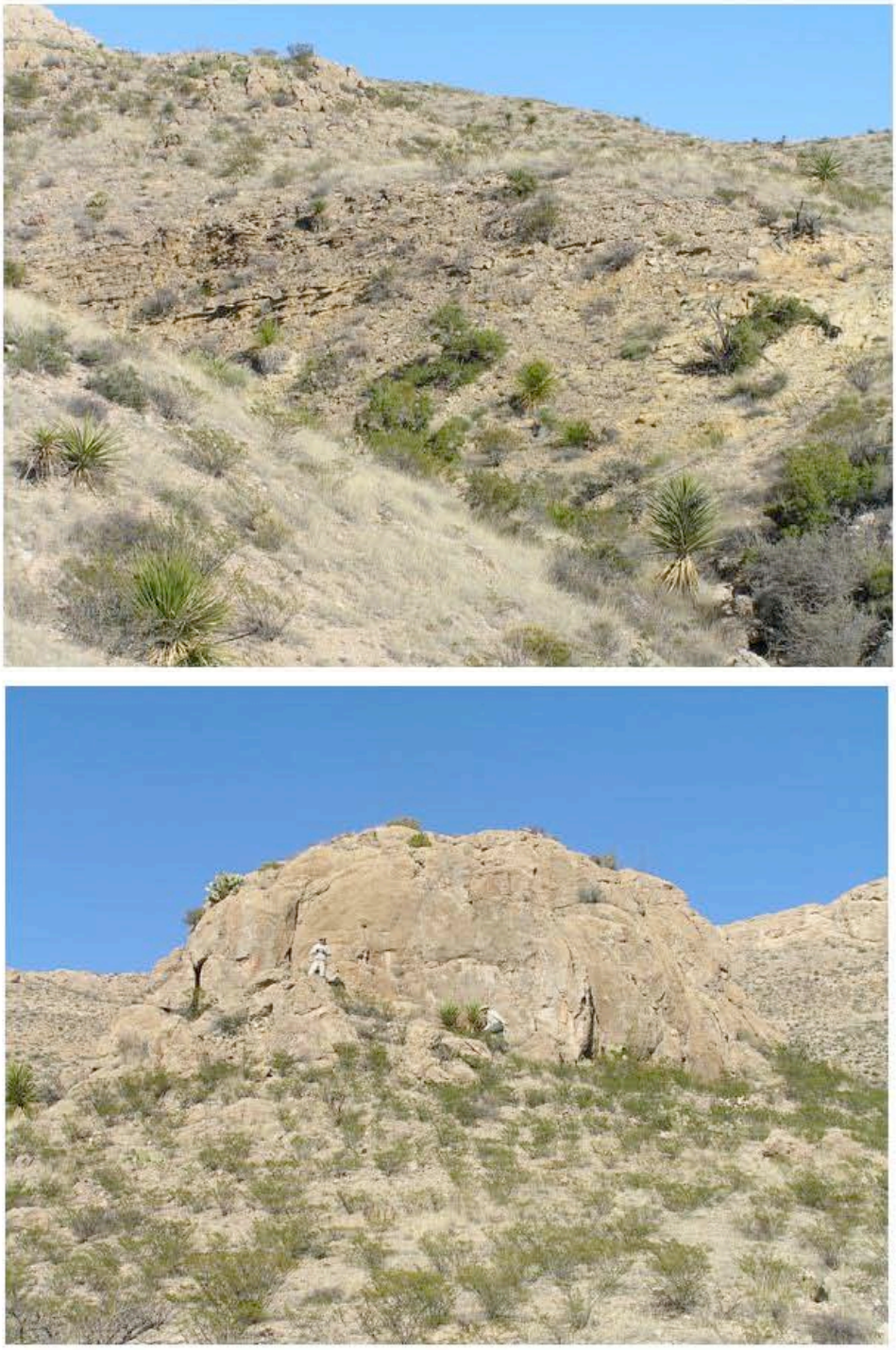

Figure 2.30: Top: The SW section base is the light tan sandstone/siltstone to the right, then moving left up section with the megabreccia at the upper left. Bottom: Megabreccia exposed just to the left of the SW section (note field partner and author for scale).

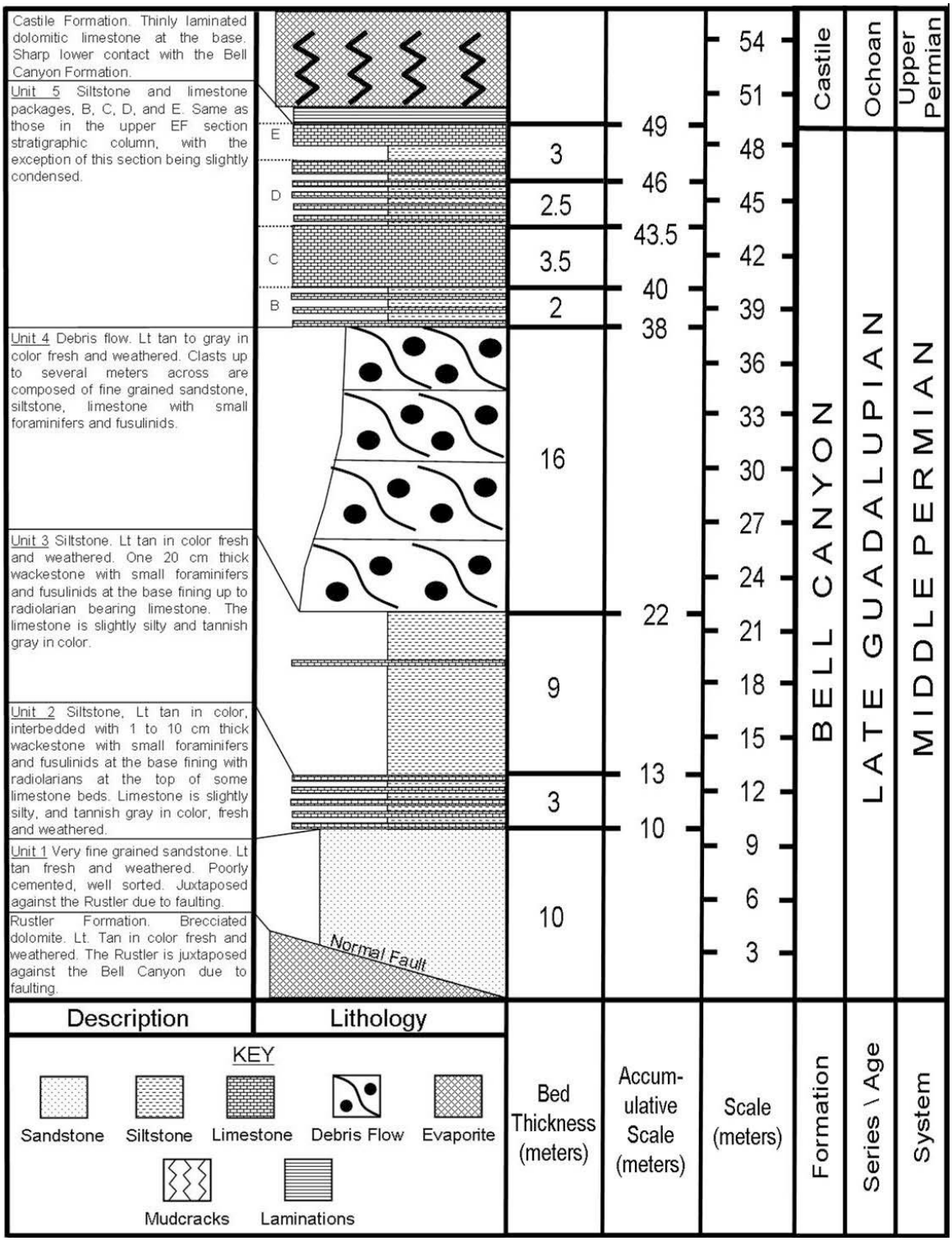

Figure 2.31: SW section stratigraphic column.

The last section measured on the southeastward traverse is the AV section (figure 2.1). This section exposes the most of the upper part of Bell Canyon Formation in the map area with 55 meters exposed (figure 2.32). There are two major debris flows exposed in the section, the lowermost of which exhibits channelization and deformation of the underlying strata (figure 2.33). The two debris flows are separated by several meters of deformed thin bedded siltstone. The separation of these two debris flows are not shown on the geologic map in Appendix A because the scale of the map would not resolve the distinction between the two. In this interval of siltstone there is a 0.5 – 1.0 meter thick brachiopodal wackestone (figures 2.33 bottom and 2.34). This brachiopod rich limestone may possibly be correlative to the brachiopod rich limestone exposed just northwest of the top of the K section. Addition field work will be necessary to verify this hypothesis. Parts of the Reef Trail equivalent strata exposed in the AV section are highly condensed compared to strata of the EF section, but the thickness of about 7 meters is similar (figure 2.35).

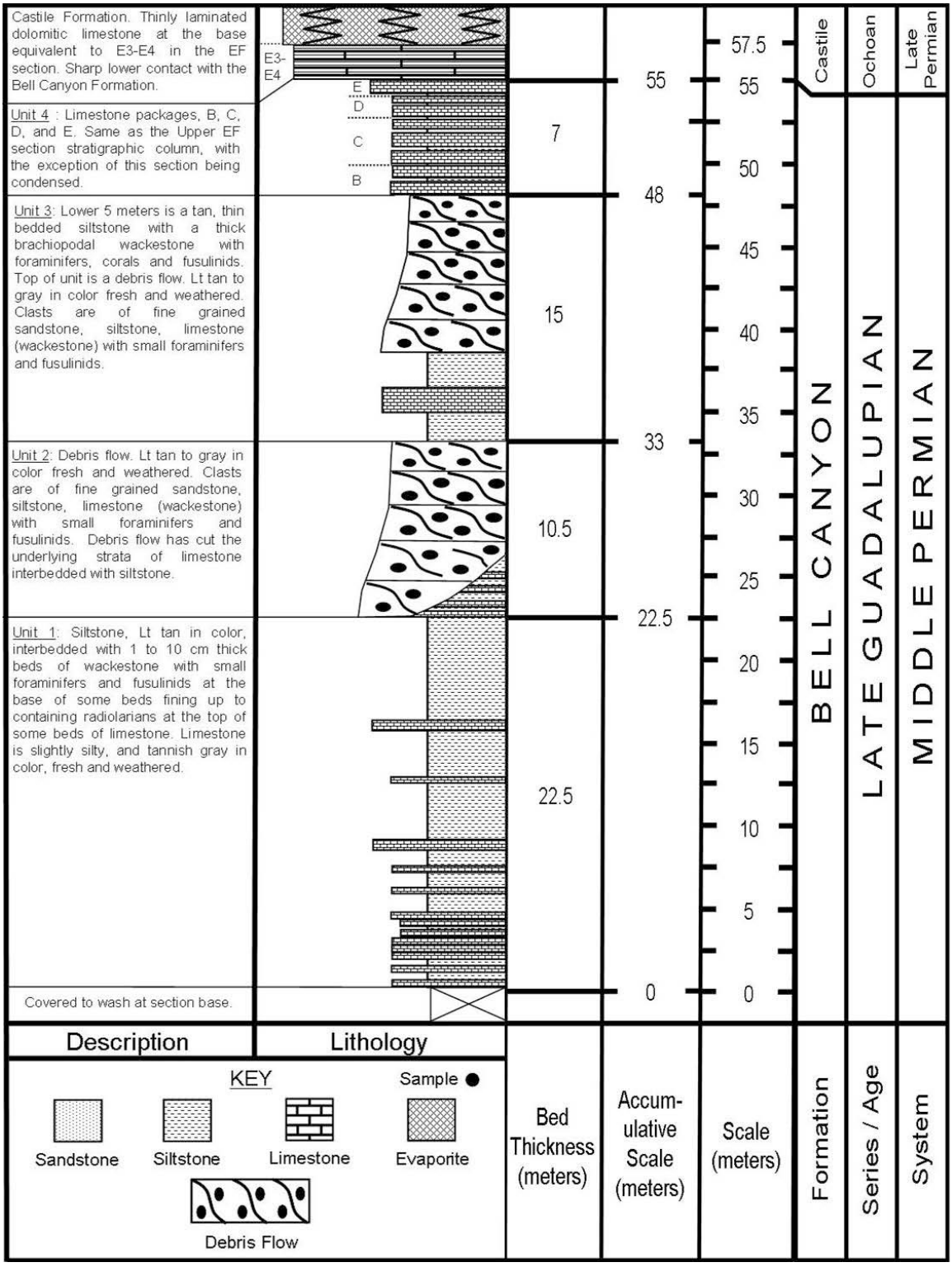

Figure 2.32: AV section stratigraphic column.

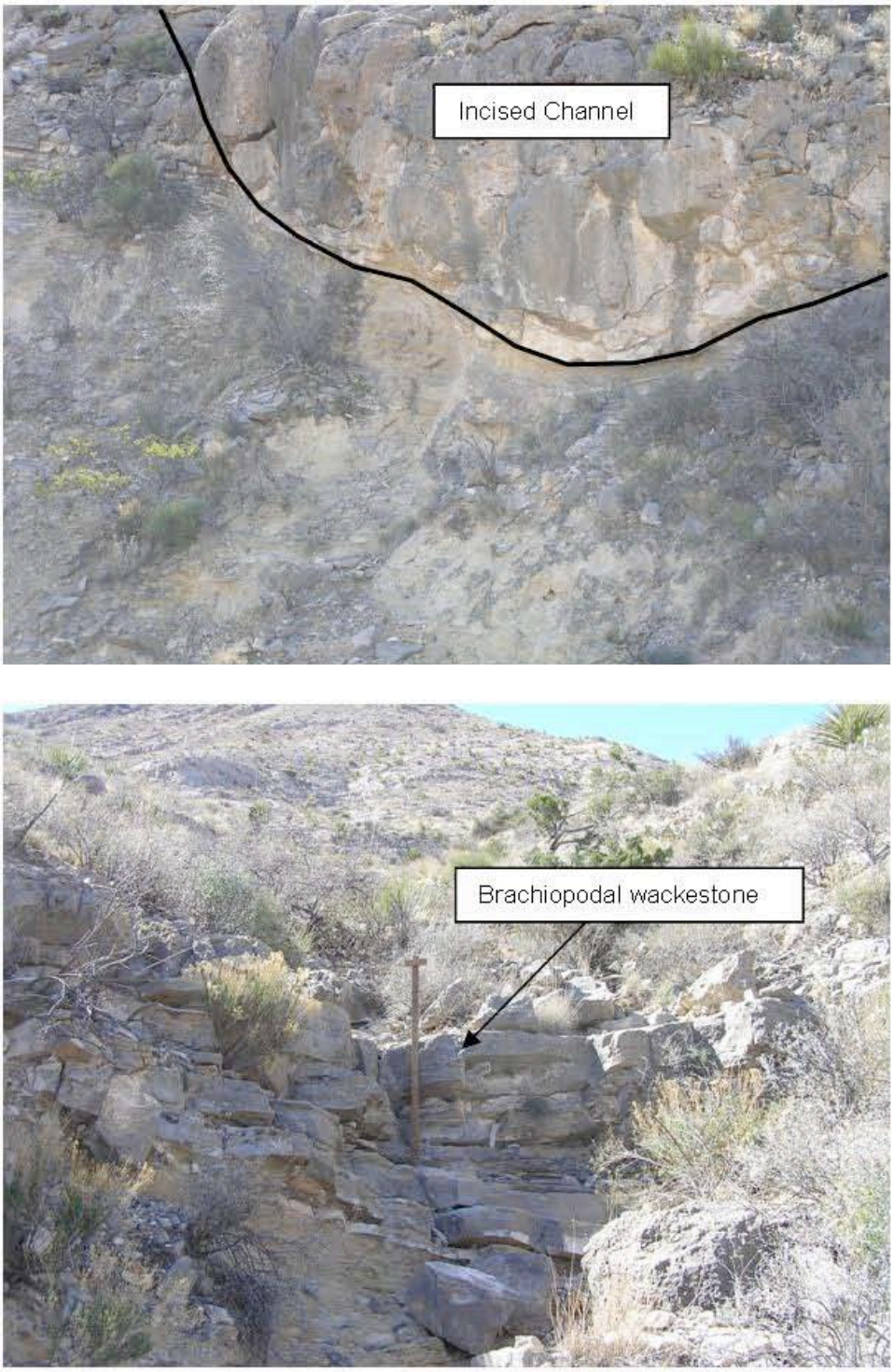

Figure 2.33: Top: The debris flow in the AV section channelizing and deforming the underlying strata. Bottom: The Jacob staff is in 10 cm increments and is resting against a brachiopodal wackestone.

Figure 2.34: Top: A thick brachiopodal wackestone a few meters above the lower debris flow in the AV section (figure 2.29). Bottom: Close-up of the brachiopod rich bed.

Figure 2.35: Strata of the upper part of the AV section equivalent to the upper part of the EF section.

The M, EF, SJ, SW, and AV sections can be correlated across the map area (figure 2.36). The M section itself only has strata of the uppermost beds of the Bell Canyon Formation, and can be correlated to Units C, D, and E of the EF section. In Kennedy's thesis (Kennedy, 2009) map area to the north-northwest, the M section can be traced for over a kilometer where it thickens and is exposed better above and below to include strata equivalent in the lower part of that present in the lower part of the SW section and in the upper part to the Castile. To the south-southeast in the map area, the M section extends about the same distance and thickens above and below in a similar manner. The EF, SJ, SW, and AV sections exhibit complete sections of strata between the top of the EF debris flow and the base of the Castile Formation that can be correlated across the map area. As mentioned earlier in this chapter, the EF section is divided into

units A-E. Unit A is the extensive debris flow in the EF section. Units B-D are primarily beds of thin to thick limestones, with interbedded siltstones in units B and D. The two lower beds of unit E (E1-E2) are the upper beds of the Bell Canyon Formation. Beds E3-E5 comprise the Basal Limestone Member of the Castile Formation and can also be correlated across the map area although their thicknesses and the amount of interbedded siltstone can vary.

Unit A, the EF debris flow, is also correlative across the map area. The upper part of the debris flow correlates better than the lower part of the debris flow. The lower part of the debris flow can vary in thickness and in composition probably due to differences in timing and localization of individual episodes of deposition and of the debris flow. For example, the reefal megabreccia in the base of the debris flow is not correlative continuously across the map area due to its deposits being localized in channels.

The strata exposed below the debris flow in sections SW and AV can be tentatively correlated due to stratigraphic correlations, but fossil evidence does not yet support the correlation of these strata.

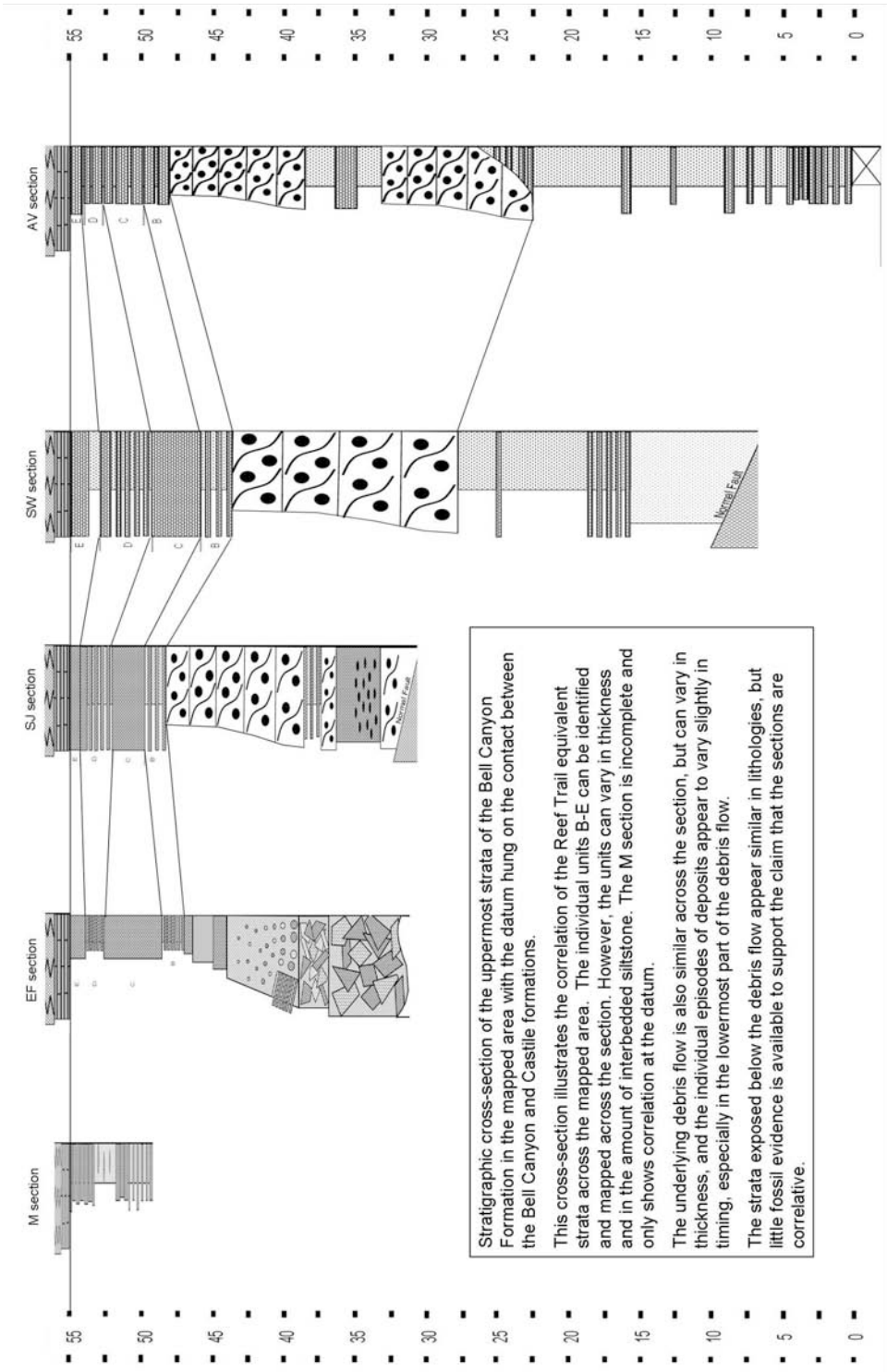

Figure 2.36: Stratigraphic cross-section of strata of the upper part of the Bell Canyon Formation Reef Trail Equivalent strata of the map area. Starting with the M section, then to the EF section and traveling southeast along a fault trend to the SJ, SW, and AV sections.

2.2.7 Debris Flows

The Bell Canyon Formation of the map area contains four distinctive debris flows in each of the measured sections except the K section, and they can be recognized and mapped to the northwest and southeast from FM 2185 (see geologic map, Appendix A). These debris flows have been discussed earlier in this chapter and to simplify this next discussion, the individual debris flows have been designated the same letter as the road cut in which each debris flow is present, i.e., the debris flow present in the EF section road cut will be referred to as the EF debris flow. In this chapter, a brief overview and recap of the B, A and G debris flows will be discussed with a detailed discussion of the EF debris flow to follow. The timing of the debris flows in the map area is still unclear, but they can be tentatively timed approximately as the same as the beginning of deposition of each individual Bell Canyon Formation limestone member equivalent strata.

The oldest debris flow in the map area is in the B debris flow, and it has been described in detail by Kennedy (2009) in his Master's thesis. It is divided into five distinctive layers or flow events with a total thickness of 15 meters. The base of the debris flow can be seen in a gully immediately south of the B section road cut (figure 2.6). Each of the lower four flow events of the B debris flow is approximately one meter thick and the flows have cobble to pebble size clasts at their bases. They grade up to a wackestone or packstone and the flows are lenticular in shape (figure 2.26 Bottom). These lower debris flows contain clasts with radiolarians, small foraminifers and the fusulinacean *Polydiexodina.* The last flow episode in the B debris flow is approximately

10 meters thick and at its base is composed of up to several meters across sub rounded and poorly sorted clasts of limestone, carbonate mudstone, and siltstone (figures 2.27, 2.28 Top, and 2.37). This debris flow fines upwards to a fine grained lenticular packstone that contains radiolarians, small foraminifers, the fusulinacean *Polydiexodina*, and the conodont *Jinogondolella aserrata.*

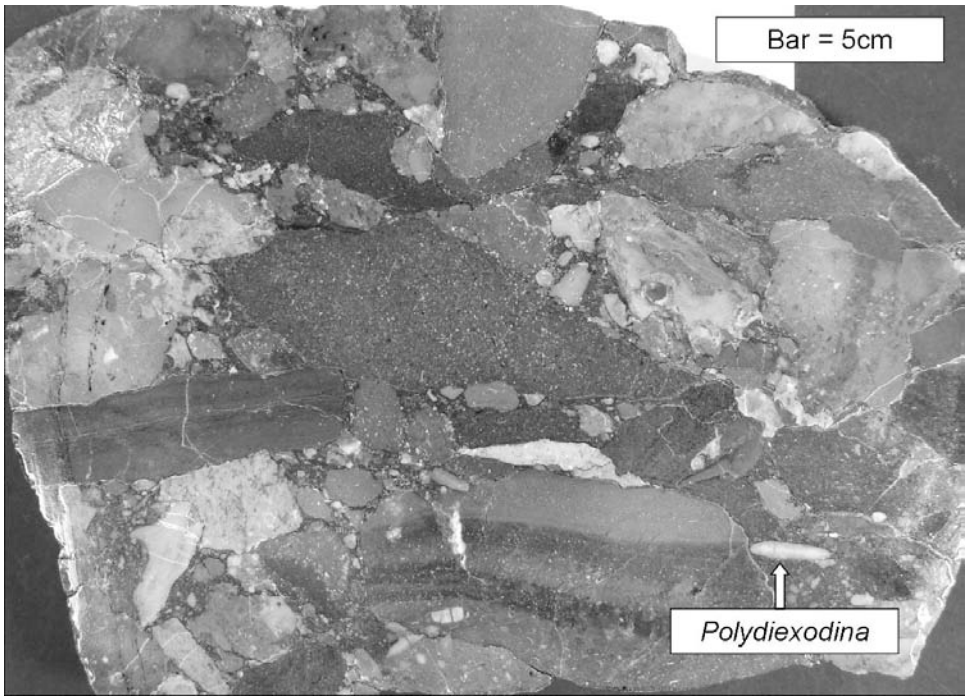

Figure 2.37: Polished slab, sampled from the B section road cut approximately 3.5 meters down from the top of the B debris flow.

The A and G debris flows are the thinnest debris flows in the map area and are separated by approximately 25 meters of strata. The oldest of the two debris flows is the A debris flow and it is approximately 2.5 meters thick and is composed of pebble size rounded and poorly sorted clasts of limestone containing brachiopods, bryozoans, small

foraminifers and the fusulinacean *Polydiexodina*. The A debris flow in the A section road cut (figure 2.1) has a large swell exposed. This swell is probably a small filled channel (figure 2.38). The G debris flow is approximately 2.5 meters thick and is composed of cobble to pebble size rounded and poorly sorted clasts of limestone containing brachiopods, bryozoans, small foraminifers, and in abundance, the fusulinacean *Polydiexodina* (figure 2.39). The uppermost 10-20 cm of the G debris flow has many clasts that are *Polydiexodina* rich packstone.

The G debris flow can be traced to the southeast to the base of the K section where it is displaced by a small fault (figure 2.14).

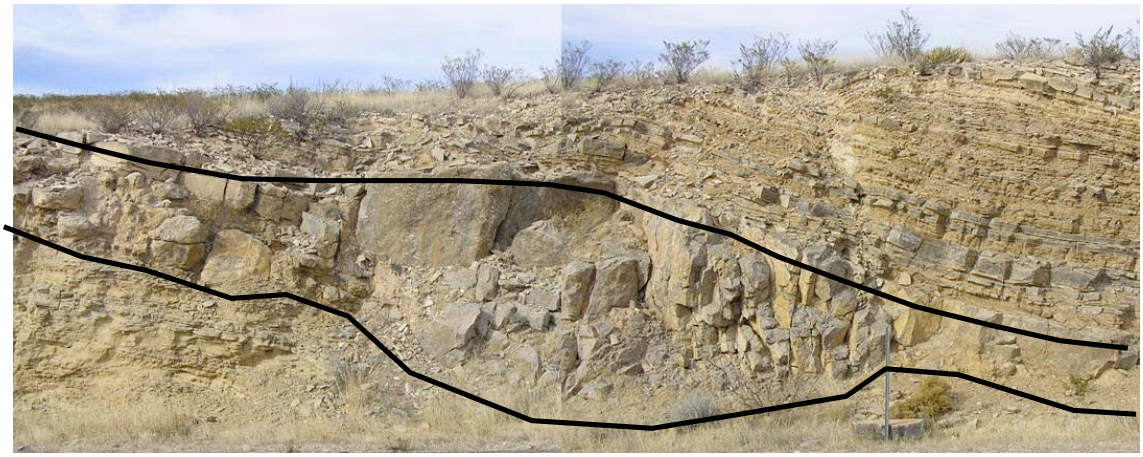

Figure 2.38: A section road cut (figure 2.1). Note the swell in the A debris flow. This swell is probably a small filled channel.

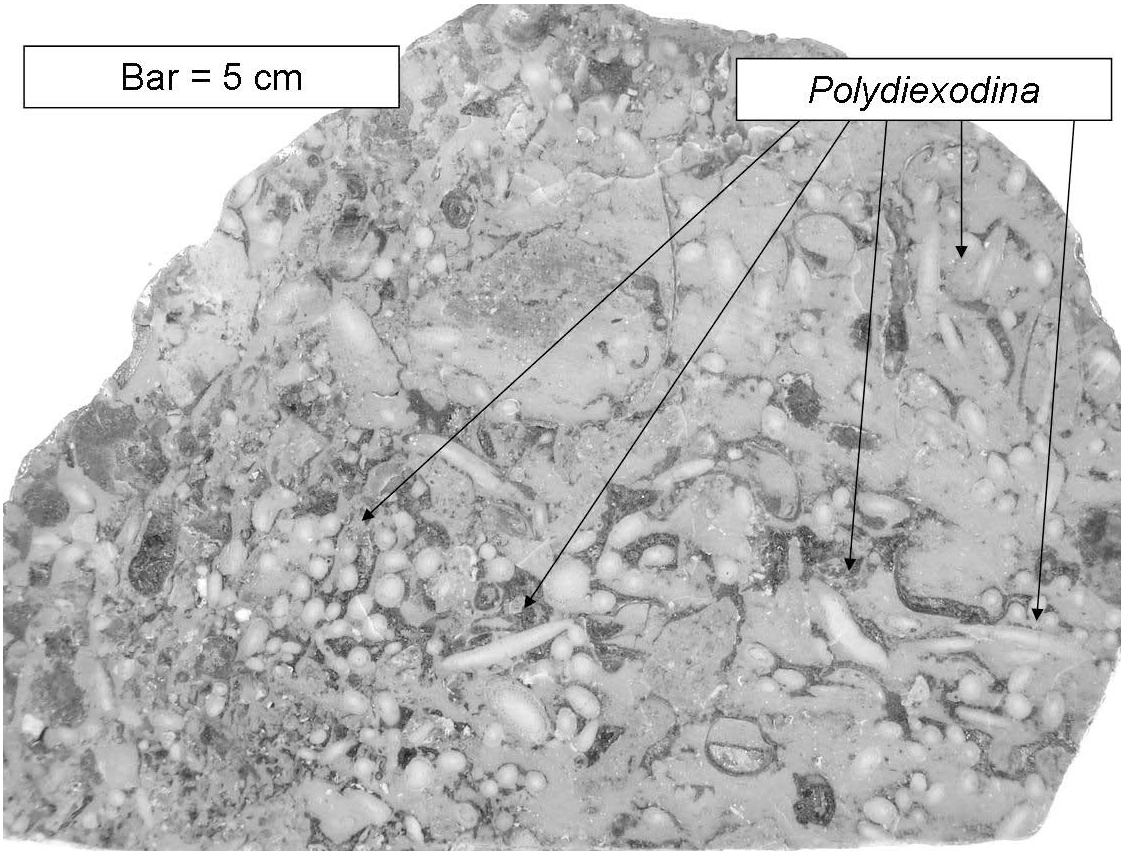

Figure 2.39: Polished slab, sampled from the G section road cut from the top of the G debris flow. Note the abundance of the fusulinacean *Polydiexodina*

The youngest debris flow in the map area is the EF debris flow that can be map along two trends from both the EF road cut and just south of the M section road cut (see geologic map, Appendix A). The equivalent EF debris flow located in outcrops just southeast of the M section is also referred to as the EF debris flow, but the exposures there are not as extensive as are the ones southeast from the EF section road cut. The EF debris flow, exhibits several distinctive lithofacies including packages of strata that have fining upward textures, nearly two meters of varve-like laminations in the upper part, a large clast breccia near the base with fragments of the fusulinacean *Polydiexodina*, and a

megabreccia composed of reef rock at the base. The following subchapter is a discussion of the lithofacies and biofacies of the EF debris flow.

2.2.7.1 EF Section Debris Flow

The EF debris flow was measured and described from the base of the EF section road cut (Units A1-A6, figure 2.40). Eight samples were taken from the EF debris flow in different lithologies and were cut into slabs and polished (Samples DEF 00, DEF 0, DEF 1, DEF 2, DEF 3, DEF 4, DEF 5, and DEF 6; figure 2.40). This debris flow exposes approximately 15.3 meters of strata in the road cut, but varies in thickness throughout the map area. Additional exposures of the EF debris flow can be seen along fault lines trending southeast from the EF and M section road cuts. The EF debris flow can be divided into several different lithological sections: very coarse breccia at the base (units A1 and A2), a fining up debris flow of boulder to pebble sized clasts (unit A3), a medium grained packstone to a laminated section (units A4 and A5), and finally a very fined grained normally graded packstone (unit A6). Oriented fusulinacean and smaller foraminifers shown in thin section in many of the illustrations from the EF and M. sections are from the collection of M. and G. Nestell that will be the subject of a paper describing the foraminifers of the upper part of Reef Trail Member equivalent strata in the Apache Mountains.

At the base of the EF debris flow two episodes of large clast breccias are exposed (units A1 and A2, figure 2.41). The lower breccia (unit A1) is referred to as the megabreccia in the map area, and it is composed of very large (several meters across) poorly sorted, sub-angular clasts of reefal material, light tan to gray in color. The reefal

material of the megabreccia exhibits the same outcrop appearance and the same composition as some parts of the Capitan Reef exposed in the Guadalupe Mountains (Bell, personal communication, 2007). Clasts contain phylloid algae, bryozoans, *Archaeolithoporella, Tubiphytes*, and sponges (figures 2.42 and 2.43, samples DEF 00 and DEF 0).

Unit A1 varies in thickness and is not continuous throughout the map area. The exposures in the map area of unit A1 have the appearance of reefal mounds. A first working hypothesis at to their origin was that these reefal mounds were in situ bioherms that were later covered by a massive debris flow. Detailed investigation of the constituents of unit A1 discovered that the reefal mounds were a mass of disoriented clasts of reefal material, and it was a debris flow in itself. Reefal clasts with disoriented geopedal structures also helped disclaim the original hypothesis of unit A1 as in situ bioherms (figure 2.44). New field evidence supports a new hypothesis that unit A1 incised and filled channels during its depositional process, which would explain the mound like exposures of the reefal debris and its discontinuity across the map area. A preserved incised and filled channel can be observed in the AV section to support the channel fill hypothesis for unit A1 (figure 2.33).

The upper sections (units A2-A6) of the EF debris flow are continuous throughout the map area with slight thinning to the southeast. Unit A2 is the unit most resistant to weathering and was the better mapping horizon of the EF debris flow. It is composed of poorly sorted, angular clasts of limestone, siltstone, and few clasts of reefal material, gray and reddish-tan to light tan in color (figure 2.45). This unit contains fragments of

brachiopods, bryozoans, and several genera of fusulinaceans including *Polydiexodina.* In the EF section road cut this unit measures 2 meters thick.

Unit A3 is 5 meters thick and is a fining upwards carbonate debris flow with large blocks of strata up to several meters across incorporated into the surrounding matrix at the base. In one outcrop approximately one mile south along the strike of the debris flow from FM 2185 there is a large block of stratified basin material in the SJ section (figure 2.28). This block appears to be stratigraphically in place when first observed because it is approximately 3 meters thick and 5-6 meters wide. It was measured and described as being a section between two episodes of debris flows. Microfossil data gathered after laboratory work placed this block as being older than the surrounding debris flow because of the presence of abundant (Polydiexodina) and other fusulinaceans and the presence of chert stringers in the limestone not seen in other sections in the map area. Tracing out the block edges verified that it is a very large block of strata incorporated into the debris flow. A smaller block of stratified basin material can be observed in the EF section road cut (figure 2.46). It was also thought to have been in place until micro fossil data was studied from the block (figures 2.47-2.51). Figure 2.46 also shows interpreted debris flow matrix injected in between layers of the strata in the block. The block was possibly ripped from the wall of a channel as the debris flow moved down gradient.

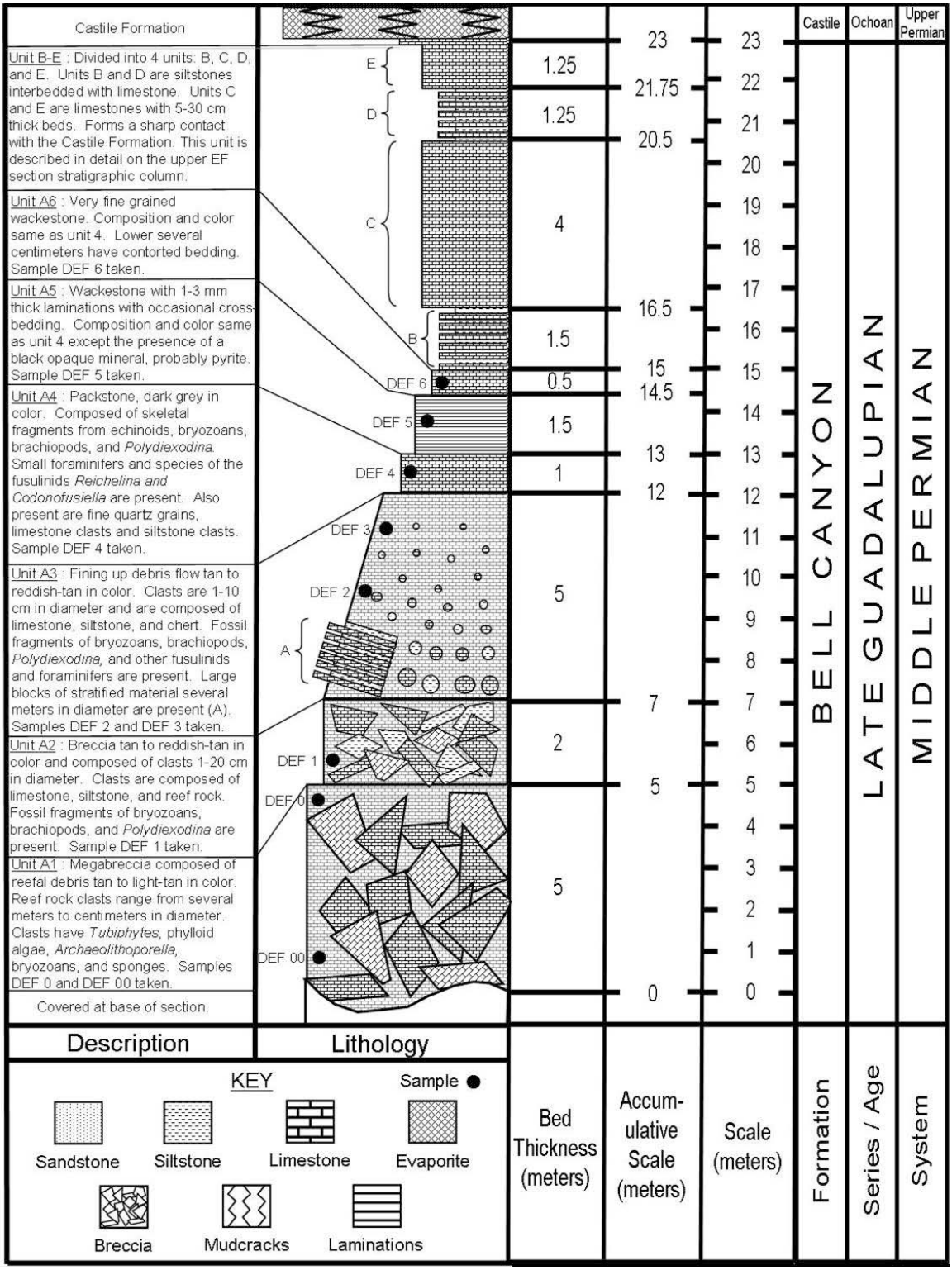

Figure 2.40: Stratigraphic column of the EF section road cut.
This stratigraphic column is also shown in figure 2.21.

Figure 2.41: Top: Outcrop of the reefal debris (unit A1) in the EF section road cut on the north side of FM 2185. Bottom: Unit A2 exposed in the EF section road cut on the north side of FM 2185.

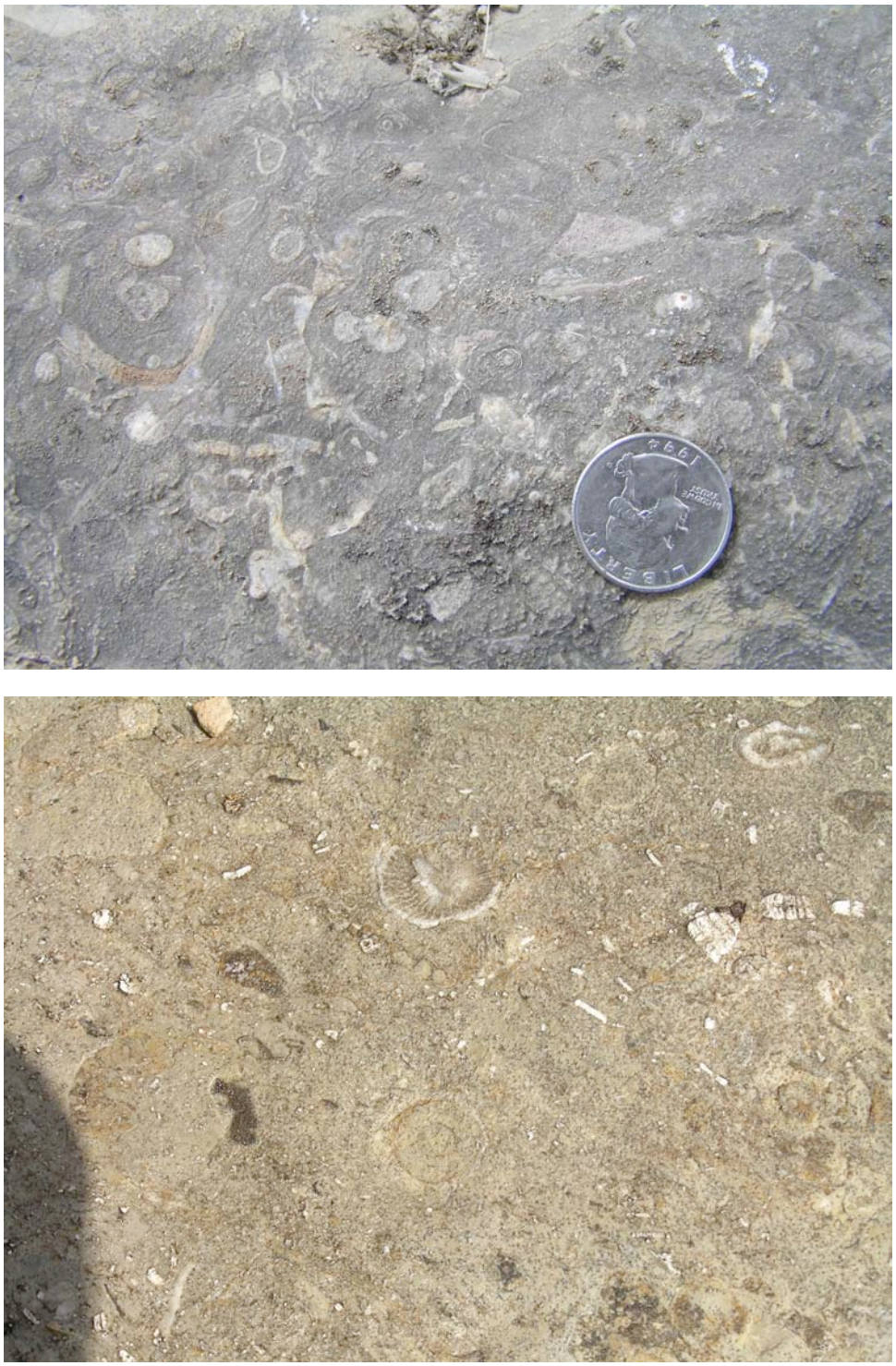

Figure 2.42: Top and bottom: Close-up of outcrops of the reefal debris (unit A1) in the EF section road cut (figure 2.41 Top) to display the general reefal texture. Coin for scale is 2.5 cm in diameter.

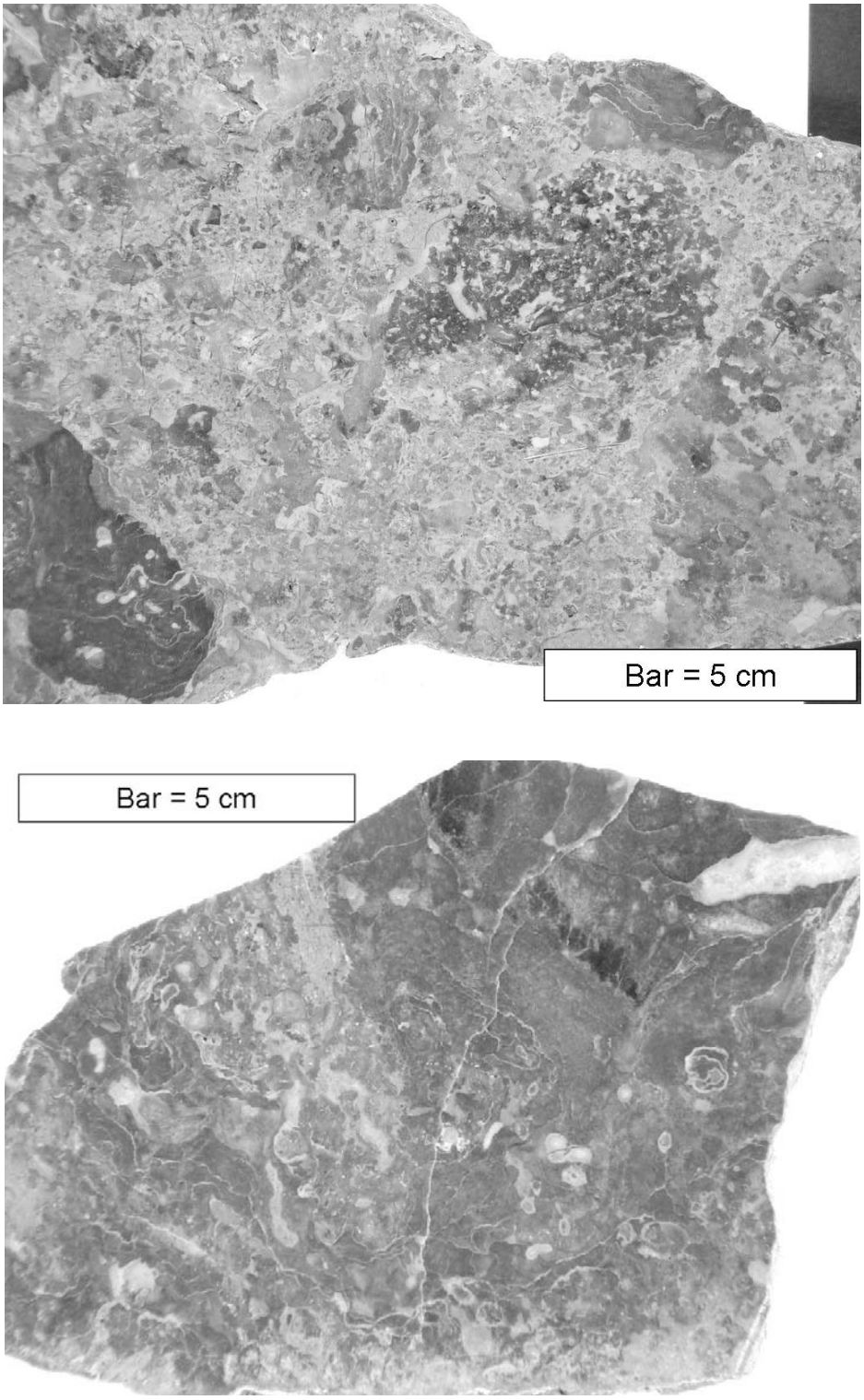

Figure 2.43: Top and bottom: Slabs of the reefal debris (unit A1) in the EF section road cut samples DEF 00 (Top) and DEF 0 (Bottom) display the general reefal texture.

Figure 2.44: Disoriented geopedal structure (arrow is pointing up), signifying that the reefal clast is not in situ (see figure 2.4 for photo location).

Unit A3 continues up normally graded, tan to reddish-tan in color with pebble sized clasts fining up to coarse sized grains composed of bryozoan, brachiopod, *Polydiexodina* fragments and other small fusulinacean fragments, and chert, siltstone and limestone clasts (figure 2.52, samples DEF 2 and DEF 3 with micrographs in figures 2.53-2.56). This section is also resistant to weathering and produces easily mappable outcrops in the field.

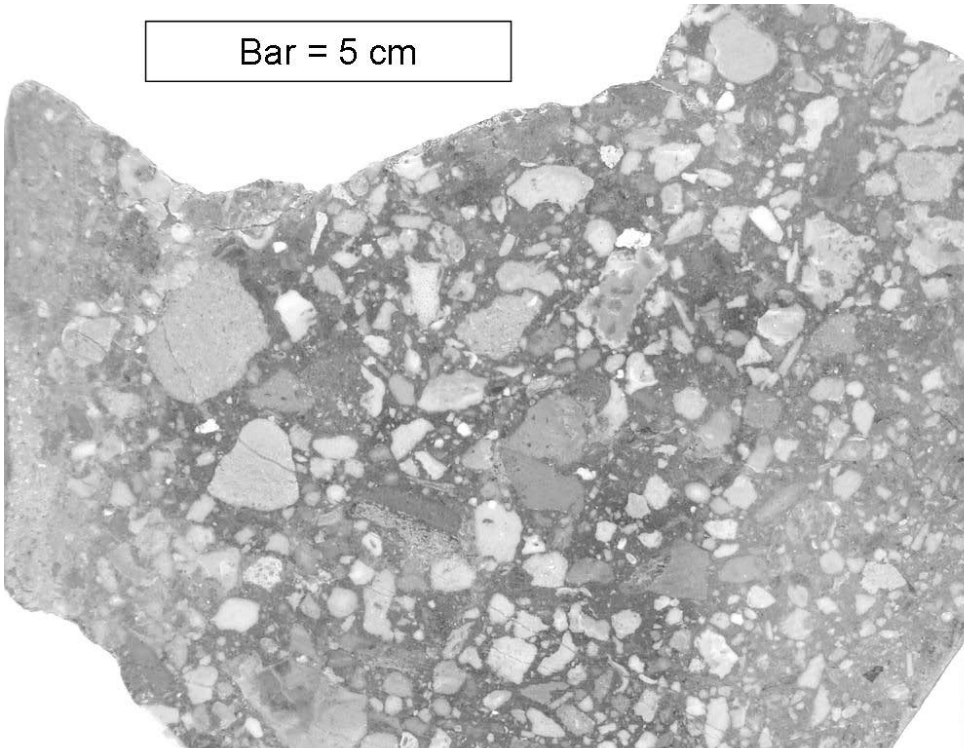

Figure 2.45: Sample DEF 1 from unit A2 from the EF debris flow from the EF section road cut. Note angular to rounded clasts of varying sizes.

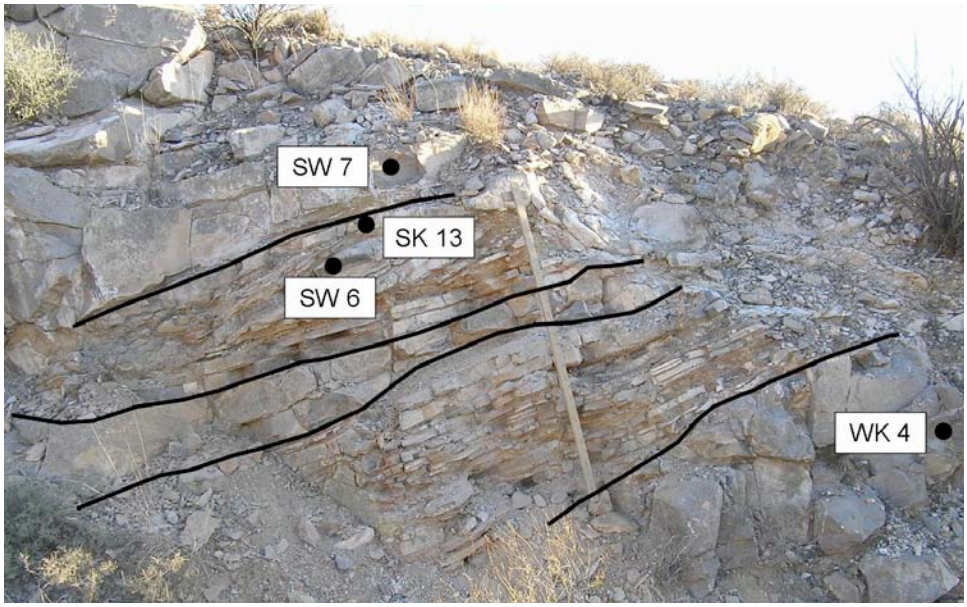

Figure 2.46: Lamar Limestone Member equivalent in age block in the base of the A3 unit of the EF debris flow. Lines trace out the incorporated older block of strata. The rock above the top line and below the bottom line and in between the two lines through the middle of the block of strata is the A3 unit matrix. Samples WK 4, SW 6, SK 13, and SW 7 were taken. Located in the south side of the EF section road cut.

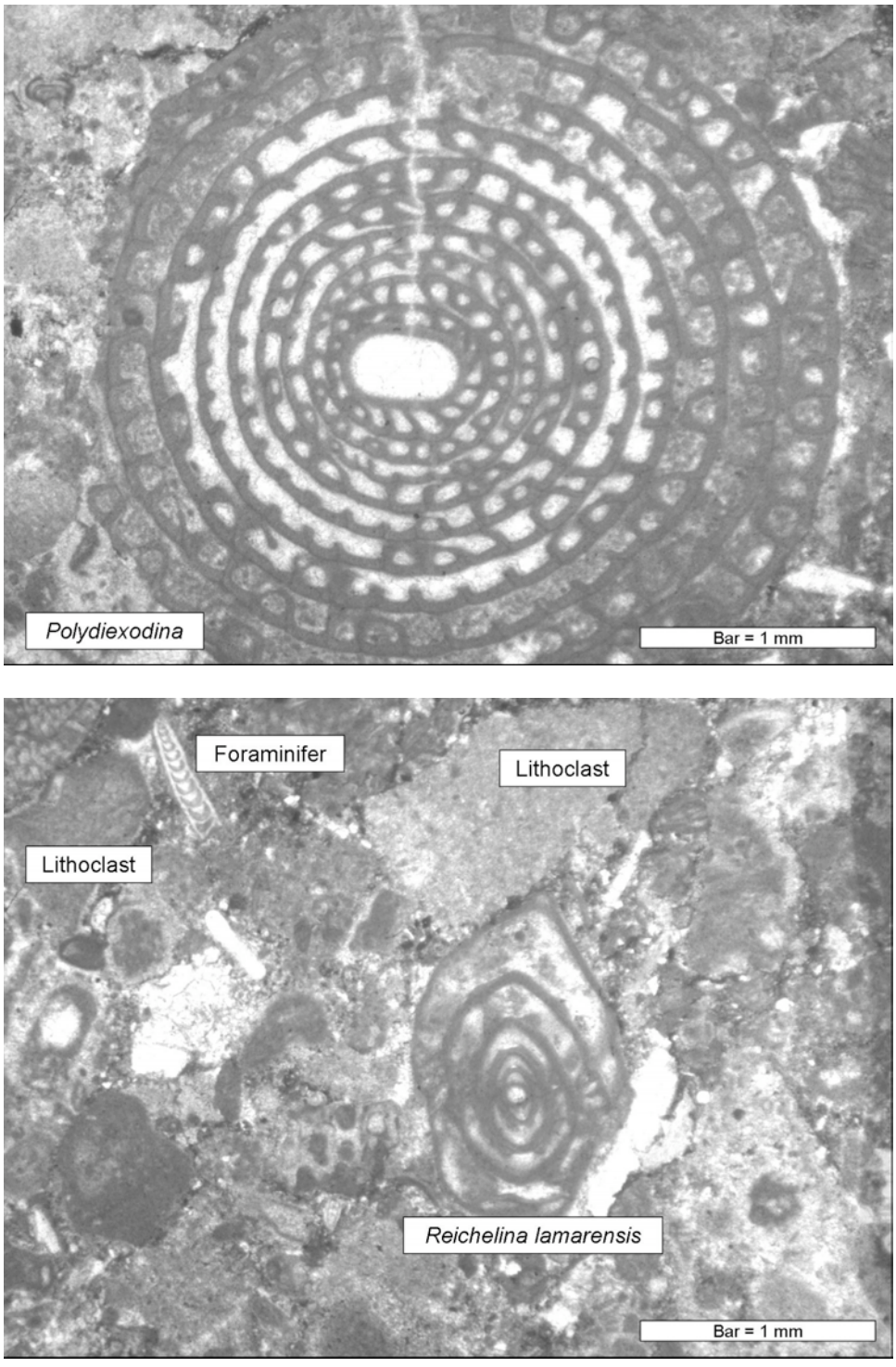

Figure 2.47: Top and Bottom micrographs: Sample WK 4 from just below a block of strata in the A3 unit of the EF debris flow (figure 2.46). Wackestone containing lithoclasts, algae, foraminifers, fusulinaceans: *Polydiexodina* and *Reichelina cf R. lamarensis*, and other indistinguishable fossil fragments.

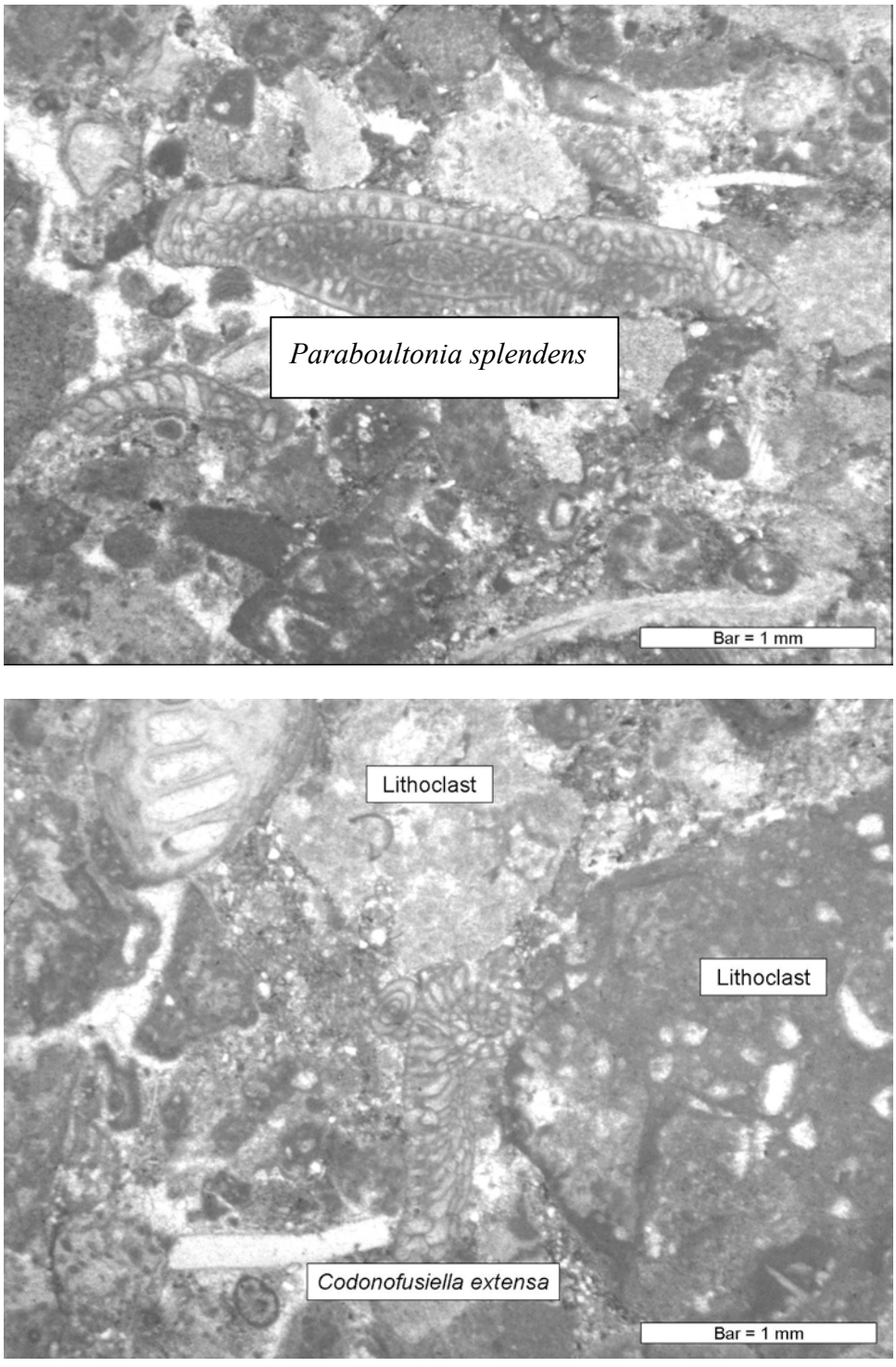

Figure 2.48: Top and Bottom micrographs: Sample WK 4 from just below a block of strata in the A3 unit of the EF debris flow (figure 2.46). Wackestone containing lithoclasts, the fusulinacean: *Paraboultonia splendens*, and other indistinguishable fossil fragments.

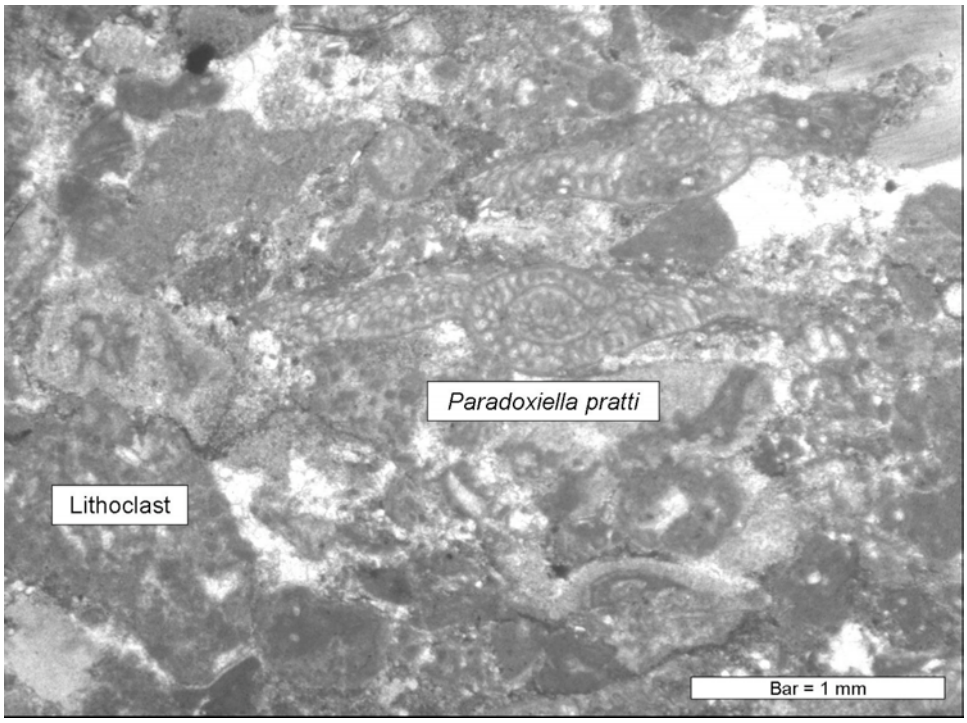

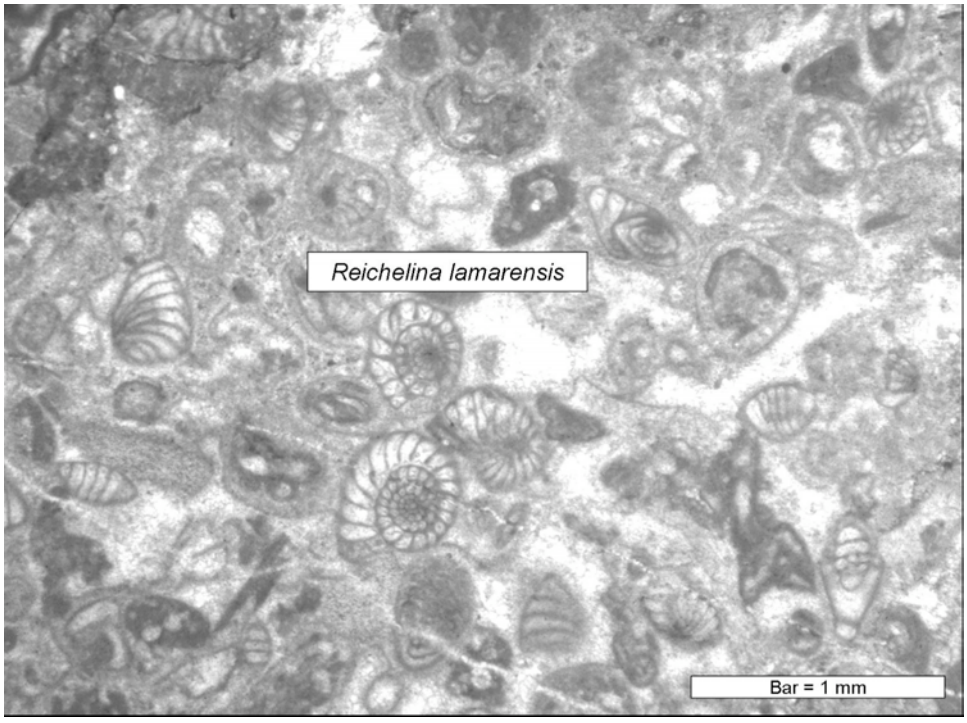

Figure 2.49: Top and Bottom micrographs: Sample SW 6 from a block of strata in the A3 unit of the EF debris flow (figure 2.46). Wackestone containing lithoclasts, fusulinaceans: *Paradoxiella pratti* and *Reichelina lamarensis*, and other indistinguishable fossil fragments.

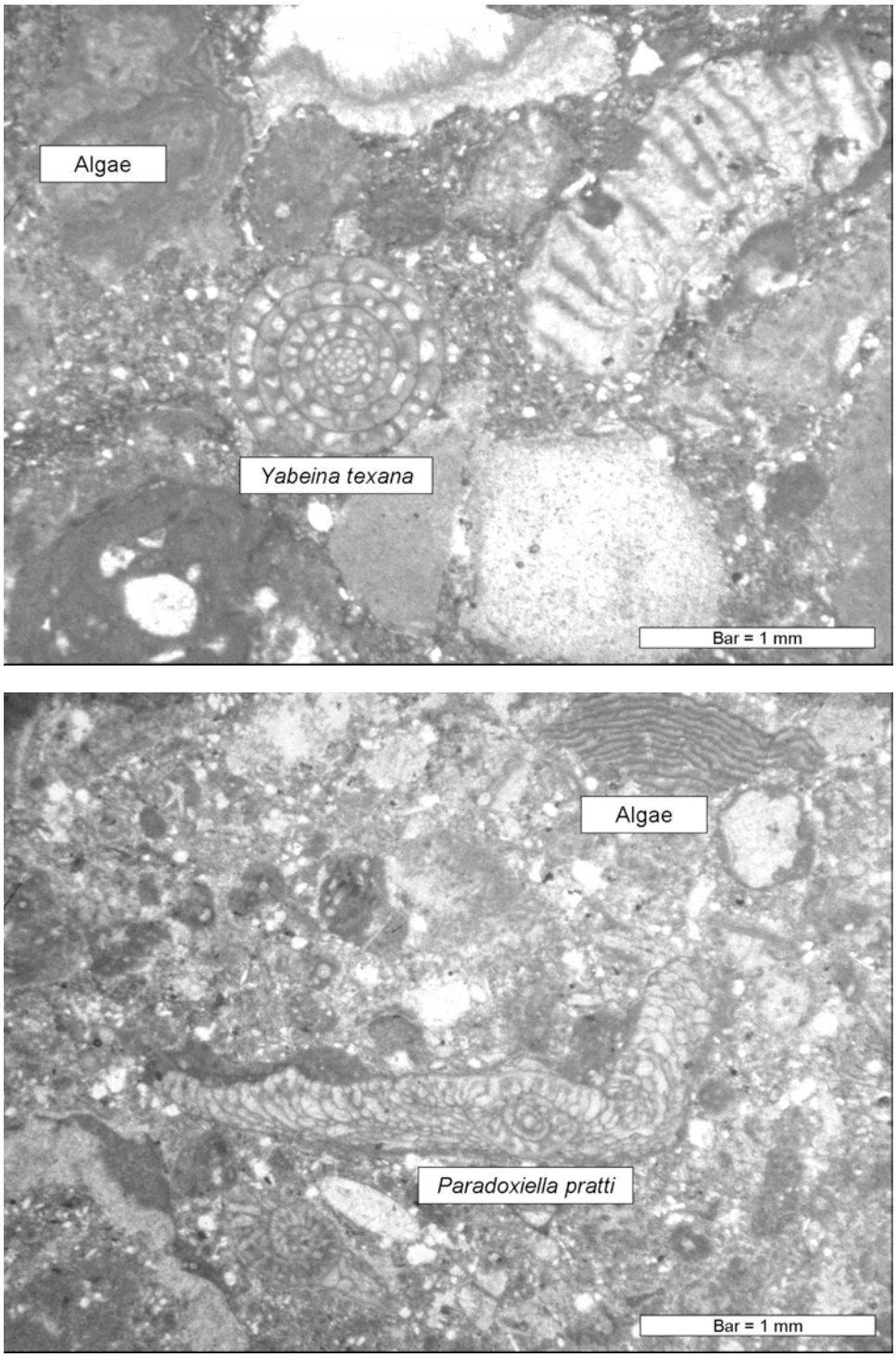

Figure 2.50: Top and Bottom micrographs: Sample SK 13 from a block of strata in the A3 unit of the EF debris flow (figure 2.46). Wackestone containing lithoclasts, algae, fusulinaceans: *Paradoxiella pratti* and *Yabeina texana*, and other indistinguishable fossil fragments.

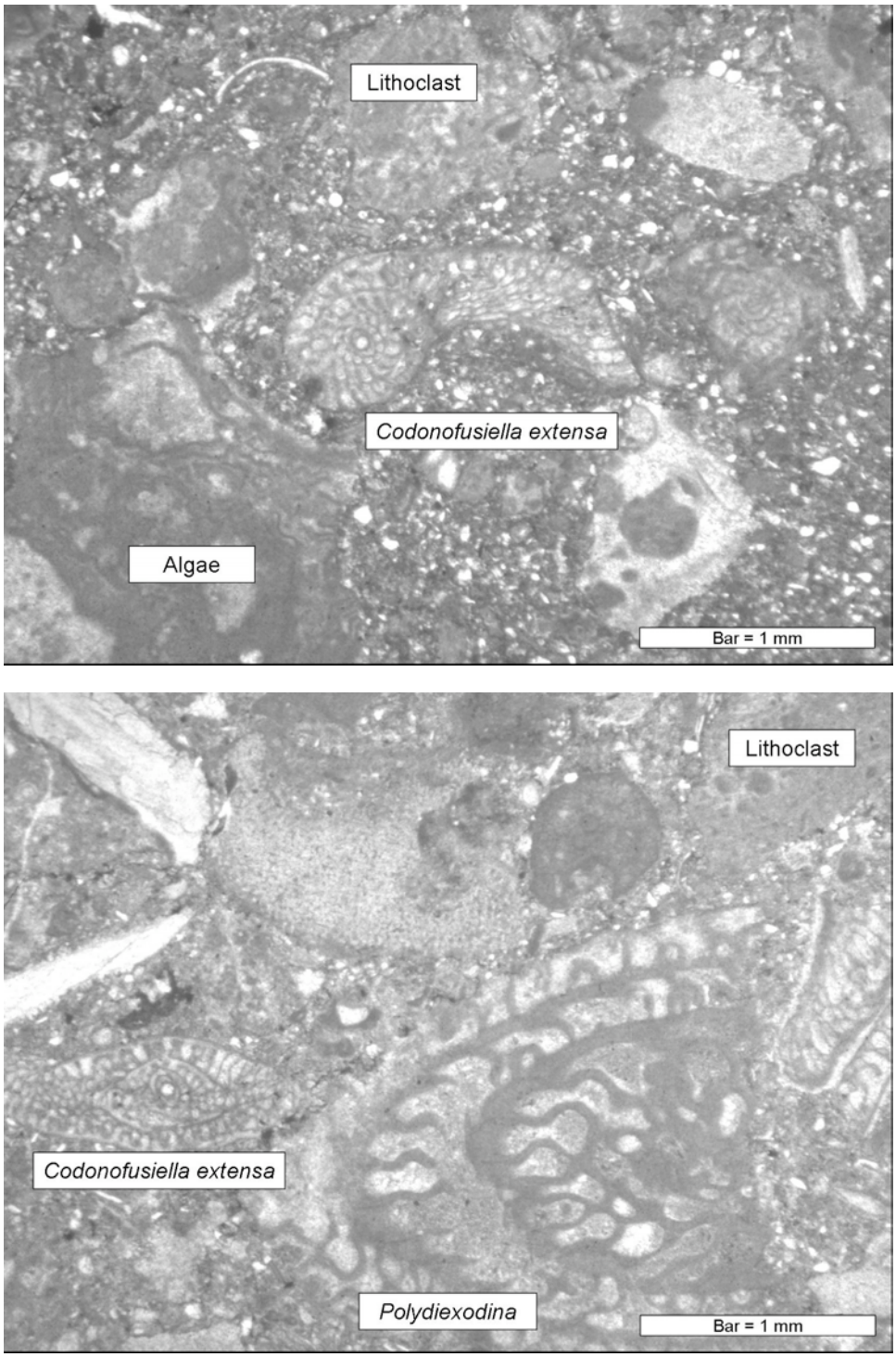

Figure 2.51: Top and Bottom micrographs: Sample SW 7 from just above a block of strata in the A3 unit of the EF debris flow (figure 2.46). Wackestone containing lithoclasts, algae, fusulinaceans: *Polydiexodina* and *Codonofusiella extensa*, and other indistinguishable fossil fragments.

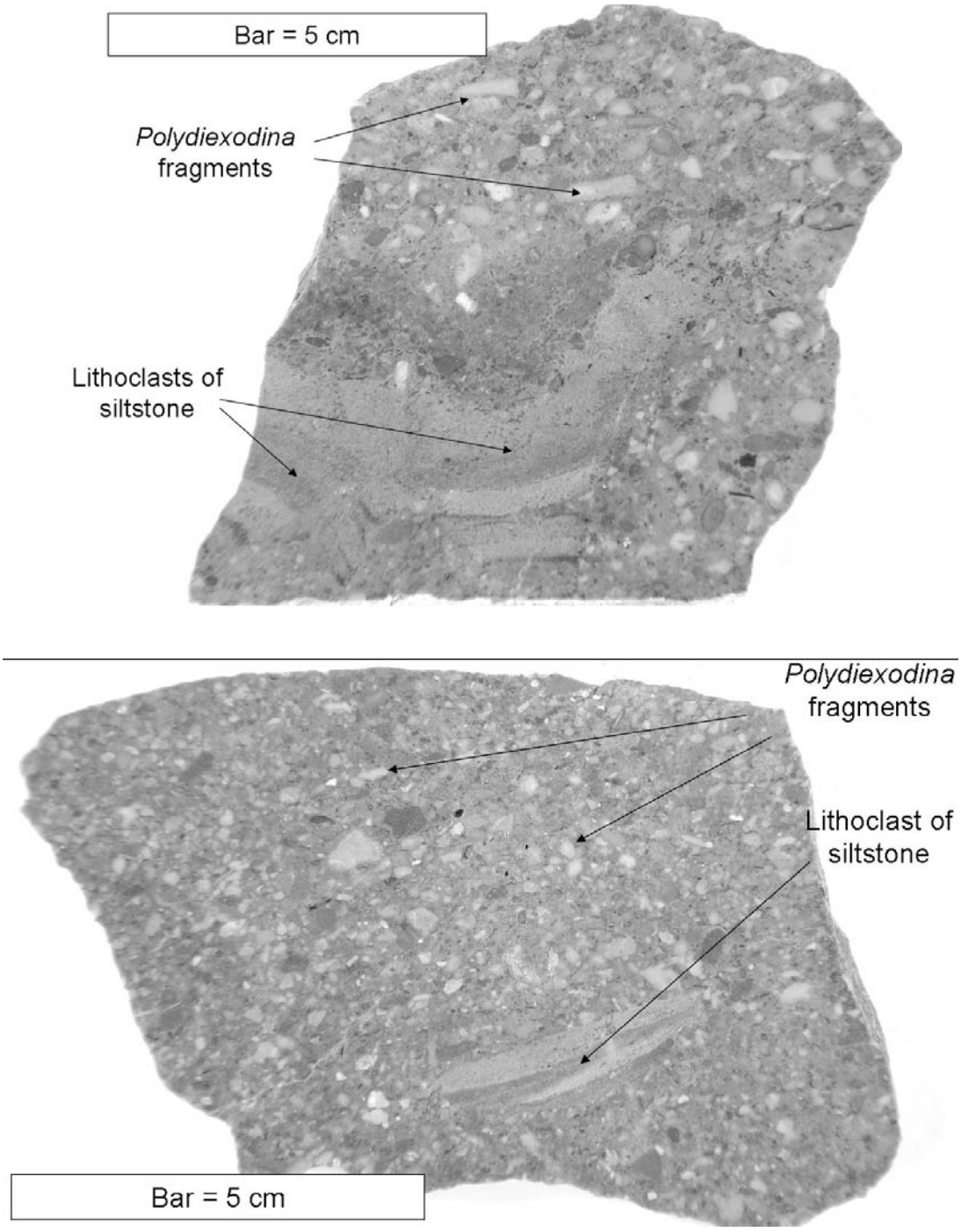

Figure 2.52: Samples DEF 2 (Top) and DEF 3 (Bottom) from unit A3 in the EF debris flow in the EF section road cut. Samples contain lithoclasts of siltstone and limestone, fossil fragments of the fusulinacean *Polydiexodina*, and other indistinguishable fossil fragments.

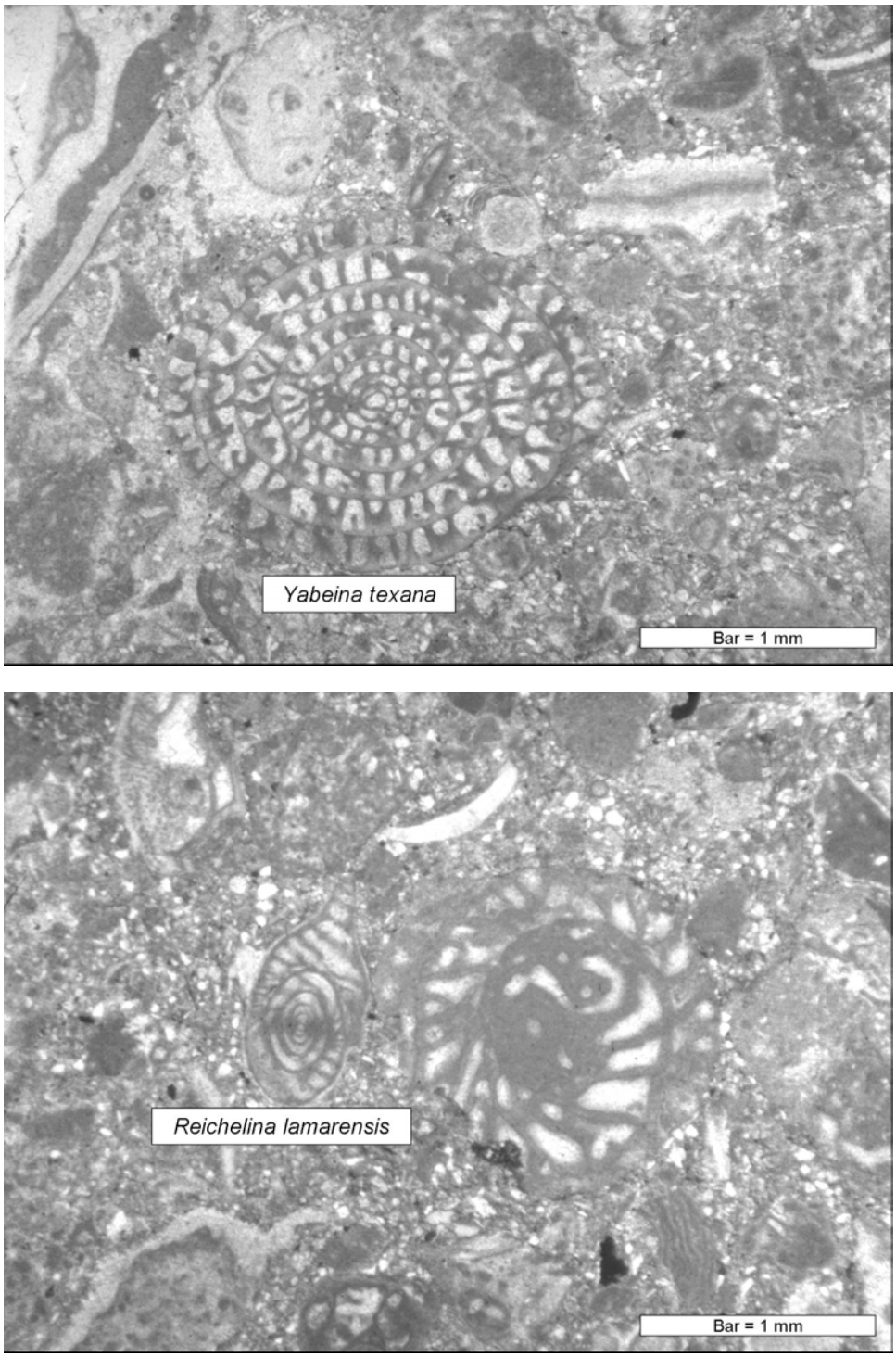

Figure 2.53: Top and Bottom micrographs: Sample DEF 2 the A3 unit of the EF debris flow (figure 2.40). Wackestone containing lithoclasts, algae, fusulinaceans: *Yabeina texana* and *Reichelina lamarensis*, and other indistinguishable fossil fragments.

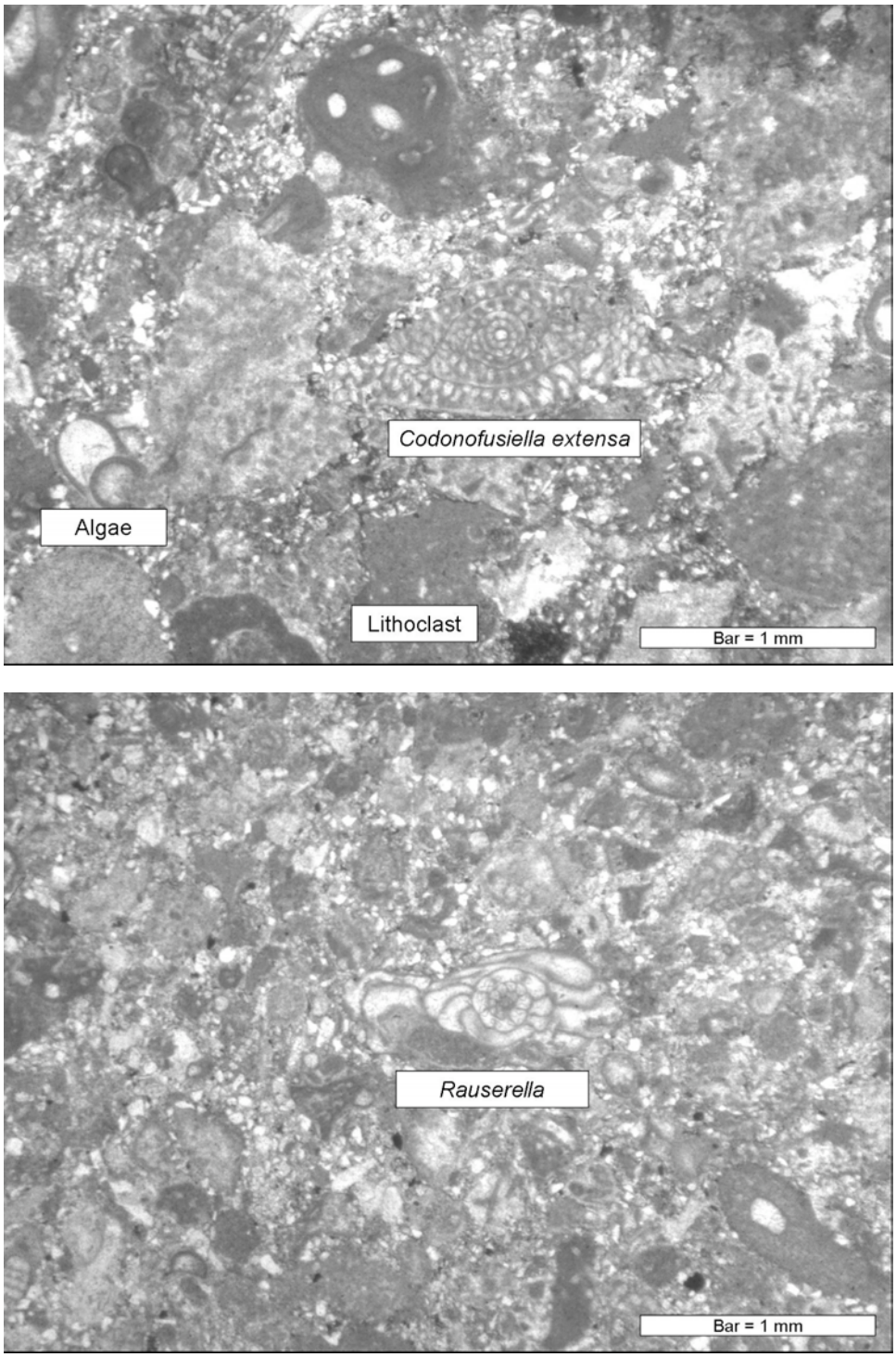

Figure 2.54: Top and Bottom micrographs: Sample DEF 2 of the A3 unit in the EF debris flow (figure 2.40). Wackestone containing lithoclasts, algae, fusulinaceans: *Codonofusiella extensa* and *Rauserella*, and other indistinguishable fossil fragments.

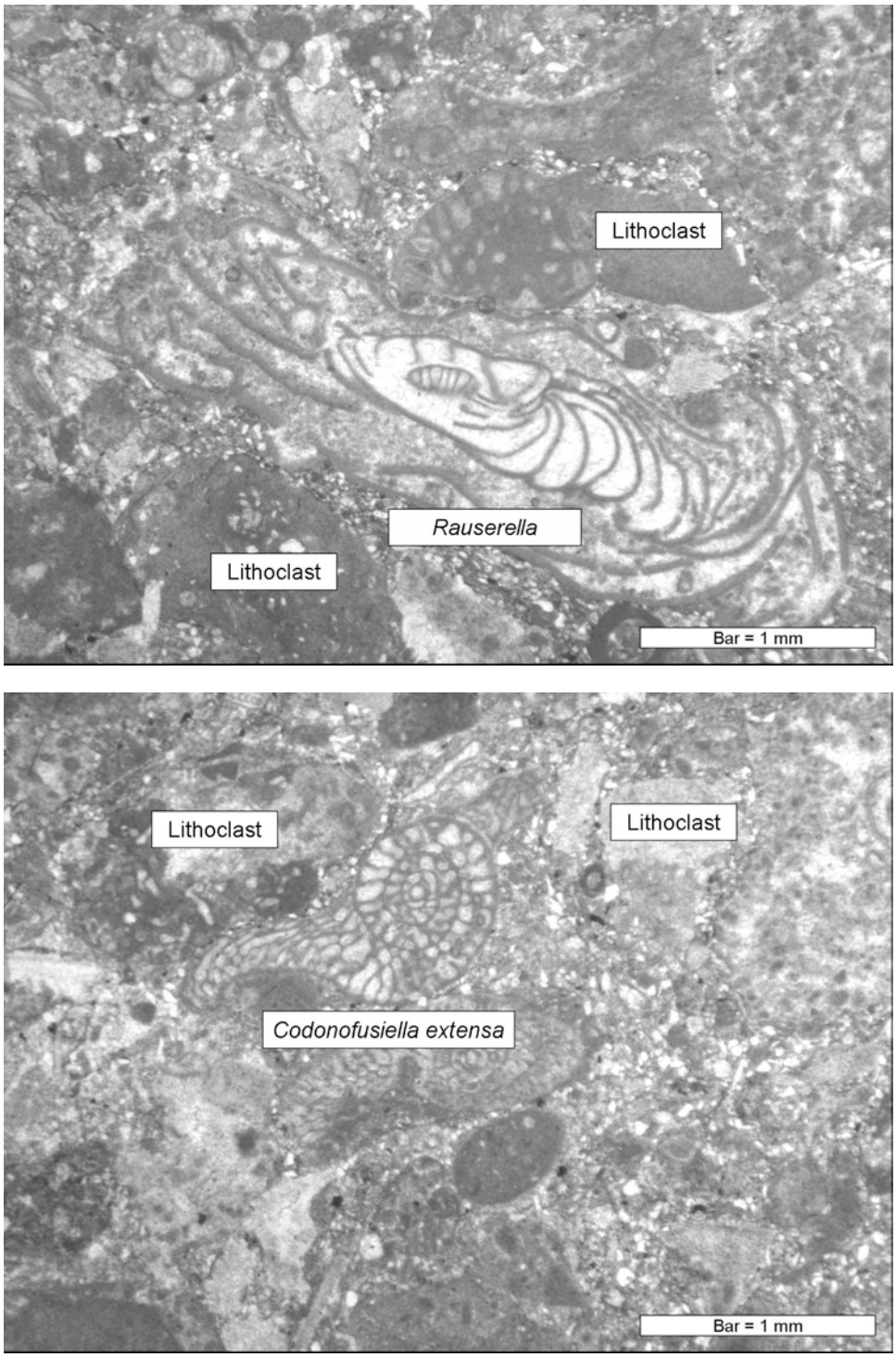

Figure 2.55: Top and Bottom micrographs: Sample DEF 3 of the A3 unit in the EF debris flow (figure 2.40). Wackestone containing lithoclasts, algae, fusulinaceans: *Codonofusiella extensa* and *Rauserella*, and other indistinguishable fossil fragments.

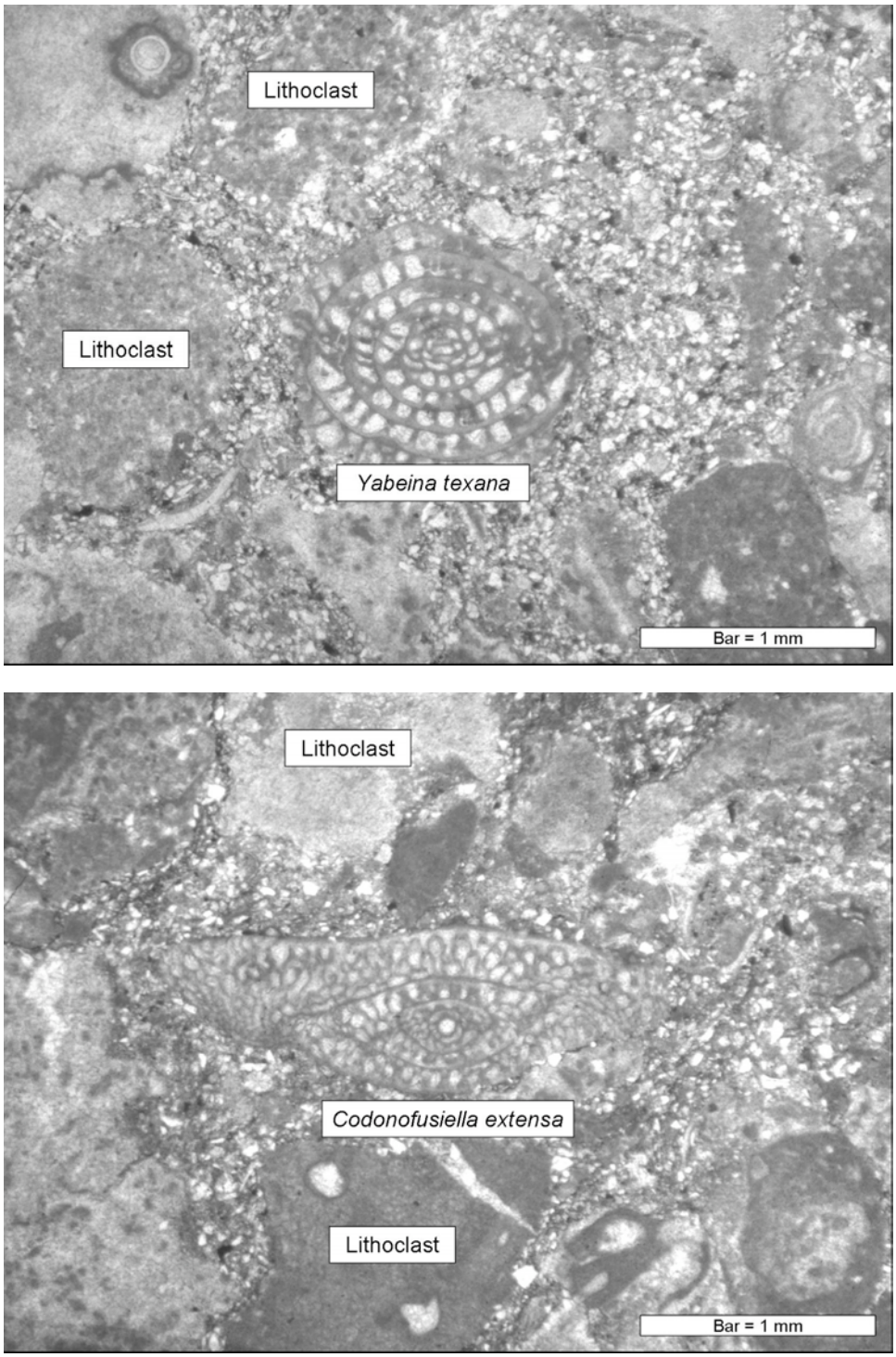

Figure 2.56: Top and Bottom micrographs: Sample DEF 3 of the A3 unit in the EF debris flow (figure 2.40). Wackestone containing lithoclasts, algae, fusulinaceans: *Codonofusiella extensa* and *Yabeina texana*, and other indistinguishable fossil fragments.

The next three sections (units A4-A6) are dark gray in color and grade into each other fining up to the top of the EF debris flow (figure 2.17 sample DEF4, figure 2.18, and 2.19 samples DEF5 and DEF6). All three samples are different in texture and grain size, but are composed of the same types of grains: small foraminifers, *Reichelina, Codonofusiella,* and *Polydiexodina* fragments, echinoid spines, bryozoans, brachiopods, fine grains of quartz, and medium to fine grains of limestone and siltstone. The lower section of the three (unit A4) is a slightly fining up, packstone with grain sizes ranging from very coarse to silt.

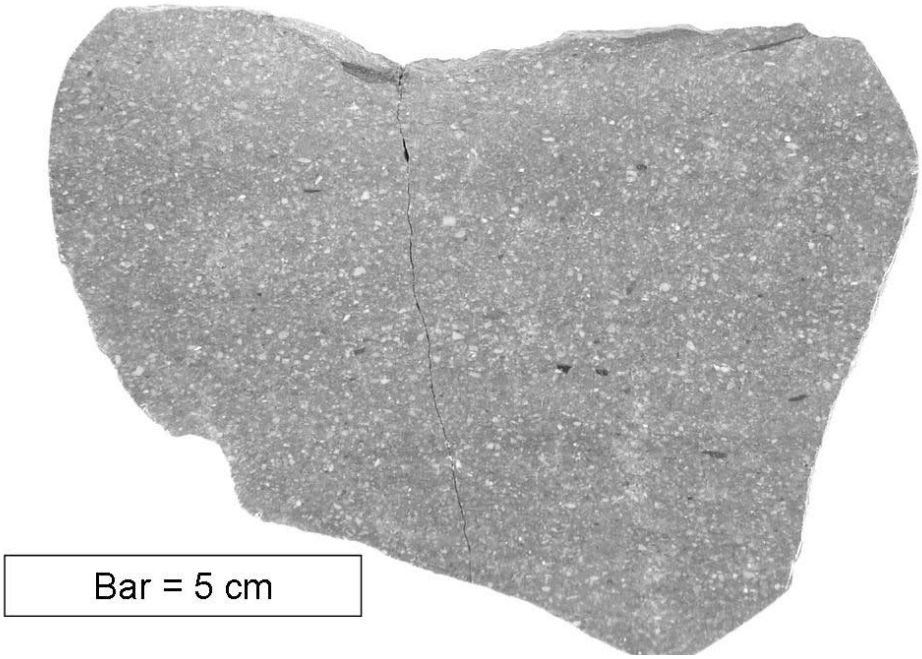

Figure 2.57: Samples DEF 4 from unit A4 in the EF debris flow in the EF section road cut. Sample is a coarse grained packstone with lithoclasts of siltstone and limestone, fossil fragments of echinoids, brachiopods, bryozoans and of the fusulinacean *Polydiexodina*, whole fusulinaceans include *Reichelina and Codonofusiella* and other indistinguishable fossil fragments.

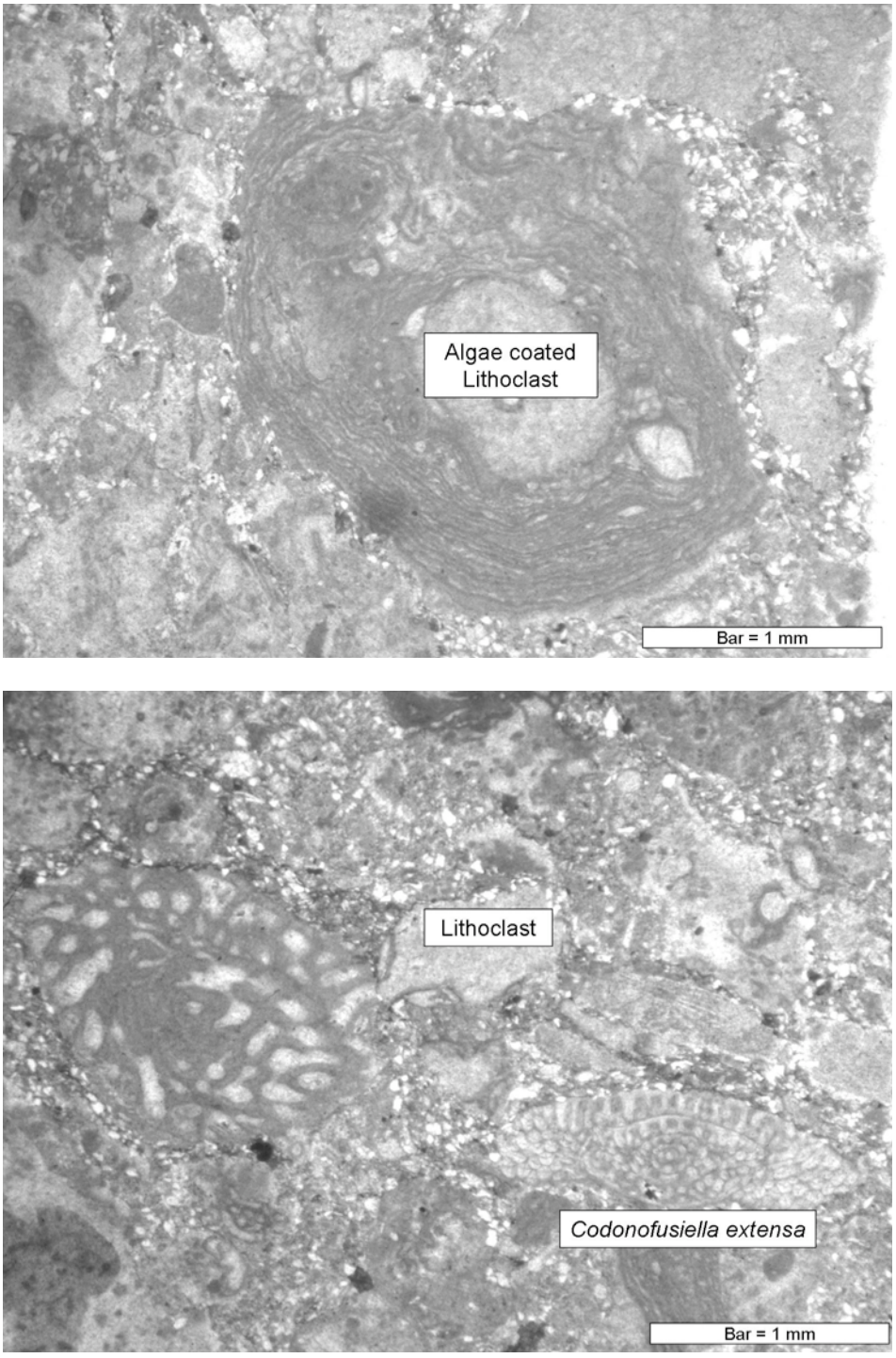

Figure 2.58: Top and Bottom micrographs: Sample DEF 4 of the A4 unit in the EF debris flow (figure 2.40). Packstone containing lithoclasts, algae, fusulinacean: *Codonofusiella extensa*, and other indistinguishable fossil fragments.

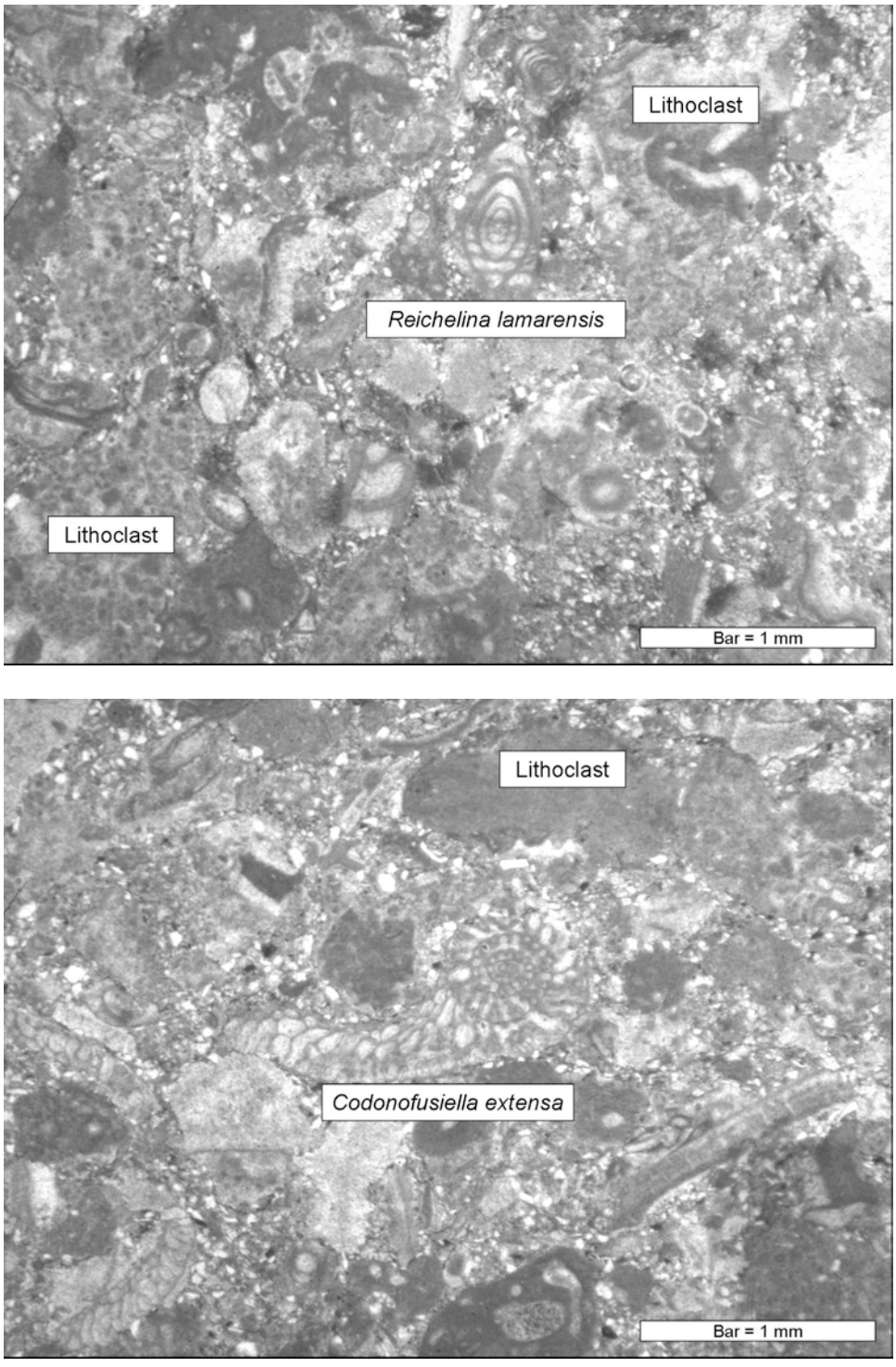

Figure 2.59: Top and Bottom micrographs: Sample DEF 4 of the A4 unit in the EF debris flow (figure 2.40). Packstone containing lithoclasts, algae, fusulinaceans: *Codonofusiella extensa* and *Reichelina lamarensis* and other indistinguishable fossil fragments.

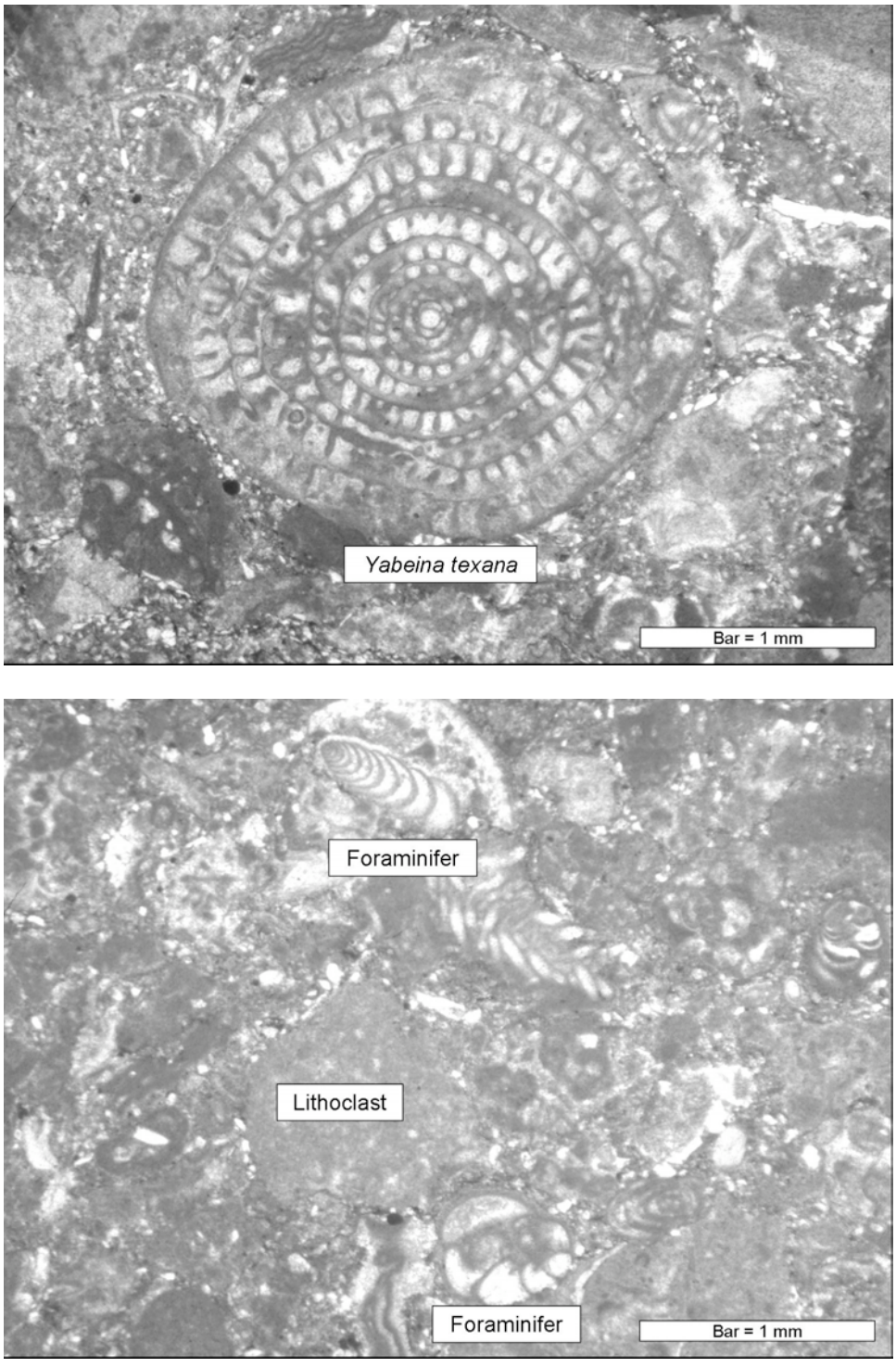

Figure 2.60: Top and Bottom micrographs: Sample DEF 4 of the A4 unit in the EF debris flow (figure 2.40). Packstone containing lithoclasts, algae, fusulinacean: *Yabeina texana*, and other indistinguishable fossil fragments.

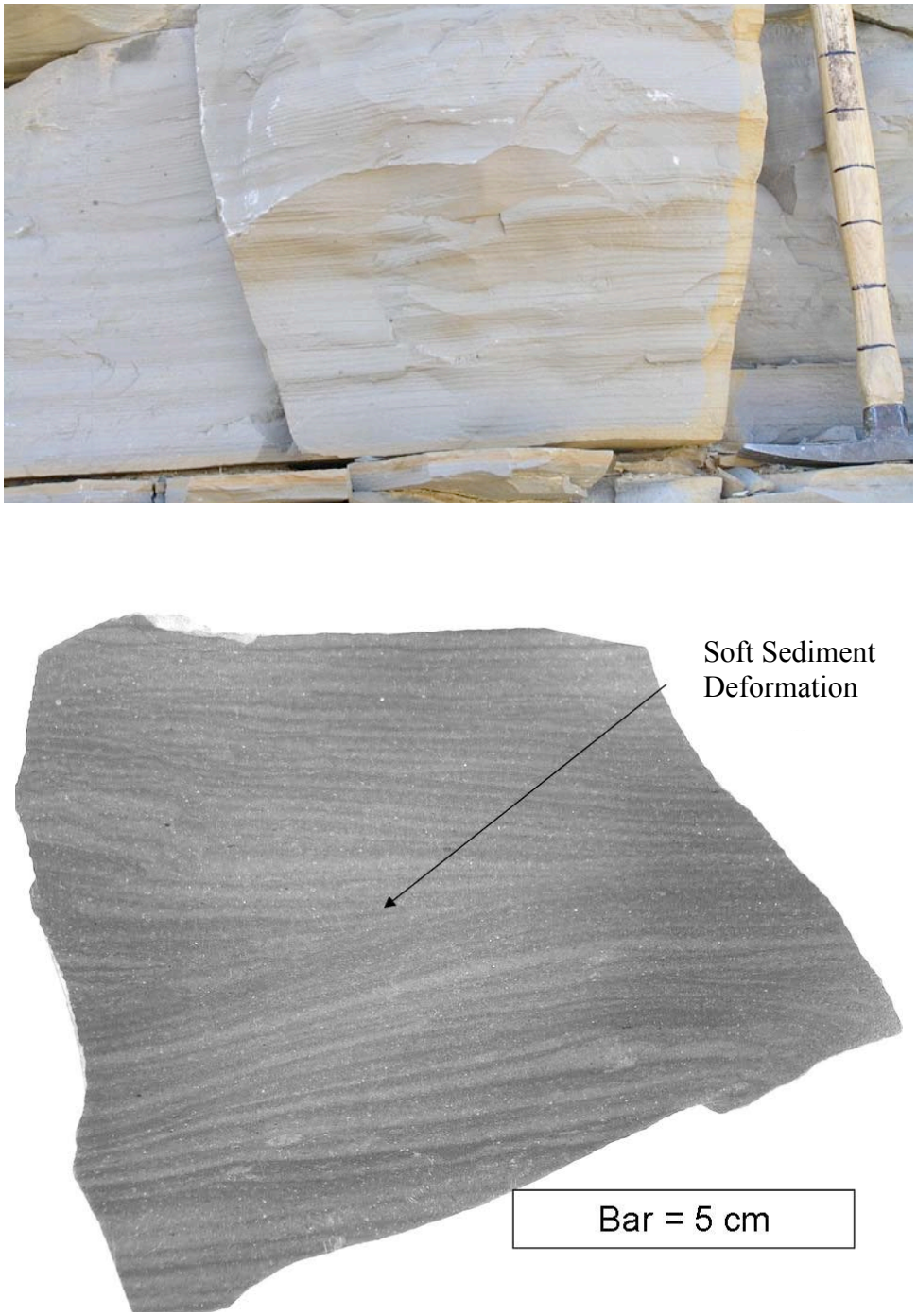

Figure 2.61: The laminated section of the upper EF debris flow (unit A5) in the EF section road cut along FM 2185. Top: Laminated section in the road cut. The hammer handle marks are in 5 cm graduations. Bottom: Slab of sample DEF 5 (figure 2.40) showing soft sediment deformation in the laminations.

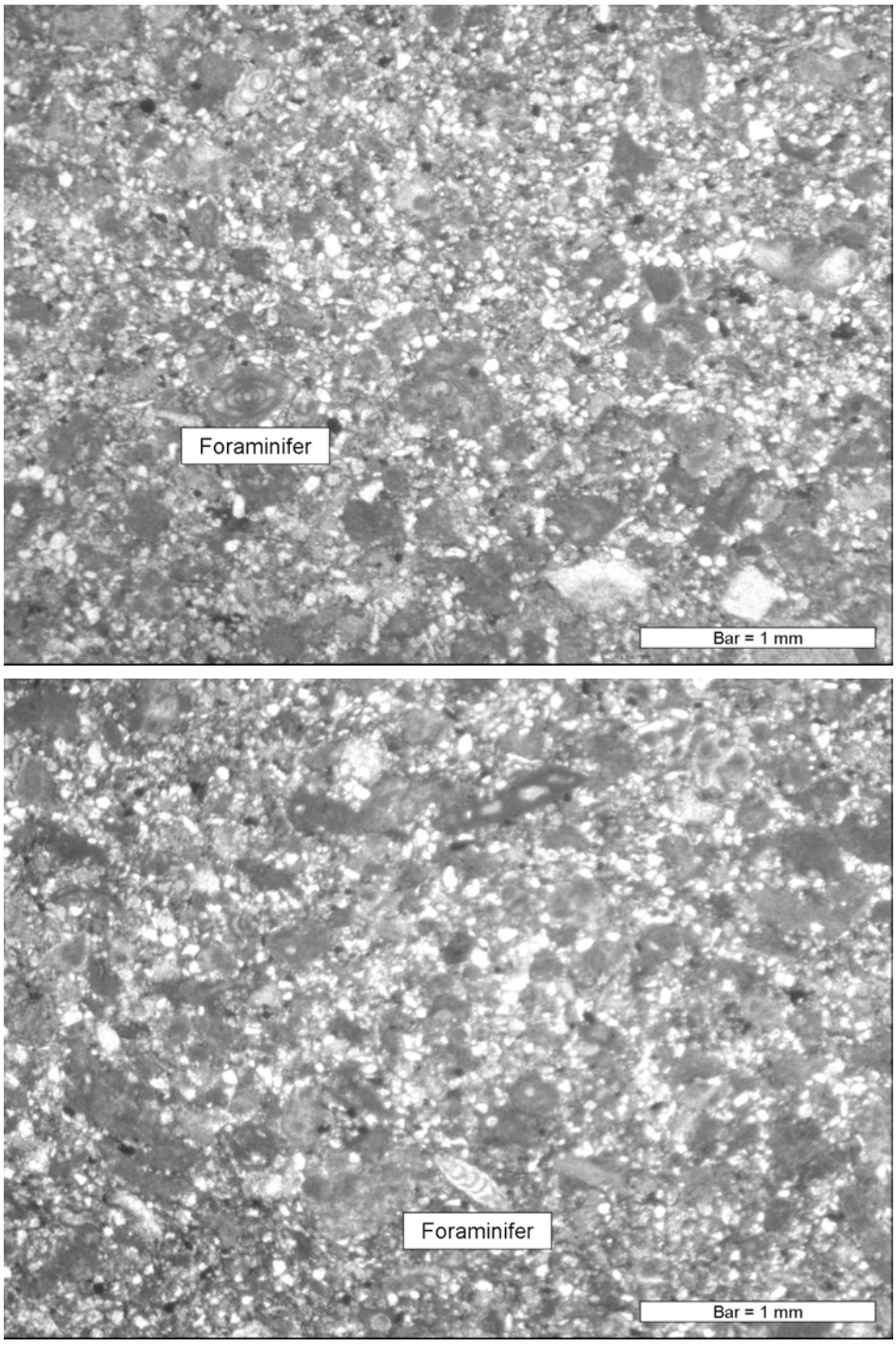

Figure 2.62: Top and Bottom micrographs: Sample DEF 5 of the A5 unit in the EF debris flow (figure 2.40). A packstone containing lithoclasts, foraminifers, and other indistinguishable fossil fragments.

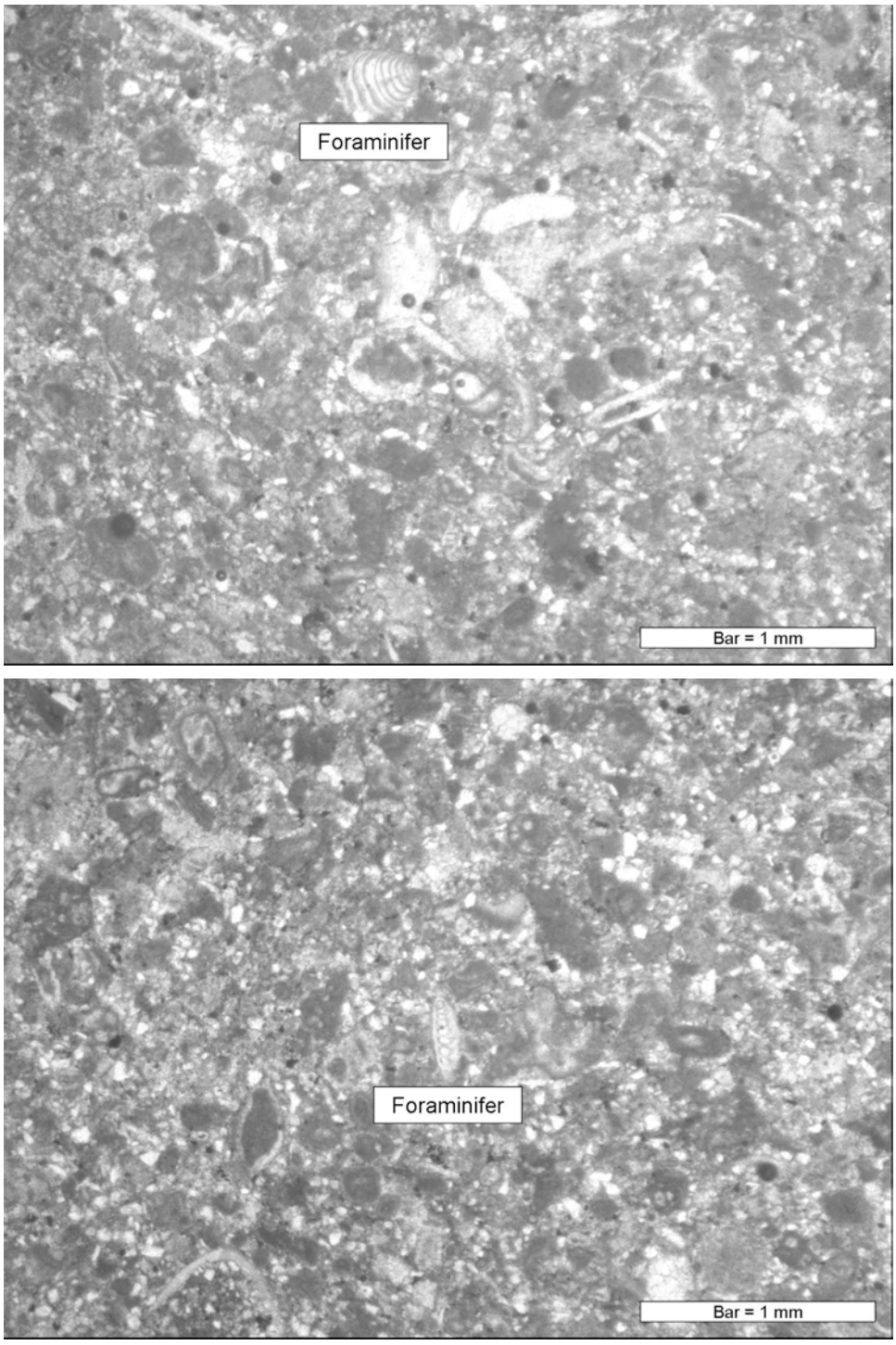

Figure 2.63: Top and Bottom micrographs: Sample DEF 6 of the A6 unit in the EF debris flow (figure 2.40). A packstone containing lithoclasts, foraminifers, and other indistinguishable fossil fragments.

Unit A5 exhibits alternating light and dark colored laminations that exhibit soft sediment deformation (figures 2.61 and 2.62). The dark laminations contain an opaque mineral, possibly pyrite, and the light laminations appear to have larger grains than the dark laminations. The last section (unit A6) of the EF debris flow is a very fine grained, slightly normally graded carbonate packstone with slight contortions to the lower few centimeters, probably due to slumping, or soft sediment deformation. Small foraminifers are present (figures 2.63 and 2.64).

Figure 2.64: Sample DEF 6 of the A6 unit in the EF debris flow (figure 2.40). A very fine grained packstone containing foraminifers, and other indistinguishable fossil fragments.

The paleodirection of flow has been difficult to determine for the EF debris flow. It appears to thin towards the east-northeast suggesting that the flow originated from the west-southwest. The closest shelf edge would have been to the southwest and would most likely be the source. Cross bedding in not present in the EF debris flow, or it is not well exposed anywhere else in the map area. Channels cut by the EF debris flow are rarely exposed and only exhibit one plane of exposure. The flow direction may be determined by observing oriented sponge spicules. In hand samples dissolved for conodonts, partially dissolved samples with abundant sponge spicules, appear to have the spicules oriented in one direction. Oriented samples were not taken in the field because this discovery was not found until after the fieldwork was concluded and the laboratory work was underway. Continued fieldwork is scheduled to expand the map area at a later date and oriented samples will be collected to address the problem with determining the flow direction of the debris flow.

The term "debris flow" is used in this thesis to maintain a consistency with the previous works in and around the map area. The term "gravite" may be a more appropriate and modern term, which describes a deposit that results from a down slope movement caused by gravity (Gani, 2004). The rheologies of the "debris flows" in the map area need to be thoroughly studied before a definite modern term is assigned.

2.3 Castile Formation

Richardson (1904) named the Castile Formation after the Castile Springs on the Gypsum Plains. It is an evaporate that was deposited during the Ochoan (Late Permian) and traditionally consists of alternating, varve-like, dark gray to light gray laminations of gypsum, calcite, and dolomite. These laminations range from 1-5 mm thick and can be planar to crenulated. Some outcrops exhibit preserved mud cracks throughout the laminations. The Castile Formation conformably overlies the Bell Canyon Formation with the Basal Limestone Member as the unit at its base. This basal unit of the Castile Formation was discussed in section 2.2 as to its age designation based on the presence of the conodont subspecies *Clarkina postbitteri hongshuiensis*.

The Castile Formation was map only to show its extent in the map area and was not the main focus of this thesis, but some interesting discoveries prompted the writer to include a more detailed description of the non-typical lithologies of the Castile Formation in the map area of the northwestern Apache Mountains.

At the Castile Formation base, the Basal Limestone Member forms a prominent mapping horizon throughout the map area and is rarely covered, due to its resistance to weathering. The upper contact of the Castile Formation with the Rustler Formation is highly unconformable and the contact is difficult to determine in most of the map area because the strata of Castile Formation grades into a rock similar in lithological characteristics of the strata of the Rustler Formation. Where the upper contact is indistinguishable in the map area, the weathering properties of the two different formations was the defining characteristic to estimate the contact. The upper part of the

Castile Formation in the map area tends to form smooth shallow slopes and the Rustler Formation tends to form rough steep slopes.

The Castile Formation as exposed in the Apache Mountains is approximately 50-60 meters thick in the map area and has several different textures up through its extent (figure 2.65). Above the contact with the Bell Canyon Formation the Basal Limestone Member is approximately 1.0-1.5 meters thick, has dark to medium gray laminations ranging from 3-7 mm thick, a strong petroliferous odor, and is pinkish towards the top with pink calcitic and dolomitic nodules. The next 5.5 meters of overlying strata is a laminated evaporite that exhibits in the lower part preserved mud cracks in crenulated 1-3 mm thick laminations that are reddish-tan to brown in color (figure 2.66 A). The next 7 meters of section are varve-like light to medium gray 0.5-2 mm thick laminations with slight crenulations (figure 2.66 B). This section of strata is very characteristic of the typical Castile Formation exposures in the type area of the Guadalupe Mountains. The next 10 meters of the Castile Formation is a matrix supported conglomerate composed of fragments of rock from the underlying previously described Castile section ranging 1-20 cm in diameter, and with sparse reddish tan sandstone and siltstone clasts 1-20 cm in size, with rare reddish tan sandstone boulders up to 20-60 cm in size in a matrix of unknown microcrystalline evaporite (figure 2.67). The next 10 meters of section is a clast supported breccia composed mostly of fragments of laminated older Castile Formation strata ranging from 5-20 cm in size with microcrystalline cement. The brecciated section of the Castile Formation in the map area is very similar in structure and composition to the strata of the middle part of the Tessey Formation in the Glass Mountains described by

King (1931) (figure 2.68). The remaining 20 meters to the formation top is a light tan to reddish-brown undistinguishable breccia (figure 2.69). The Rustler Formation drapes over the Castile Formation forming an unconformable contact; which is most likely due to extensive dissolution (figure 2.70) (Owen, 1951).

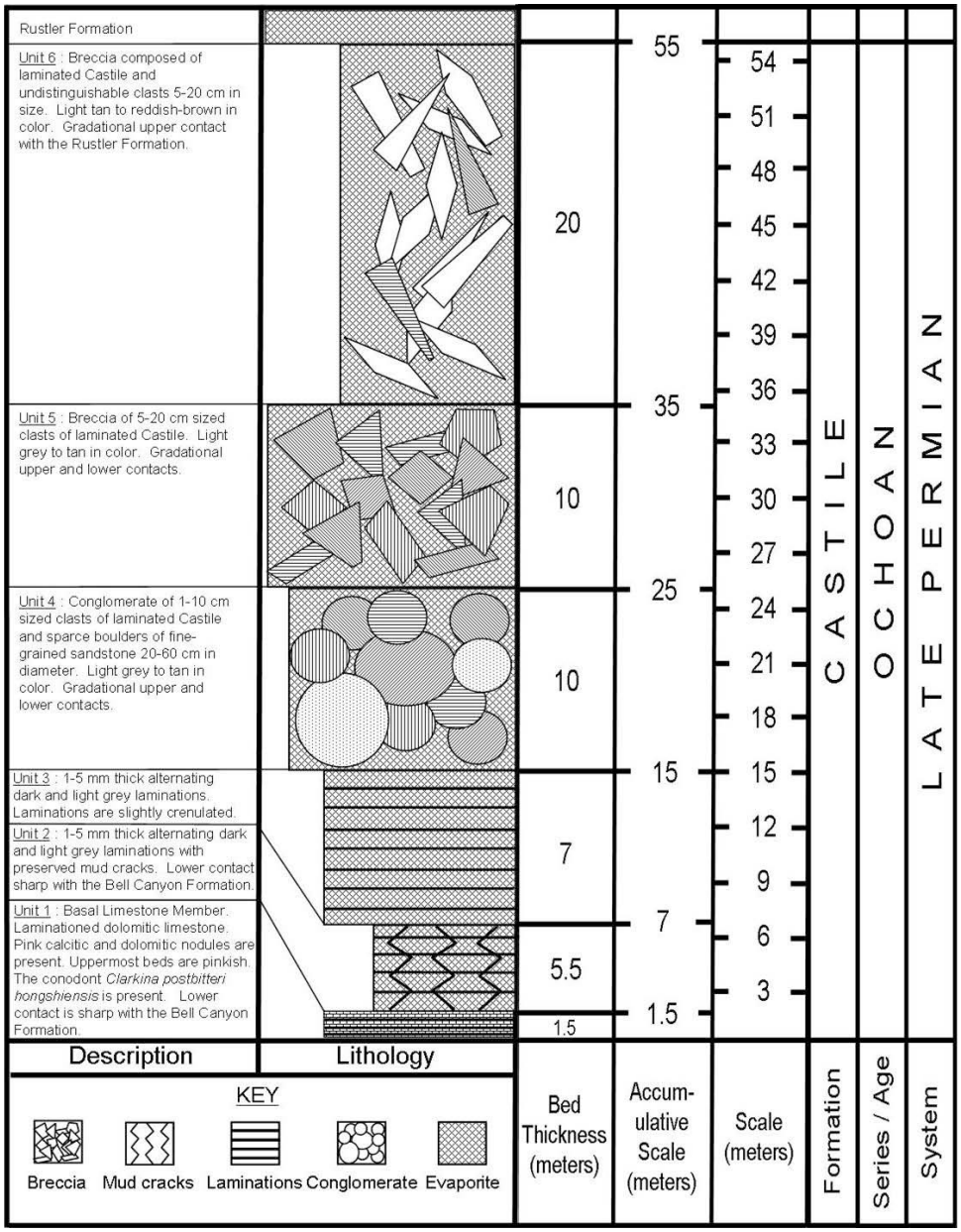

Figure 2.65: Castile Formation stratigraphic column.

Figure 2.66: Photos A and B exhibit typical exposures of the lower section of the Castile Formation in the map area. Photo A shows mud cracks in the lower part of the Castile Formation a few meters above the EF section road cut on FM 2185. This texture can also be seen in the basal Castile in the M section road cut on FM 2185. Photo B illustrate exposures of the more "traditional" laminated Castile Formation near the Guadalupe Mountains. Jacob staff is in 10 cm divisions. Photo B location is shown in figure 2.4.

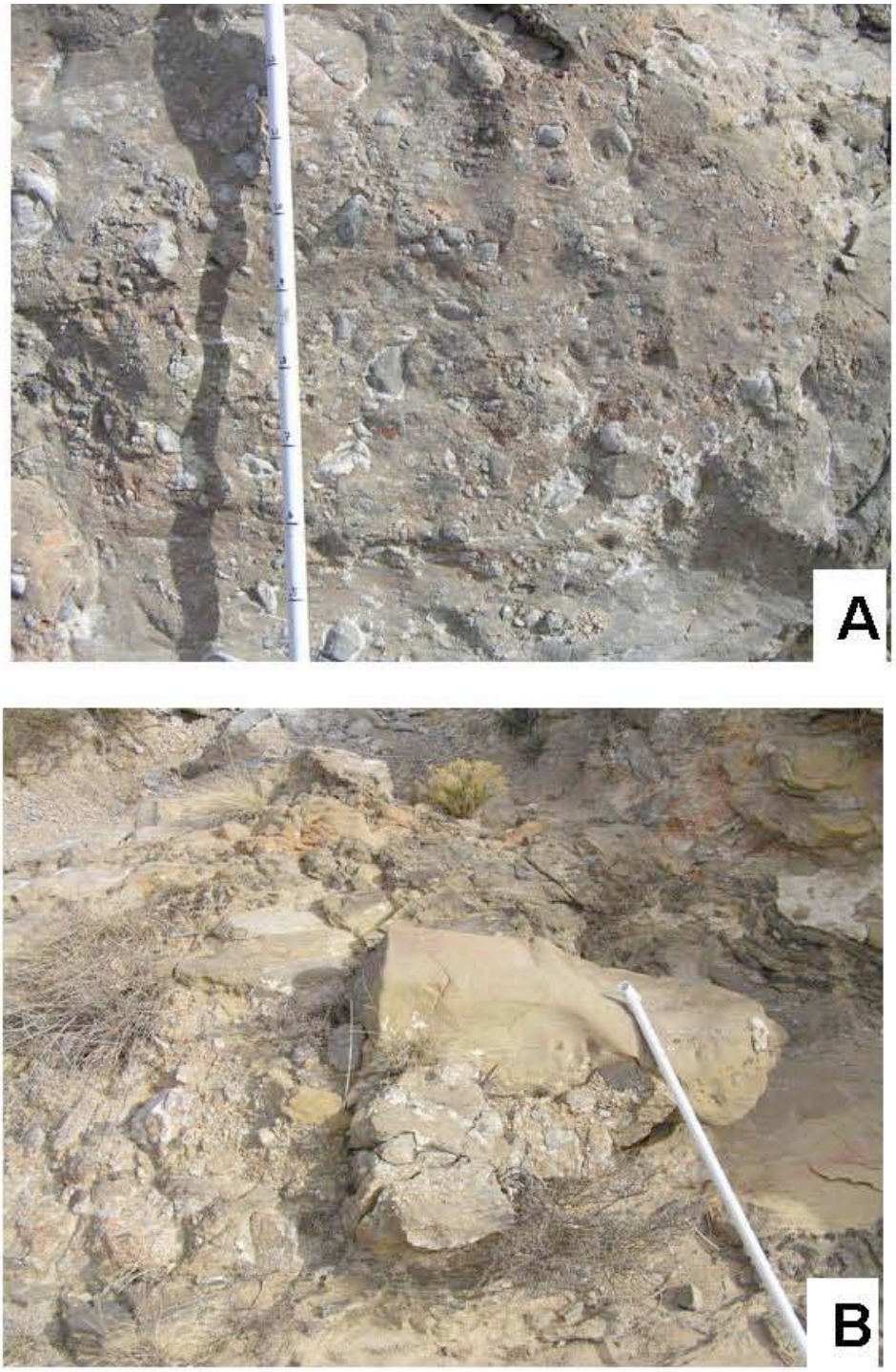

Figure 2.67: Photos A, and B exhibit typical exposures of the conglomerate section of the Castile Formation in the map area. Photo B shows a large sandstone boulder. Jacobs staff is in 10 cm divisions. These photo locations are shown in figure 2.4.

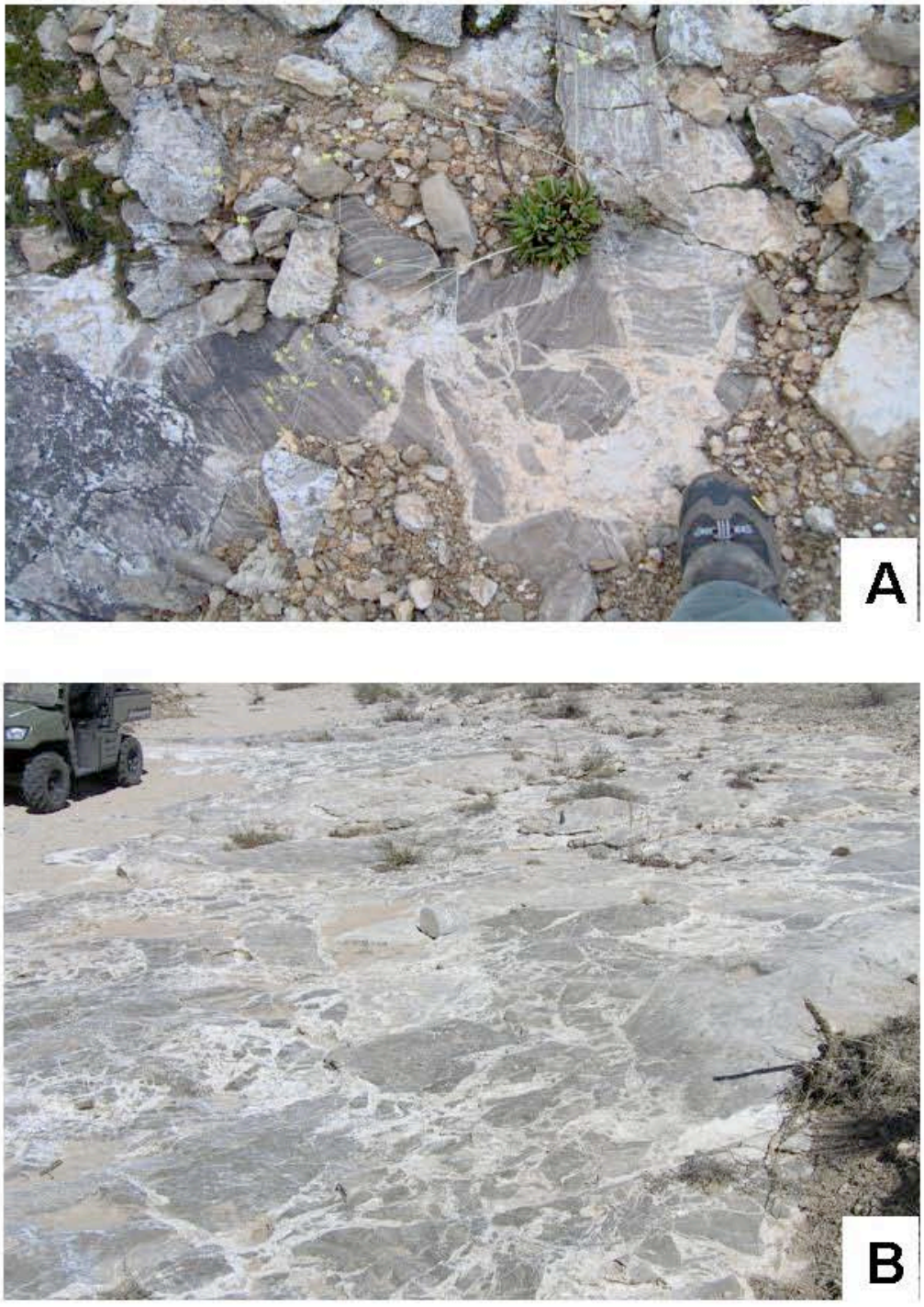

Figure 2.68: Photos A and B exhibit typical exposures of the breccia section of the Castile Formation in the map area. The top left of photo B is an All-Terrain-Vehicle (ATV) for scale. These photo locations are shown in figure 2.4.

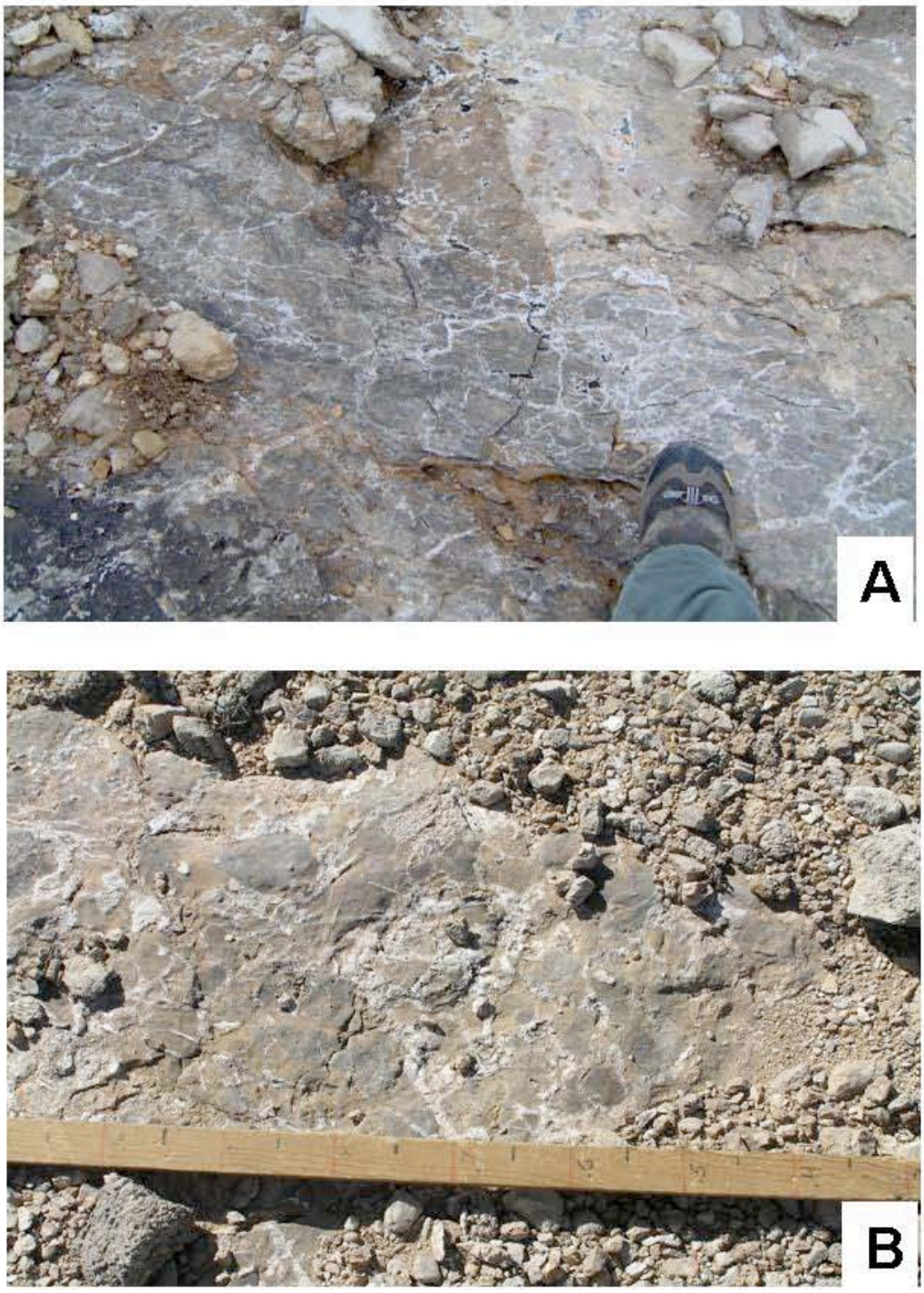

Figure 2.69: Photos A and B exhibit typical exposures of the upper section of the Castile Formation in the map area. The Jacob staff is in 10 cm divisions. These photo locations are shown in figure 2.4.

2.4 Rustler Formation

The Rustler Formation was also named by Richardson in 1904. The age designation of the Rustler Formation has been questionable to either Late Paleozoic or Early Mesozoic (Adams, 1944). Walter (1953) described molluscan fossils collected in the uppermost part of the Rustler Formation, near the Guadalupe Mountains, that are similar to Russian and Indian upper Permian faunas, thus suggesting that the strata of the Rustler Formation was deposited during the Ochoan age (Late Permian). Fossils in the map area have not been found, most likely because fossils have only been found in the uppermost beds of the Rustler Formation, and in the map area the entire extent of the formation is not present, and only the lowermost beds of strata appear to be present. This formation forms significant topographic highs in the map area (Appendix A), and the thickest exposure of this formation is approximately 60 meters thick, measured from the lower contact with the Castile Formation to the top of the hill about 1000 feet southwest from the AV section across a fault (Appendix A). The Rustler Formation is generally a yellowish gray to pale yellowish brown, thick bedded dolomite (Owen, 1951). The contact between the Castile and Rustler Formations in the western Delaware basin has been described by Adams (1944) as an angular unconformity. This angular unconformity has not been identified in the map area of this thesis. The contact is frequently difficult to determine, especially due to the lithological similarities of the two formations at the contact and also due to the nature of the strata of the Rustler Formation to drape over that of the Castile Formation (figure 2.70) due to possible dissolution (Owen, 1951). In rare outcrops, a 3-5 meter thick, thin to medium bedded, tan to red, fine grained sandstone is

present at the contact with the Castile Formation (figure 2.71). Kennedy (2009) conducted a more lithological study of the basal Rustler Formation sandstone and wrote in his thesis:

> "Grains within the sandstone are rounded to subrounded and consist largely of quartz (majority), and minor amounts of feldspar (orthoclase), lithics and heavy minerals set in a carbonate matrix. Plagioclase feldspar within the sandstone has largely been altered to clay suggesting large volumes of fluid have been transported through the sandstone since Upper Permian time."

However this basal sandstone of the Rustler Formation is so rare in outcrops that it is not useful as a continuous mappable unit.

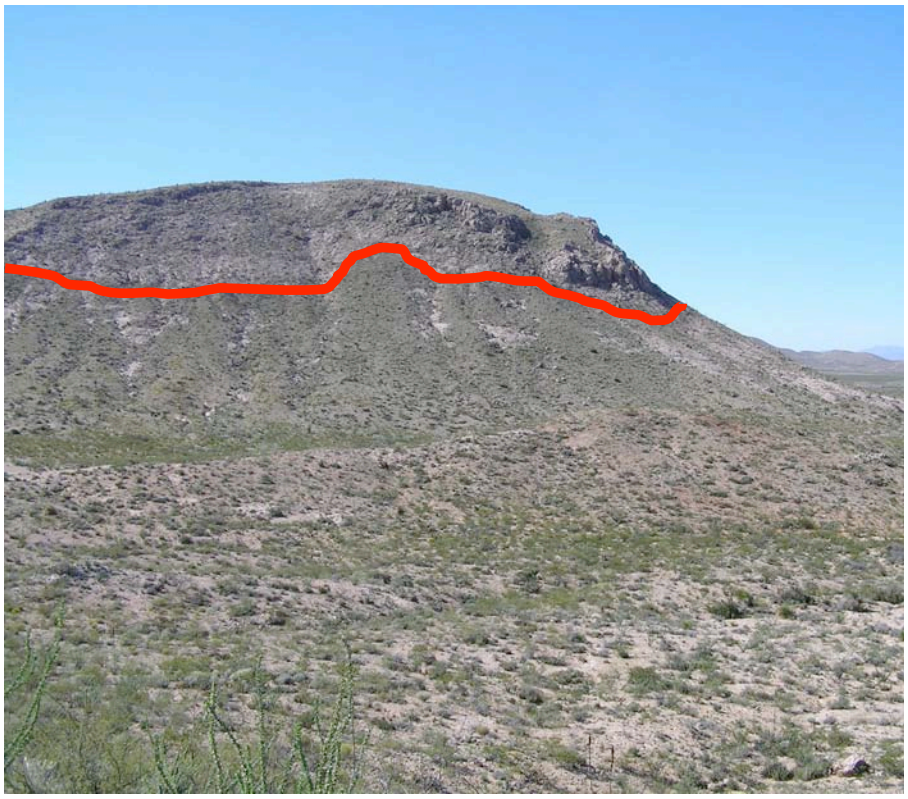

Figure 2.70: Rustler Formation (top of the hill) draping over the Castile Formation (red line marks the contact). This "Rustler Hill" is the 4645' bench marked hill in the northeast quadrant of the map area, approximately ¼ mile southeast from the M section (Appendix A and also located on figure 2.4).

Figure 2.71: Top: Red sandstone at the base of the Rustler Formation. Bottom: Close up of sandstone in the Rustler Formation, bar equals 10 cm. Photo locations shown in figure 2.4.

2.5 Cenozoic Deposits

The exposures in the broad low-lying valleys of the map area are filled with alluvium deposits of cobble to silt sized grains with occasional gravel lenses (Appendix A). The floors of the recent washes and draws are covered with rounded gravel primarily composed of limestone. Some of the sandstone and siltstone clasts are probably derived from the Permian rocks of the surrounding strata of the Delaware and Apache mountains. These Cenozoic sediments most likely were deposited during rare fluvial intervals due to localized flash flooding (figure 2.72).

Figure 2.72: Quaternary gravel in a dry wash on the Castile Formation.
Photo location shown in figure 2.4.

CHAPTER 3

STRUCTURE

The oldest known tectonic features near the Apache Mountains are in Pre-Cambrian rocks in the southern part of the Sierra Diablo Mountains, near Van Horn, southwest of the map area (figure 3.1). These Pre-Cambrian rocks are poorly exposed and offer insufficient data to fully understand the relationship between the tectonic features they display and the ones exposed in the Apache Mountains (King, 1948).

Late Pennsylvanian tectonic features are widely exposed in the Sierra Diablo Mountains and King (1948) has interpreted that the Sierra Diablo area was uplifted, faulted, and deeply eroded during the Late Pennsylvanian, pre-Wolfcamp time. The faults in the Sierra Diablo trend west-northwest which lie parallel to the tectonic features exposed in the Apache Mountains (King, 1948).

As the Delaware basin area began to subside during the Late Pennsylvanian, Pre-Wolfcamp time, three monoclinal flexures bordering the west and northwest edge of the basin began to form: the Bone Spring, Babb, and Victorio flexures (figure 3.1) (King, 1948). The Bone Spring flexure trends to the northeast near the Guadalupe Mountains. This flexure is overlain by the Captain Reef along the same trend. The Babb and Victorio flexures are located in the southern Sierra Diablo Mountains and trend west-northwest with the reef zone in the Apache Mountains following the same trend (King,

1948). Mesozoic tectonics little affected the Apache, Guadalupe and Delaware mountains area leaving the region as a broadly warped structure (King, 1948).

The Apache, Guadalupe, and Delaware mountains were formed from the uplifting of major fault blocks during the Late Cenozoic; the Delaware uplift (Wood, 1965). The major fault trends associated with these mountain ranges are north-northwest and west-northwest normal faulting with very steep, near vertical planes (King, 1948), and follow the same trends as the above mentioned flexures. Along with the Bone Spring, Babb, and Victorio flexures, three other tectonic features exist in the Guadalupe, Delaware and Apache mountains region: the Border fault zone, Stocks fault, and the Seven Heart graben complex (figure 3.1). The north-northwest trend of faults along the west side of the Guadalupe and Delaware mountains is called the Border fault zone and runs from just north of the Guadalupe Mountains to just south of the Apache Mountains (King, 1948). The Stocks fault runs in a west-northwest trend along the north side of the Apache Mountains intersecting the Border fault zone. The Seven Heart graben complex exists where the Border fault zone and Stocks fault intersect (figure 3.1) (King, 1948, McNutt, 1948). Present fieldwork has established similar findings to those of King and McNutt as to the trends of the major faults present in the map area.

Four dominant north-northwest trending normal faults have been identified in the map area (faults 1, 3, 4, and 5; figure 3.2) by traverse, aerial photography, cross-sections, and vegetation change (*Agave lechuguilla* is more abundant on exposures of the Castile and Rustler Formations than on exposures of the Bell Canyon Formation). The north-northwest trending faults have estimated displacements, calculated from cross-sectional

work, ranging from 200 to 600 feet with the down thrown blocks to the west. Fault 1 is continuous through the map area, and it is also the largest fault in the map area. Its displacement increases from the south with about a 400 foot throw to the north with roughly a 600 foot throw. Fault 4 was map from cross-sectional work.

Subordinate west trending faults have also been identified; one on the northwest side of FM 2185 (not map), and the other (fault 6, figure 3.2) covered in a valley trending west in the southeastern part of the map area. This fault doesn't appear to have much displacement. It is identified only by the slight dip change from the north side of the valley at six degrees to the northwest to the south side of the valley at five degrees to the south. Approximately 100 meters southeast from FM 2185 along the EF debris flow from the EF section road cut, a change in dip occurs which suggests a minor fault (fault 2, figure 3.2) within the Castile Formation trending near north. The general dipping trend of the strata in the map area is northeast 5-10 degrees. Several fractures can be found in the map area with spar (dog-tooth) calcite fill (figure 3.3). The size of these fractures range from 1-50 cm in width. The displacement of these fractures is on the scale of 0.25-5 meters (figure 3.4).

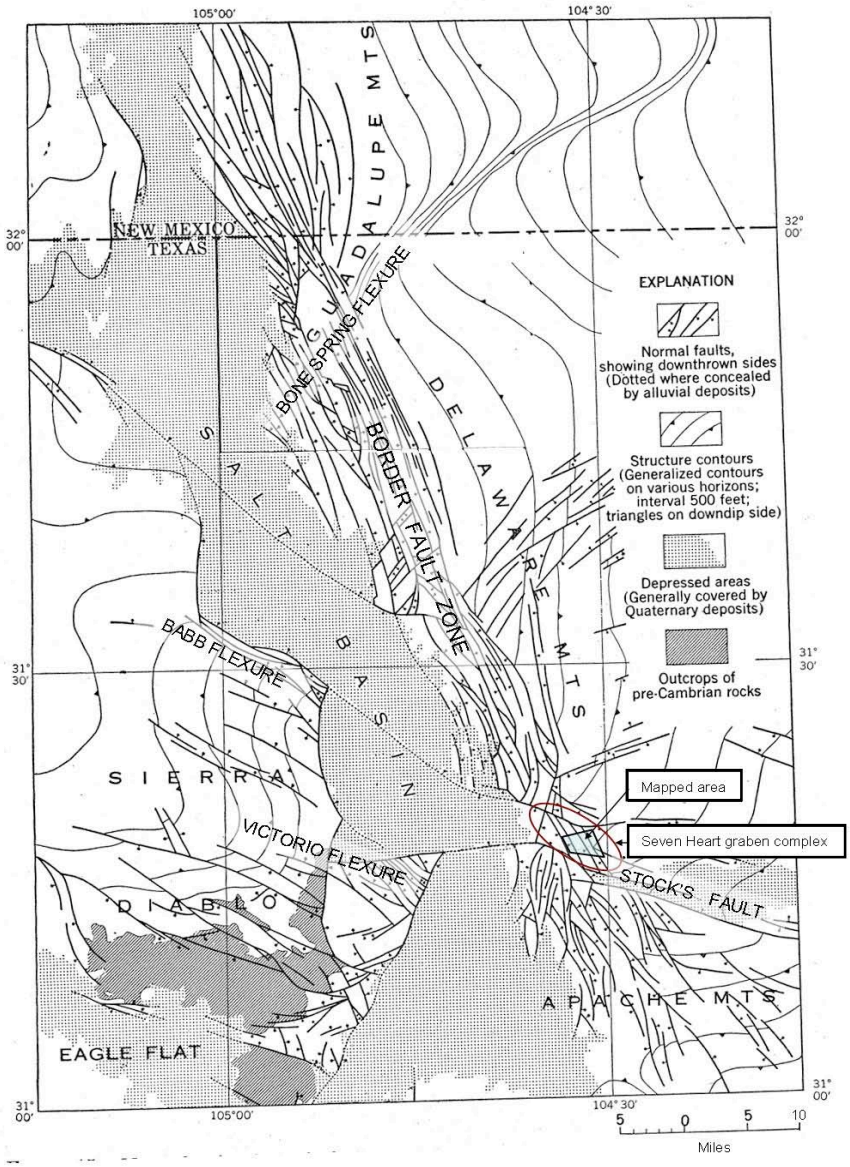

Figure 3.1: Regional structure map showing the major tectonic features of the region (Modified from King, 1948). The map area is in the southeastern portion of the map. The Seven Heart graben complex is outlined in red and is located at the intersection of the Border fault zone trending north-northwest along the Delaware Mountains and the Stock's fault trending west-northwest along the Apache Mountains. The Babb and Victorio flexures trend west-northwest along with the Stock's fault and the Apache Mountains reef trends. The Bone Spring flexure trends north-northeast along the Guadalupe Mountains reef trend.

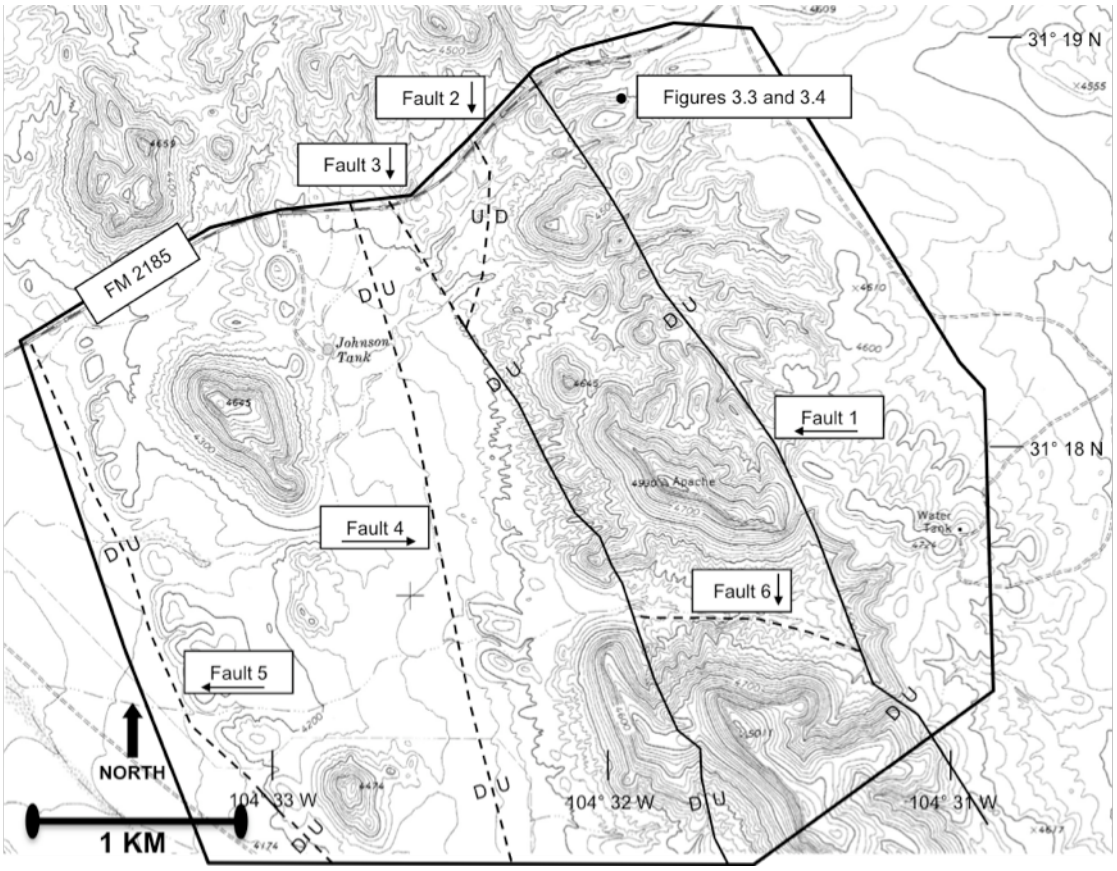

Figure 3.2: Major faults in the map area, outlined in a solid bold line. Solid lines indicate exposed faults, and dashed lines indicate covered or inferred faults. Fault 1 is the largest and most continuous fault in the map area. It has a maximum displacement of about 600 feet at its north end. The displacement of faults 3, 4 and 5 are less than 300 feet. Faults 2 and 6 have displacements of less than 20 feet. One minor fault is indicated by the small circle and is illustrated in figure 3.4.

Figure 3.3: Dog-tooth calcite fill in one of the many fractures in the map area. Hammer is 30 cm in length for scale. Location of this fracture is shown in figure 3.2.

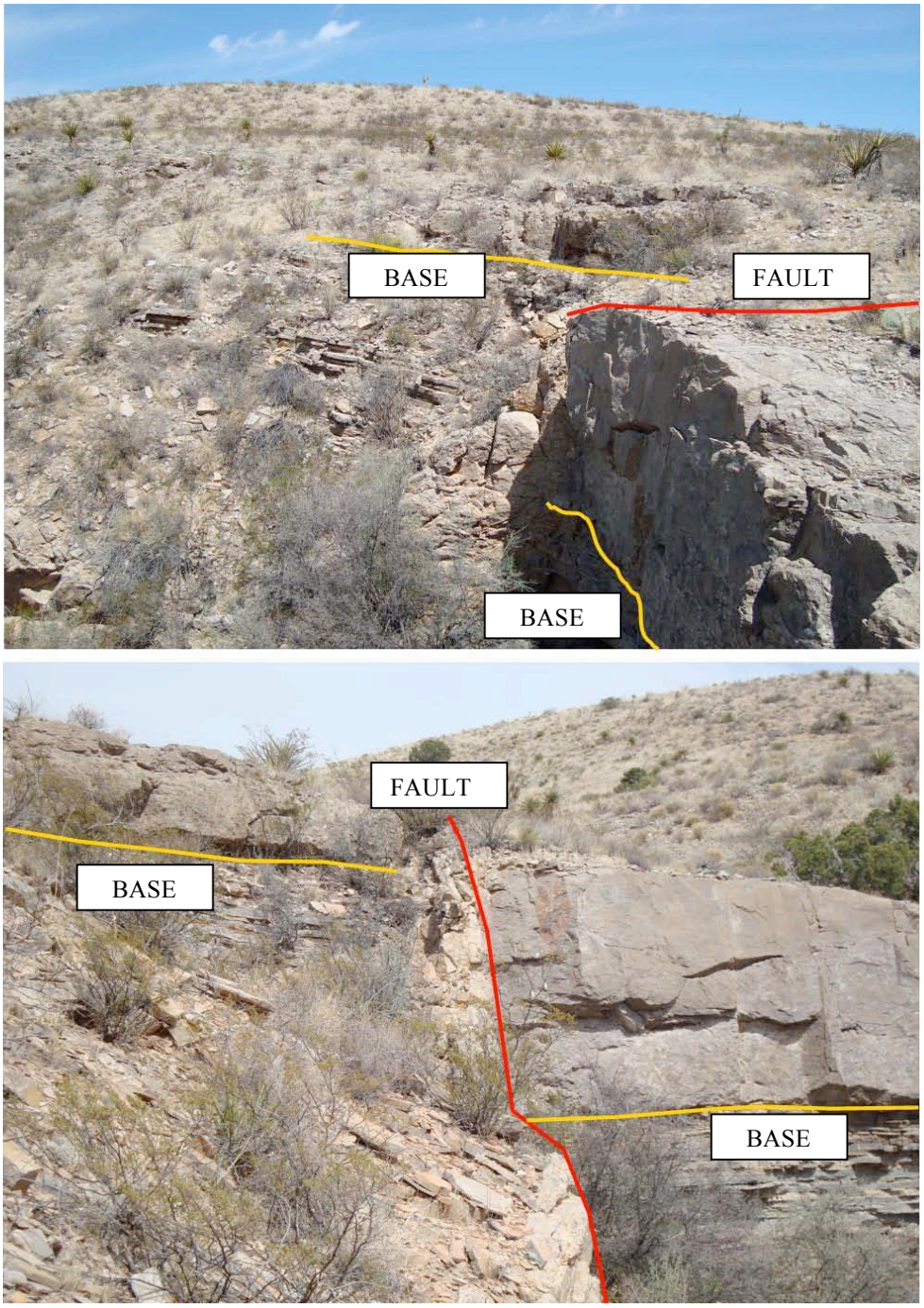

Figure 3.4: Minor fault cutting the G debris flow with a 2 meter displacement. Red lines show the fault trace and the yellow lines mark the base of the debris flow. Top: Viewing perpendicular to and across the fault. Bottom: Viewing into the strike of the fault. Location of this fault is shown in figure 3.2.

CHAPTER 4

CONCLUSIONS

The study of the exposed rock in the northwestern Apache Mountains has provided a better understanding of the age relationships of the faunal successions of the uppermost Guadalupian strata by defining the EF section as at least partially equivalent to the Bell Canyon Reef Trail Member and with faunal evidence supporting that the B, A, G, and K sections are pre-Lamar Limestone Member equivalent.

The Pre-Lamar strata of the Bell Canyon Formation in the Guadalupe Mountains, which includes the Hegler, Pinery, Rader, and McCombs Limestone Members, can be generally correlated to strata of the B, A, G, and K sections in the Apache Mountains by the presence of the fusulinacean genus *Polydiexodina* and conodont species *Jinogondolella aserrata* and *J. postserrata.* Further study of the conodonts, radiolarians, and foraminifers in progress by the Nestells and Wardlaw will determine the detailed correlation of the two areas. Part of the Reef Trail Member of the Bell Canyon Formation in the Guadalupe Mountains can be correlated to the EF section in the Apache Mountains by the presence of the fusulinacean species *Paraboultonia splendens* Skinner and Wilde and the conodont species *Clarkina postbitteri hongshuiensis* Henderson, Mei, and Wardlaw. This correlation has extended the working knowledge of the proper placement of the upper boundary between the Lopingian and Guadalupian Series.

The EF debris flow is exposed on south-southeast trends from the EF and M section road cuts along fault cuts, and it varies in thickness due to its channelization of

the underlying strata. The very basal, megabreccia unit of the EF debris flow is composed mostly of small to large pieces or blocks of reefal clasts, most likely sourced from the reef edge to the south from the present Apache Mountains core. The debris flow continues to fine up from several meter wide clasts to cobble and pebble sized to fine grained clasts with fine laminations from turbidity flows.

The detailed geologic map (Appendix A) shows major structural trends and covered faults, the distribution of strata of the Rustler, Castile, and Bell Canyon Formations, a cross-section perpendicular to the fault trend, and the locations of the road cut sections and their associated debris flows.

APPENDIX A

GEOLOGIC MAP

(See Supplemental File)

REFERENCES

Adams, J.E., 1944, Upper Permian Ochoa Series of Delaware basin, West Texas and southeastern New Mexico. Bull. Amer. Assoc. Petrol. Geol., v. 28, p. 1596-1625.

Anderson, R.Y., Walter, D.E. Jr., Kirkland, D.W., and Snider, H.I., 1972, Permian Castile varved evaporite sequence, West Texas and New Mexico. GSA Bulletin, v. 83, p. 59-86.

Blanchard, W.G., Jr., and Davis, M.J., 1929, Permian stratigraphy and structure of parts of southeastern New Mexico and southwestern Texas. Bull. Amer. Assoc. Petrol. Geol., v. 13, p. 957-995.

Bybee, H.P., 1931, Some Major Structural Features of West Texas. University of Texas Bulletin, 3101, p. 19-26.

Crandall, K.H., 1929, Permian stratigraphy of southeastern New Mexico and adjacent parts of western Texas. Bull. Amer. Assoc. Petrol. Geol., v. 13, p. 927-944.

Cys, J.M., 1983, Potential Middle Permian (Guadalupian) stratotype in West Texas. Permophiles, v. 7, p. 5.

DeFord, R.K., 1951, Apache Mountains of Trans-Pecos Texas Guidebook. West Texas Geol. Society Guidebook No. 51-26. 56p.

Dunbar, C.O. and Skinner, J.W., 1937, Permian Fusulinidae of Texas, *in* The Geology of Texas, Vol. III, Upper Paleozoic ammonites and fusulinaceans. Univ. Texas Bull.3701, p. 523-733.

Dutton, S., Holtz, M., Tremblay, T., Zirczy, H., 2000, Expansion of Gas Reservoir Data Base, Permian Basin, Texas. The Permian Basin: Proving Ground for Tomorrow's Technologies: West Texas Geological Society Publication Number 00-109. p. 197-204.

Dutton, S.P., W. A. Flanders, and M.D. Barton, 2003, Reservoir characterization of a Permian deep-water sandstone, East Ford field, Delaware Basin, Texas. Bull. Amer. Assoc. Petrol Geol. v. 87, p. 609 – 627.

Dutton, S.P., 2008, Calcite cement in Permian deep-water sandstones, Delaware Basin, West Texas: Origin, distribution, and effect on reservoir properties. Bull. Amer. Assoc. Petrol. Geol. Bulletin, v. 92, p. 765-787.

Gani, M.R., 2004, From Turbid to Lucid: A straightforward approach to sediment Gravity flows and their deposits. The Sedimentary Record, v. 2, no. 3, p. 4-8.

Gradstein, F.M., Ogg, J.G., Smith, A.G., Bleeker, W. and Lourens, L.J., 2004, A new Geologic Time Scale with special reference to Precambrian and Neogene. Episodes, v. 27, no. 2, p. 83-100.

Girty, G.H., 1908, The Guadalupian Fauna. U.S. Geol. Survey Prof. Paper 58. 651 p.

Harms, J.C., 1974, Brushy Canyon Formation, Texas: A deep-water density current deposit. Geological Society of America Bulletin, v. 85, p. 1763-1784.

Harms, J.C. and Williamson, C.R., 1988, Deep-water density current deposits of Delaware Mountain Group (Permian), Delaware Basin, Texas and New Mexico. Bull. Amer. Assoc. Petrol. Geol., v. 72, p. 299-317.

Hill, C.A., 1999, Reevaluation of the Hovey channel in the Delaware Basin. West Texas. Bull. Amer. Assoc. Petrol. Geol., v. 82,. p. 277-294.

Hills, J.M., 1972, Late Paleozoic sedimentation in West Texas Permian Basin. Bull. Amer. Assoc. Petrol. Geol., v. 56, p. 2303-2322.

Hills, J.M., 1984, Sedimentation, Tectonism, and Hydrocarbon generation in the Delaware Basin, West Texas and southeastern New Mexico. Bull. Amer. Assoc. Petrol. Geol., v. 68, p. 250-267.

Jin, Y., Shen, S., Henderson, C.M., Wang, X., Wang, W., Wang, Y., Coa, C., Shang, Q., 2006, The Global Stratotype Section and Point (GSSP) for the Boundary between the Capitanian and Wuchiapingian Stage (Permian). Episodes, v. 29, no. 4, pp. 253-262.

Kennedy, W., 2009, Geology of part of the northwestern Apache Mountains, southeast Culberson County, West Texas, USA. Master's thesis, The University of Texas at Arlington, Texas. 84 p.

King, P.B., 1935, Outline of structural development of Trans-Pecos Texas: Bull. Amer. Assoc. Petrol. Geol., v. 19, p. 221-261.

King, P.B., 1947, Permian correlations, Bull. Amer. Assoc. Petrol. Geol., v. 31, p. 774-778.

King, P.B., 1948, Geology of the Southern Guadalupe Mountains, Texas. U. S. Geol. Surv. Prof. Paper, 215. 183 p.

King, P.B., and King, R.E., 1928, The Pennsylvanian and Permian stratigraphy of the Glass Mountains. Texas University Bulletin, 2801, p. 109-145.

King, P.B. and Newell, N.D., 1956, McCombs Limestone Member of Bell Canyon Formation, Guadalupe Mountains, Texas. Bull. Amer. Assoc. Petrol. Geol., v. 40, p. 386-387.

Kirkland, D.W., 2003, An explanation for the varves of the Castile evaporites (Upper Permian), Texas and New Mexico, USA. Sedimentology, v. 50, p. 899-920.

Lambert, L.L., Wardlaw, B.R., Nestell, M.K., and Nestell, G.P., 2002. Latest Guadalupian (Middle Permian) conodonts and foraminifers from West Texas. Micropaleontology, 48, p. 343-364.

Lloyd, E.R., 1929, Capitan Limestone and associated formations of New Mexico. Bull. Amer. Assoc. Petrol. Geol., v. 13, p. 645-658.

McNutt, G.R., 1948, Geology of southern Delaware Mountains and northwestern Apache Mountains, Texas. Univ. Oklahoma, PhD. Dissertation. 82 p.

National Park Service website: www.nps.gov/gumo/naturescience/geologicformations.htm

Nestell, G.P., Nestell, M.K., 2006, Middle Permian (Late Guadalupian) foraminifers from Dark Canyon, Guadalupe Mountains, New Mexico. Micropaleontology, v. 52, p. 1-50.

Nestell, M.K., Nestell, G.P., Bell, G.L. Jr., 2006a, Van Horn to Apache Mountains to southern Delaware Mountains, Texas Permian (Late Guadalupian-Lopingian). Field Trip Guidebook, Permian Basin Section, SEPM pub. 2006-46.

Nestell, M., Nestell, G., Wardlaw, B., and Sweatt, M., 2006b, Integrated biostratigraphy of foraminifers, radiolarians and conodonts in shallow and deep water Middle Permian (Capitanian) deposits of the "Rader slide", Guadalupe Mountains, West Texas. Stratigraphy, v. 3, p 161-194.

Nestell, G.P., Nestell, M.K., Wardlaw, B.R., Bell, G.L. Jr., and Yermolayev, J.B., 2007a, Integrated biostratigraphy of conodonts, foraminifers and radiolarians from the Uppermost Guadalupian (Middle Permian) in the Apache Mountains, West Texas. Abstracts with Programs, v. 39, no. 3, p. 68.

Nestell, M.K., Bell, G.L. Jr., Wardlaw, B.R., Nestell, G.P., Lambert, L.L., Maldonano, A.L., Noble, P.J., 2007b, Biostratigraphic significance of a new potential key reference section for the Latest Guadalupian Reef Trail Member of the Bell Canyon Formation (Middle Permian), West Texas. Abstracts with Programs, v. 39, no. 3, p. 68.

Newell, N.D., Rigby, J.K., Fischer, A.G., Whiteman, A.J., Hickox, J.E., and Bradley, J.S., 1953, The Permian Reef Complex of the Guadalupe Mountains region, Texas and New Mexico, a study in Paleoecology. San Francisco, W.H. Freeman and Company. 236 p.

Owen, D.E., 1951, Geologic Structure of Seven Heart Gap, Culberson County, Texas. University of Texas, M.A. Thesis. 57 p.

Richardson, G.B., 1904, Report of a reconnaissance in Trans-Pecos Texas north of the Texas and Pacific Railway. Univ. Texas Bull. 23 (min. Survey Ser. 9). 119 p.

Richardson, G.B., 1914, Description of the Van Horn Quadrangle. U.S. Geol. Survey Geol. Atlas, Van Horn folio No. 194.

Silver, B.A., Todd, R.G., 1968, Permian cyclic strata, northern Midland and Delaware basins, West Texas and southeastern New Mexico. Bull. Amer. Assoc. Petrol. Geol., v. 68, p. 250-267.

Skinner, J.W. and Wilde, G.L., 1955, New fusulinids from the Permian of West Texas. Journal of Paleontology, v. 29, p. 434-444.

Snider, J.L., 1955, Geology of the Seven Heart Quadrangle Culberson County, Texas. University of Texas, M.A. Thesis. 69 p.

Walter, J.C. Jr., 1953, Paleontology of the Rustler Formation, Culberson County, Texas. Journal of Paleontology, v. 27, p. 679-702.

Wardlaw, B.R., Lambert, L.L., Nestell, M.K., 2001, Latest Guadalupian-Earliest Lopingian Conodont Faunas from West Texas. Permophiles, v. 39, p. 31.

Wilde, G.L. and Todd, R.G., 1968, Guadalupian biostratigraphic relationships and Sedimentation in the Apache Mountain region, West Texas. *in* Silver, B.A., ed., Guadalupian facies, Apache Mountain area, West Texas. Guidebook 68-11: Midland, Society of Economic Paleontologists and Mineralogists, Permian Basin Section, p. 10-31.

Wilde, G.L., Rudine, S.F. and Lambert, L.L., 1999, Formal Designation: Reef Trail Member, Bell Canyon Formation, and its significance for recognition of the Guadalupian-Lopingian boundary, *in* Geologic framework of the Capitan Reef, Soc. Econ. Paleont. and Min., Special Pub., No. 65. p. 63-83.

Wood, J.W., 1965, Geology of Apache Mountains, Trans-Pecos Texas. Univ. of Texas, PhD. Dissertation. 241 p.

BIOGRAPHICAL INFORMATION

Michael James Sweatt began studying at the University of Texas at Arlington in 2002. He earned his B.S. degree in Geology in 2006 and began work on his Master's degree later that same year. He is presently working for XTO Energy as an associate geologist in Ft, Worth, TX. Future endeavors may include pursuing his Ph.D. in Environmental Science at the University of Texas at Arlington to extend his Master's work to include the additional work needed in this paper and to also include the upper part of the Cherry Canyon Formation exposed far to the north of his and Walter Kennedy's map areas.